FORMATION OF CYCLIC CARBONATES FROM ALKENES AND CO_2 USING GOLD NANOPARTICLE CATALYSTS STABILIZED IN TETRAALKYLPHOSPHONIUM IONIC LIQUIDS

A thesis submitted to the College of Graduate Studies and Postdoctoral Studies

In partial fulfillment of the requirements for the degree of

Master of Science

In the Department of Chemistry

University of Saskatchewan

Saskatoon, Saskatchewan, Canada

by

VY THAO PHUNG

April 2018

Permission to Use

In presenting this thesis in partial fulfilment of the requirements for a Postgraduate degree from the University of Saskatchewan, I agree that the Libraries of this University may make it freely available for inspection. I further agree that permission for copying of this thesis in any manner, in whole or in part, for scholarly purposes may be granted by the professor or professors who supervised my thesis work or, in their absence, by the Head of the Department or the Dean of the College in which my thesis work was done. It is understood that any copying or publication or use of this thesis or parts thereof for financial gain shall not be allowed without my written permission. It is also understood that due recognition shall be given to me and to the University of Saskatchewan in any scholarly use which may be made of any material in my thesis.

Requests for permission to copy or to make other use of material in this thesis in whole or part should be addressed to:

Dean
College of Graduate and Postdoctoral Studies
University of Saskatchewan
116 Thorvaldson Building, 110 Science Place
Saskatoon, Saskatchwan S7N 5C9
Canada

Department Head
Department of Chemistry
University of Saskatchewan
110 Science Place
Saskatoon, Saskatchewan S7N 5C9
Canada

Abstract

Cyclic carbonates have found extensive uses in numerous industrial applications. Conventional methods for cyclic carbonate formation, however, often employ toxic phosgene precursors in which hydrochloric acid is being produced as a by-product. In recent years, routes for the direct synthesis of cyclic carbonates from alkenes instead of epoxides have been sought due to the lower cost and greater availability of alkenes as the starting materials. Among the investigated catalysts, gold nanoparticles (Au NPs) have shown excellent catalytic activity for alkene epoxidation as they allow rapid chemical transformations and are less prone to over-oxidation and self-poisoning during selective oxidation reactions.

Highly stable Au NPs were synthesized in the trihexyl(tetradecyl)phosphonium chloride ionic liquid ([P66614][Cl] IL), a greener alternative to traditional volatile organic solvents. This composite system is novel as the Au NPs act as the catalyst for the epoxidation of alkenes, whereas the IL functions as a solvent for CO_2 and a catalyst for the ring-opening of the intermediate epoxides and CO_2 (via the chloride nucleophile).

The focus of this thesis is to optimize the conditions needed for the one-pot activation of alkenes and CO_2 to form cyclic carbonates via studying the required conditions for each reaction. It was found that while epoxidation of alkenes such as propylene and styrene by tert-butyl hydroperoxide can be catalyzed by Au NPs stabilized in the IL solvent, care has to be taken to ensure that the NPs do not get oxidized during the reaction. The cyclic carbonate reaction was found to be effectively catalyzed by the IL chloride anion and has pseudo-first order kinetics with respect to CO_2. Increased rates and conversions were further seen at elevated CO_2 pressures (i.e. 2.4 MPa) and stirring the system at 600 rpm helped to take the reaction out of the mass-transfer

limited range. The established reaction conditions were then being examined for the direct synthesis of cyclic carbonates from alkenes and CO_2. Moderate conversion and selectivity were observed. A non-halide tetraalkylphosphonium IL, trihexyltetradecylphosphonium bis(trifluoromethylsulfonyl)imide ([P66614][NTf_2]), was also tested to compare with [P66614][Cl] for the same reaction.

Acknowledgements

As this fulfilling MSc journey comes to an end, I am thankful for everyone who has helped and supported me along the way.

To my research supervisor, Dr. Robert Scott, for giving me this opportunity to work in his group. Without his academic freedom, patience, encouragement, forgiveness, and valuable scientific inputs, I will not be where I am today. I also thank my academic advisor, Dr. Stephen Foley, as well as Drs. Andrew Grosvenor and Lee Wilson for their valuable input throughout my MSc program.

To all the past and present members of the Scott group, Dr. Abhinandan Banerjee, Dr. Mahesh Gangishetty, Dr. Yali Yao, Robin Theron, Sudheesh Kumar Veeranmaril, William Barett, Brandon Chivers, Kazeem Sulaiman, and Maryam Alyari, thank you for all of the fond memories and for making everyday a joy to be in the lab. I truly enjoyed all the time we spent outside and inside the lab, and I appreciate all of your advices, encouragements and suggestions along the way.

To Larhonda Sobchishin at the Western College of Veterinary Medicine Image Centre and Ken Thoms for helping me with my TEM, MS and GC-MS analysis. I also thank Drs. Keith C. Brown and Jianfeng Zhu for their help with NMR measurements.

To the laboratory manager, Dr. Alexandra Bartole-Scott, for her guidance in teaching Chem112 and Chem114, and to all the staff in the Department of Chemistry, Leah Hildebrant, Bonita Wong, Tracey Friesen, Linda Duxbury, and Ronda Duke for their invaluable help.

Finally, I thank my dearest parents, Nguyet Trinh and Tuan Phung, for their unwavering support, encouragement and love throughout my years of study. To my brother, Huy Phung, you are amazing, and you inspire me more than you will ever know.

Dedication

‘I dedicate this work to my family, whose endless love inspired me in this life,

and to Ton Bi.’

Table of Contents

List of Figures

List of Schemes

List of Tables

List of Abbreviations

A11	Non-symmetrial Aluminium Salen-acac Hybrid Complex
BA1	Benzaldehyde
BA2	Benzoic acid
BMIm	1-Butyl-3-Methylimidazolium
BMMIm	1-Butyl-2,3-Dimethylimidazolium
BMPy	1-Butyl-4-Methylpyridinium
BMPy	1-Butyl-4-Methylpyridinium
$C_7F_{15}CO_2$	Pentadecaflurooctanoate
$C_8H_4F_{13}$mim	1-(3,3,4,4,5,5,6,6,7,7,8,8,8-Tridecafluorooctyl)-3-Methylimidazolium)
CHP	Cymene Hydroperoxide
CNT	Multi-Walled-Carbon Nanotubes
COD	Cyclooctadiene
COT	Cyclooctatetraene
CPy	Butylpyridinium
EMIm	1-Ethyl-3-Methylimidazolium Cation
FAP	Tris(perfluoroalkyl)trifluorophosphate
IL	Ionic Liquid
MTO	Methyltrioxorhenium
NMR	Nuclear Magnetic Resonance
NPs	Nanoparticles
NTf_2	Bis(trifluoromethylsulfonyl)imide

P44414	Tributyltetradecylphosphonium
P66614	Trihexyltetradecylphosphonium
PC	Propylene Carbonate
PO	Propylene Oxide
PS	Polystyrene
SC	Styrene Carbonate
SO	Styrene Oxide
TBAB	Tetrabutylammonium Bromide
TBHP	Tert-Butyl Hydroperoxide
TEM	Transmission Electron Microscopy
TOAB	Tetraoctylammonium Bromide
TON	Turnover Number
UHP	Urea Hydrogen Peroxide
UV-Vis	Ultraviolet-Visible

1.0 Introduction

Solvents have been widely acknowledged to have drastic effects on reaction pathway, reaction rate, and even product selectivity in chemical reactions. However, the use of volatile organic solvents at medium to large scales in industrial synthetic protocols has definite toxic environmental implications that we can no longer afford to ignore. This ranges from environmental hazards such as air and water pollution, to disposing of contaminated organic solvents after product purification. Hence, it is imperative for us to seek alternatives to solvents that are potentially damaging to the environment and living beings.

1.1 Ionic Liquids

Ionic liquids (ILs) are structurally similar to ionic surfactants: they consist of a cation and an anion where the cation alkyl chain must be long enough to disrupt lattice packing but not too long as this will increase the salt melting point as a result of increasing cohesive interactions.[1] The properties of IL, in principle, are tunable due to the nearly endless combinations of cations and anions available. The most popular cations include 1-alkyl-3-methylimidazolium, N-alkylpyridinium, and quaternary ammonium or phosphonium species (Figure 1.1).

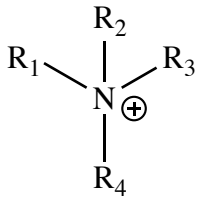

tetraalkylammonium

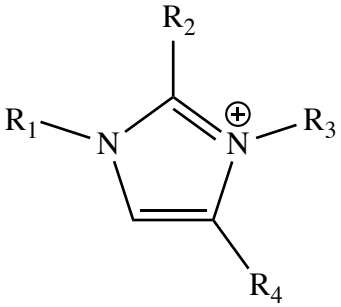

di- or trialkylimidazolium

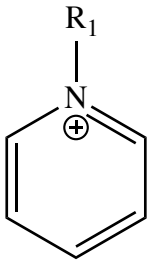

alkylpyridinium

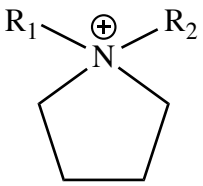

dialkylpyrazolium

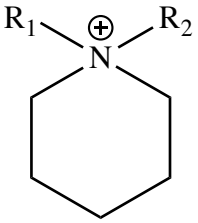

dialkylpiperidinium

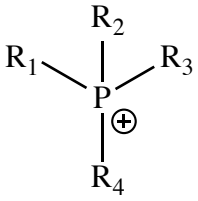

tetraalkylphosphonium

Fluorous-anions:

BF_4^- (tetrafluoroborate)
PF_6^- (hexafluorophosphate)
$CF_3CO_2^-$ (trifluoroacetate)
$CF_3SO_3^-$ (trifluoromethanesulfonate
OTf^- (triflate)
NTf_2^- (N-bis-trifimide)

Non-fluorous anions:

OAc^- (acetate)
Cl^-, Br^-, I^- (halides)
$N(CN)_2^-$ (dicyanamide)

Figure 1.1 Some common cations and anions in IL.

ILs are often synthesized via a two-step reaction: the first step involves making of the desired cations, followed by anion exchange where necessary to form the desired product.[2] Cation formation can be carried out by protonation with an acid, or by direct alkylation of alkylimidazole, trialkylamine, or trialkylphosphine precursors.[3] The anion exchange, on the other hand, can be done by either direct treatment of halide salts with a Lewis acid (i.e. $AlCl_3$) to form ILs upon contact of the two materials, or via anion metathesis between halide salts and a range of silver

salts.[4] The later method remains the most efficient for water-miscible ILs, although it is limited by the relatively high cost of silver salts and the large amount of solid Ag halide produced as by-products.[5]

1.1.1 Imidazolium Ionic Liquids

ILs were first discovered by Weiner and Gabriel backed in the 1880s;[6] and since then, they have been developed and used in numerous applications, including but not limited to biosensors, electrolytes and photopolymerization (Table 1.1).[7–22] The first room-temperature IL, ethylammonium nitrate, $[C_2H_5NH_3][NO_3]$, was reported by Paul Walden in 1914.[7] Early ILs, however, were often air- and water-sensitive due to the use of haloaluminates as counter-ions; therefore of little value for industrial applications.[8] In 1992, the Wilkes group reported air- and water-stable, low melting-point imidazolium salts with weakly coordinating anions such as hexaflurophosphate (PF_6^-) and tetrafluoroborate (BF_4^-) that allowed for much wider applications.[9–13] These ILs are often referred to as second generation ILs, and currently remain the most well investigated classes of ILs. The third generation of ILs, also are known as task-specific ILs, were introduced in the early 2000s by Abbott et al.,[14] in which a particular property, either physical or chemical, is added into the ILs by covalently incorporating a functional group into the anion, cation, or both ions.[15–18] Some ILs are synthesized with chiral cations or anions, thus are useful for asymmetric synthesis applications.[19] Others are prepared with active pharmaceutical ingredients to produce ILs with biological activities.[20–22]

Table 1.1 History and development of ILs.

Year/ Inventors	Object of invention
[7]1914 – Walden et al.	First room-temperature IL, $[C_2H_5NH_3][NO_3]$
[9]1992 – Wilkes and Zaworotko	Second generation of room-temperature imidazolium ILs with weakly coordinating anions $[PF_6^-]$ and $[BF_4^-]$
[10]1996 – Bonhote et al.	First imidazolium IL with $[NTf_2^-]$ anion
[11]1998 – Ohno and Ito	Polymeric ILs as matrixes for fast ion conduction
[12]2001 – Ye et al.	IL-derived lubricants
[13]2002 – Liang et al.	IL-based quartz crystal microbalance sensors
[14]2003 – Abbott et al.	Third generation ILs with quaternary ammonium salts
[15]2003 – Sakaebe and Matsumoto	IL-based Li batteries electrolytes
[16]2006 – Wang et al.	Surface-confined ILs as stationary phases for high performance liquid chromatography
[17]2008 – Marták et al.	Separation of lactic acid by supported IL membranes
[22]2008 – Pauliukaite et al.	IL-based biosensors
[19]2009 – Van-Buu et al.	Chiral ILs as catalysts for aza Diel-Alder reactions
[18]2010 – Tao et al.	Acidic ILs as catalysts for furfural reactions
[21]2010 – Hernández-Fernández et al.	ILs as reaction media for biocatalytic ester synthesis
[20]2011 – Ho et al.	ILs as sorbent materials for solid phase microextraction

1.1.2 Tetraalkylphosphonium Ionic Liquids

Although the chemistry of the tetraalkylphosphonium ILs have been investigated experimentally by several groups, and some have been commercially available for the past decade or so, they are surprisingly under-represented in the journal literature compared to other families of ILs. Tetraalkylphosphonium ILs often have better thermal stability, lower toxicity and lower cost compared to other classes of ILs.[23] Also, unlike imidazolium cations, they have no acidic proton, thus are more stable toward nucleophilic and basic conditions, which is important for many applications.[24,25] Wang et al., for example, reported the use of superbase-derived phosphonium ILs for CO_2 capture at an extremely high capacity (i.e. more than 1 mole of CO_2 per mole of IL) by making use of their tunable chemical reactivity.[24] Similarly, Cristiano et al. took advantage of the high polarizability and low volatility of the tetraalkylphosphonium trihalide ILs and used them as halogenation agents for alkenes, alkynes, and aromatic molecules.[25]

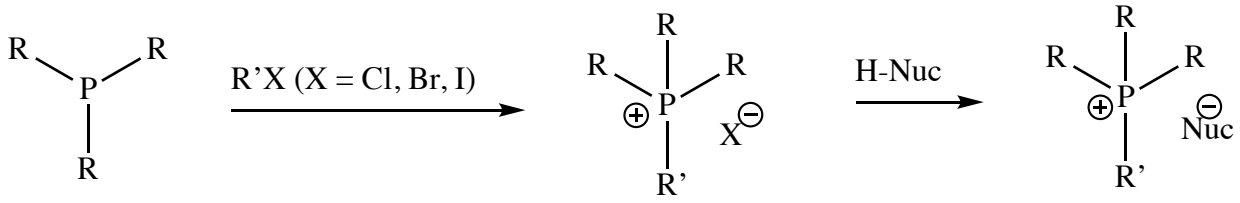

Scheme 1.1 Schematic synthesis of tetraalkylphosphonium ILs.

To prepare tetralalkylphosphonium ILs, a tertiary phosphine, PR_3, is added to haloalkenes via a nucleophilic S_N2 addition (Scheme 1.1).[26] Asymmetrical ILs can also be prepared by converting primary and secondary alkylphosphines (PRH_2 and PR_2H respectively) via free radical addition to alkenes, followed by anion exchange.[27] Despite the nearly endless anion/cation combinations, only a number of them can result in true room-temperature ILs (Figure 1.2).[28]

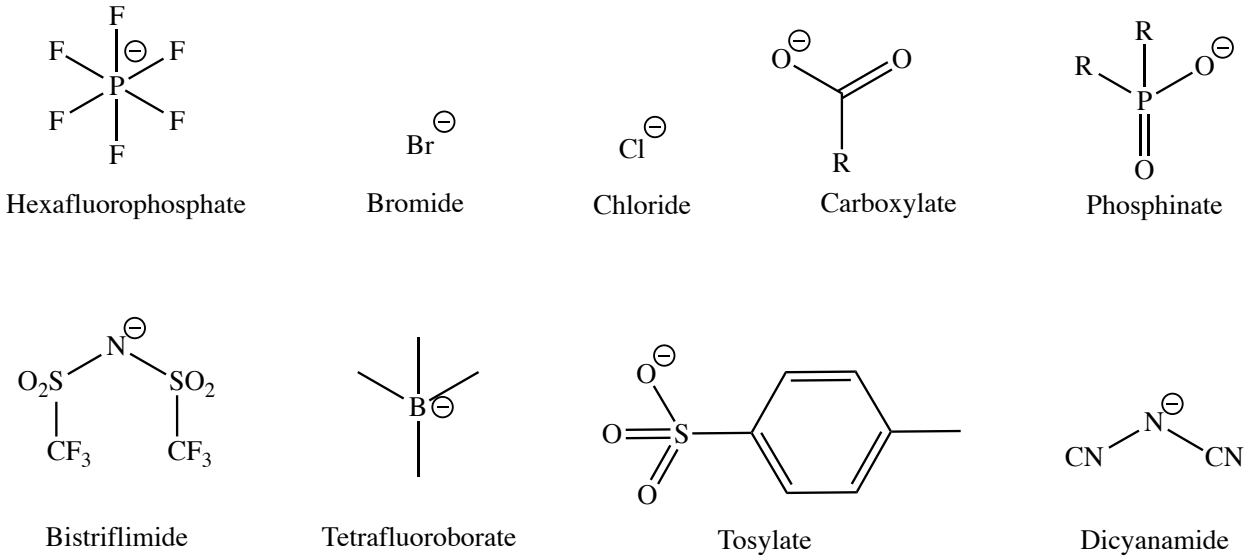

Figure 1.2 Examples of anions that can be paired with tetraalkylphosphonium cations to produce room-temperature ILs. Reprinted with permission from reference (26). Copyright © 2002 Royal Society of Chemistry.

1.1.3 Other Ionic Liquids

There are numerous other families of ILs that have been synthesized, but of late, the focus has shifted to IL families based on renewable feedstocks that can be prepared easily and without consuming large amount of organic solvents during their synthesis.[29–36] These ILs tend to have unique advantages associated with them, while still maintain interesting IL properties. Polymeric IL materials that are high in ionic conductivity, for example, can find applications as fuel cells, battery electrolytes, and antistatic agents for various polymers such as polypropylenes, polyvinylidene fluoride, polycarbonates, and polyurethanes.[29] Similarly, magnetic ILs that exhibit susceptibility to an applied magnetic field by incorporating one or more paramagnetic components into the cation or anion moiety are very useful for applications such as chloramphenicol extraction from aqueous environments,[30] uranium removal,[31] and micro-extraction of acidic pharmaceuticals

from aqueous matrixes.[32] Also, a number of ammonium-, phosphonium- and imidazolium-based ILs with biological properties have been examined for pharmaceutical-related applications.[33–36]

Despite their advantages as reaction media for catalytic syntheses, ILs have yet to be widely applied in the industry, mainly due to their high production cost and insufficient data regarding their toxicity and biodegradability.[37] For this reason, it is important to design and synthesize ILs from cheap and readily available starting materials, as well as study their environmental impact to put these solvents at the forefront as alternative solvents for scientific and commercial applications.

1.1.4 Applications of Ionic Liquids

Since the discovery of the second generation of ILs with weakly coordinating anions (i.e. $[PF_6^-]$ and $[BF_4^-]$) by Wikes and Zaworotko in 1992, ILs have been widely incorporated in numerous scientific and industrial applications, including but not limited to organic syntheses such as the Friedel-Crafts alkylations and acylations, Diels-Alder cycloadditions, enzymatic catalysis, aromatic nucleophilic substitutions, spectroscopy and electrochemistry, nanomaterials synthesis, polymerization, extraction and separation processes.[38–43] Furthermore, by pairing the appropriate anions and cations, ILs can also act as potential electrolytes for electrochemical devices, such as Li-ion batteries,[44] supercapacitors,[44] fuel cells,[45] sensors and solar cells,[46] or as solvents for metal deposition as well as for electro-finishing applications.[47]

1.2 Stabilization of Metal Nanoparticles Catalysts in Ionic Liquids

Metal NPs have found extensive uses in a number of disciplines due to their large surface area and properties.[48] However, the synthesis and stabilization of metal NPs in solution is relatively challenging due to their aggregation behavior, in which they aggregate into colloids up to several

microns in size.[49] This is because these species are only kinetically stable, whereas the thermodynamically stable species are the bulk phase.[50] To restrict their aggregation, a stabilizer or ligands must be present to ensure that the NPs will remain in solution, with little to no growth.[50] Particularly, the stabilizer needs to provide an electrostatic, van der Waals, and/or covalent stabilization between it and the NP surface, as well as a steric hindrance and/or electrostatic repulsion between the outer stabilizer sphere of adjacent particles (Scheme 1.2).[50] In general, both van der Waal and covalent stabilizers can lead to steric hindrance between metal NPs. However, while van der Waals stabilizers are in close proximity with the metal surface via combination of various weak attractive forces, covalent stabilizers are covalently bonded directly to the metal surface.

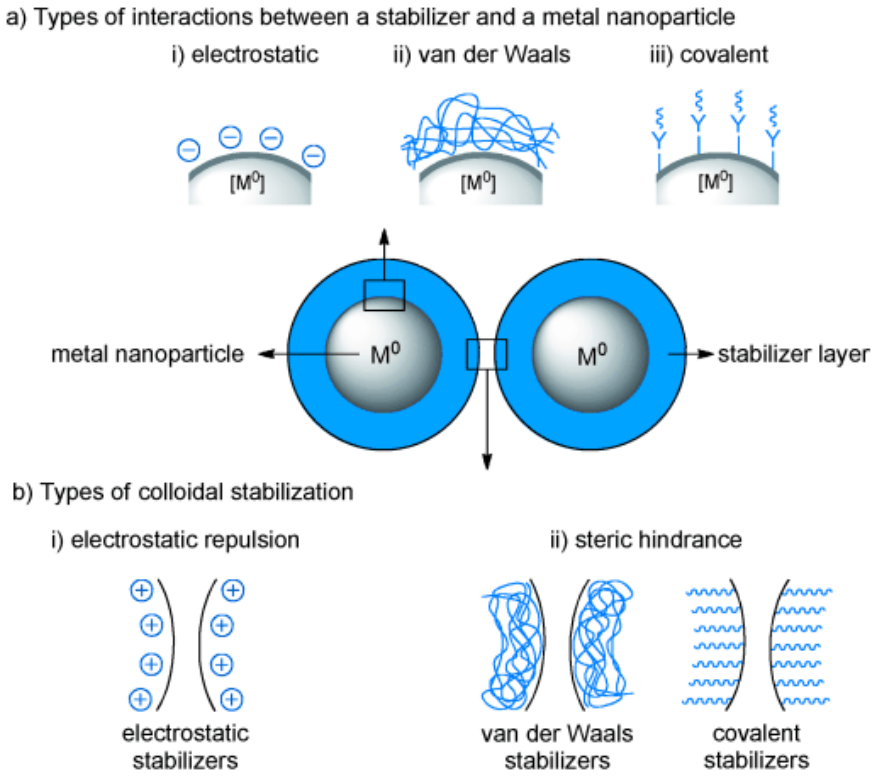

Scheme 1.2 Schematic representation of (a) interactions between the stabilizers and metal NPs, and (b) interactions between the outer stabilizer spheres of adjacent metal NPs. Reprinted with permission from reference (50). Copyright © 2012 Wiley-VCH.

Recently, ILs have been investigated experimentally by many groups as an intriguing media for metal NP formation due to their cationic and/or anionic species acting as electrostatic stabilizers.[51–53] Dupont et al., for example, synthesized Ir NPs via reduction of Ir(I) dissolved in imidazolium ILs.[51] Similarly, the Moores group employed phosphonium- and imidazolium-based ILs as reaction media to make highly stable Ru NPs.[52] Our group has also proposed a simple synthetic route for metal NPs in tetraalkyphosphonium ILs via $LiBH_4$ reduction without the use of any organic solvent or external stabilizers.[53] The synthesized NPs were found to remain stable and showed no NP agglomeration over many months.[53] Other chemical syntheses of noble metal NP/IL are given in Scheme 1.3.[54] Scheme 1.3a and 1.3d show gold or silver salts (i.e. $HAuCl_4$, $AuCl_3$ or $AgNO_3$) are being reduced by the imidazolium-based cation.[55] Ru NPs, on the other hand, are often synthesized via decomposition of metal precursors, such as [Ru(COD)(2-methylallyl)$_2$] or [Ru(COD)(COT)] (COD = cyclooctadiene, COT = cyclooctatetraene) followed by nucleophilic attack,[56] or decomposition of metal precursors by heat, microwave, and light irradiation (Scheme 1.3b).[57,58] Similar to Ru NPs, Ni NPs can be prepared by decomposition of Ni(0) in imidazolium ILs (Scheme 1.3c).[59,60]

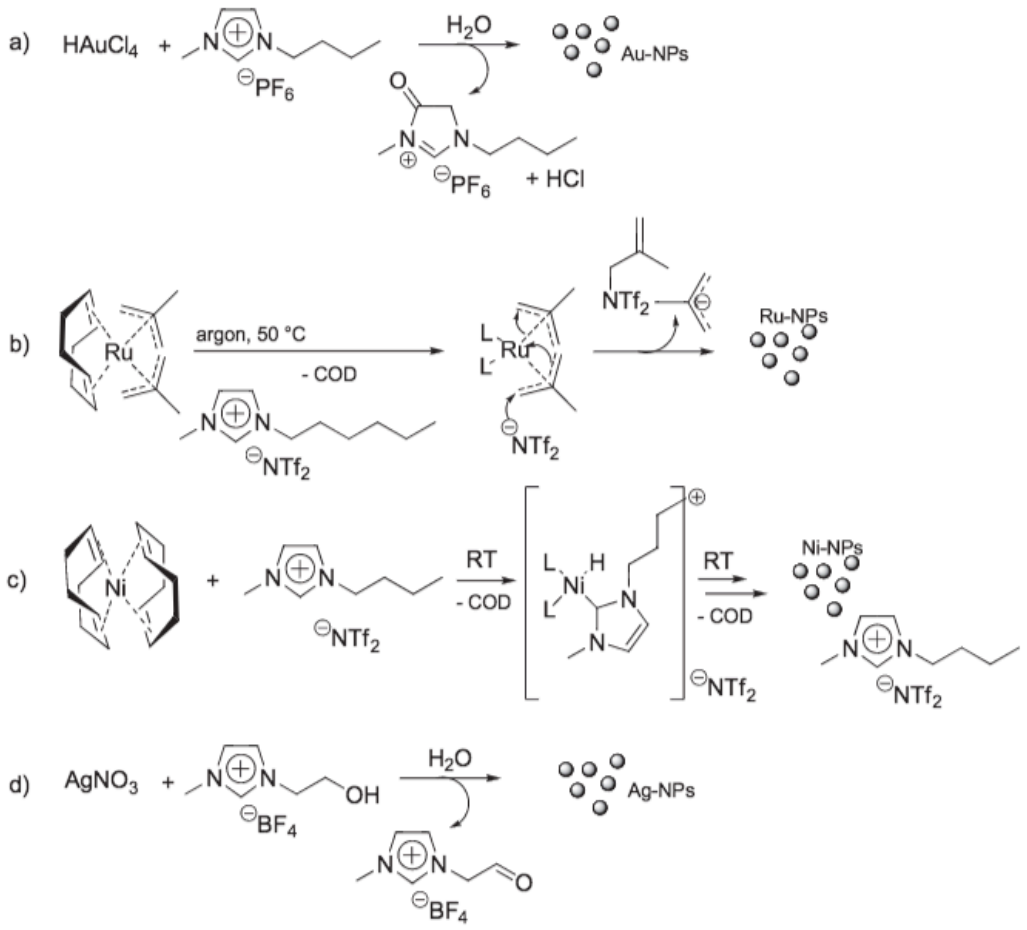

Scheme 1.3 Typical synthetic routes for NPs in IL. Reprinted with permission from reference (54). Copyright © 2013 John Wiley and Sons.

1.3 Metal Nanoparticle-Catalyzed Reactions in Ionic Liquids

The number of catalytic reactions where metal NP/IL play a role has increased rapidly over the past decade. The reactions include but are not limited to hydrogenations, selective oxidations, hydrodehalogenations, hydrosilylations, methoxycarbonylations, and Fischer-Tropsch syntheses.[61–63] Although it would be impossible to cover every single reaction, this section does intend to provide an overview on the major reaction class that have been examined over the course

of this MSc research project: selective oxidations. This is a very important reaction from an industrial standpoint as most common chemical syntheses, including drugs, dyes, perfumes, flavoring material, processed food, and cleaning products, involve one or more steps where molecules are being reduced or oxidized.[64]

1.3.1 Hydrogenation

Catalytic hydrogenation reactions of specific functional groups, such as alkenes, alkynes, imines, nitro and carbonyl groups, are crucial in synthetic chemistry from both scientific and industrial standpoints.[51] Moreover, they are among the most thoroughly studied class of reactions in which metal NPs stabilized in ILs act as catalysts. These reactions are often occurred under biphasic conditions, which potentially allow for facile product separation from the catalyst.

The first successful hydrogenation catalyzed by the NP/IL system was studied by Chauvin et al. in 1996 with Rh complexes such as $RhCl(PPh_3)_3$, $RhCl_2(PPh_3)_3$, and $[Rh(COD)_2][BF_4]$ were synthesized in $(BMIm)(BF_4)$ IL (BMIm = 1-butyl-3-methylimidazolium).[65] The reactions were performed at 1 MPa H_2 with turnovers of up to 6000, and the NPs were found to form in situ during the synthesis.[65] Since then, many others have shown the syntheses and catalytic applications of metal NPs in room-temperature ILs.[66,67] For example, Vollmer et al. reported a highly active and easily recyclable catalyst system of dispersed Ru/Rh/Ir NP/IL for the biphasic liquid-liquid hydrogenation of cyclohexene to cyclohexane that gave almost quantitative conversion within 2 h at 10 MPa H_2 and 90 ºC.[66] Later on, Yu et al. employed Au/Pt alloy NPs in nine different functionalized imidazolium ILs as electrocatalysts for hydrogen peroxide reduction.[67]

1.3.2 Selective Oxidation

Catalytic oxidations are the second most investigated class of reactions, in which ILs are used as co-catalysts with transition metal NPs by providing them with a polar, weakly coordinating media. Although metal NP/IL show good catalytic activity toward oxidation reactions, there are still a few drawbacks that need to be considered before designing an oxidative catalytic process in an IL phase. For example, both the metal NPs and the ILs are susceptible to chemical oxidation in the presence of an oxidant, especially at higher temperatures. The exposure of oxygen or water might lead to oxidative etching, Ostwald ripening, or formation of inert oxide shells for metal NPs, thus diminishing their catalytic activities.[68] ILs, on the other hand, can be oxidized by anion decomposition (halometallate ILs), anion hydrolysis (BF_4- and PF_6-contained ILs), or oxidation of the cation alkyl side chains (tetraalkylphosphonium ILs).[69,70] Other drawbacks involves the toxicity and biodegradability of ILs since the majority of reported ILs are not biodegradable and their toxicity is not well-known.[71] The viscosity of ILs can also be a problem but this can be mitigated by changing the cation and/or anion.

Despite the limitations described above, progress is still being made, especially for selective oxidations in IL media. In 2014, Shi et al. reported a graphene-supported Pt NPs in [BMIm][BF_4] and [BMIm][PF_6] ILs systems that exhibited highly electrocatalytic activity and stability toward methanol oxidation.[72] Ding et al. later on introduced supported Pd/Ni alloy NPs on multi-walled carbon nanotubes prepared by thermal decomposition in N-butylpyridinium tetrafluoroborate for formic acid oxidation.[73] In 2015, Restrepo et al. demonstrated the use of Au NPs on IL-based crosslinked polymeric materials as catalysts for the oxidation of 1-phenylethanol in water using different oxidants and microwave irradiation as the heat source.[74] Au NPs synthesized in tetraalkylphosphonium halide ILs were also used as catalysts for aerobic oxidation

of α, β-unsaturated alcohols, deep hydrogenations, and hydrodeoxygenation reactions by our group.[75]

1.3.3 Other Reactions

Beside oxidations and hydrogenations, metal NPs in ILs also act as active catalysts in various reactions such as Suzuki C-C couplings, carbonylations, and hydrosilylations.[76-85] A sampling of reactions is shown in Table 1.2. The catalytic reactions are often carried out in a multiphase system, in which the NP/IL forms the denser phase while the substrates and product remains in the upper phase, thus making it easier to recover the IL solution.[86]

Table 1.2 Examples of reactions catalyzed by IL-stabilized metal NPs.

Reaction	**Catalyst**	**Ionic Liquids**
[76]Alkene Hydroformylation	Rh	[BMIm][PF_6]
[77,78]Heck Reactions	Pd	[BMIm][PF_6] and [BMIm][NTf_2]
[79,80]Suzuki Cross–Coupling	Pd	[BMIm][BF_4] and [P66614][Cl]
[81]Stille Cross–Coupling	Pd	[NR_4][Br]
[82,83]Sonogashira Cross–Coupling	Pd	[BMIm][PF_6]
[63]Methoxycarbonylations	Pd	[BMIm][X] (X=Cl, Br) and [BMPy][X] (X= PF_6, BF_4, Cl, Br)
[84,85]Hydrosilylations	Pt, Rh	[P44414][NTf_2] and [BMMIm][NTf_2], [CPy][BF_4]

NTf_2 = bis(trifluoromethylsulfonyl)imide; NR_4 = tetraalkylammonium;
BMPy = 1-butyl-4-methylpyridinium; P44414 = tributyltetradecylphosphonium;
BMMIm = 1-butyl-2,3-dimethylimidazolium; CPy = butylpyridinium.

1.4 CO_2 Capture via Cycloaddition of CO_2 to Epoxides

Carbon dioxide (CO_2), a well-known greenhouse gas, is an ideal C1 feedstock that is renewable, non-toxic, and low-cost.[87] The conversion of CO_2 into valuable chemicals, therefore, is highly desirable, especially with the fast consumption of fossil fuels.[87] One of the most attractive and feasible strategies for CO_2 capture is to use it as a building block in the ring-opening of epoxides to yield cyclic carbonates as the desired product.[87] However, further optimization of the catalysts and the contemporary employed processes are still required to satisfy the criteria for Green Chemistry such as reducing the formation of non-selective products and solvent waste.

1.4.1 CO_2 Solubility in Ionic Liquids

While both the IL cations and anion affect the CO_2 solubility, it is believed the anions play a key factor. A study by Cadena et al. on CO_2 solubility of imidazolium ILs have shown that CO_2 primarily associates with the [PF_6^-] and [BF_4^-] anions, regardless of the cations.[88] Anion effect were later investigated experimentally by pairing [BMIm] cations with various anions, and the CO_2 solubility in ILs was found to increase in the order of [NO_3^-] < [SCN^-] < [$MeSO_4^-$] < [BF_4^-] < [Dichloroacetic acid] < [PF_6^-] < [NTf_2^-] < [Tris(trifluoromethylsulfonyl)methide] < [$C_7F_{15}CO_2^-$] ($C_7F_{15}CO_2$ = Pentadecaflurooctanoate).[89] This trend was also found to be reproducible for guanidinium- and phosphonium-based ILs when tested by Maiti et al. and Sistla et al.[90,91]

Higher CO_2 solubility was observed when longer fluoroalkyl chains were employed in the IL anions, such as the FAP anion (FAP = tris(perfluoroalkyl)trifluorophosphate).[92] The presence of fluoroalkyl groups in cations can also increase the solubility of CO_2, though the effect is only secondary compared to anion fluorination. For example, CO_2 solubility was significantly higher in fluorine-substituted such as [$C_8H_4F_{13}$mim][NTf_2] IL compared to non-fluorine-substituted ILs

such as [1-octyl-3-methylimidazolium][NTf_2] and [1-decyl-3-methylimidazolium][NTf_2] ($C_8H_4F_{13}$mim = 1-(3,3,4,4,5,5,6,6,7,7,8,8,8-tridecafluorooctyl)-3-methylimidazolium).[93] Using longer alkyl chain cations also improves the CO_2 solubility.[94] For instance, tetraalkylphosphonium ILs, especially trihexyltetradecylphosphonium bis(2,4,4-trimethylpentyl)phosphinate, were reported to have a higher solubility of CO_2 than most of the commonly used fluorinated imidazolium ILs, such as [BMIm][NTf_2], [BMIm][$C_7F_{15}CO_2$], and [1-hexyl-3-methylimidazolium][FAP].[95]

1.4.2 Alkene Epoxidation

Epoxidation of alkenes are important in chemical industry as the resultant epoxides are often used as raw materials or intermediates in the production of commercially valuable products for flavors, fragrances, paints, polymers and pharmaceuticals.[96] Different methods have been developed to prepare epoxides; however, alkene epoxidations are still an extensive route in which alkenes are oxidized to the corresponding epoxides in the liquid phase (Figure 1.3).

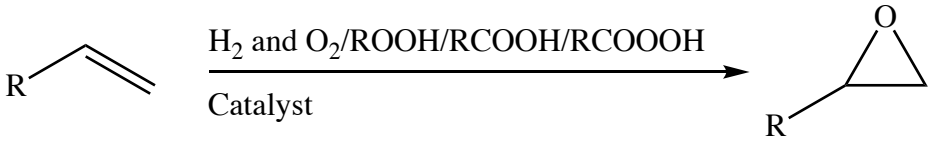

Figure 1.3 Synthesis of Epoxides from Alkenes.

Although ethylene, the simplest member in the alkene series, can be epoxidized efficiently using molecular oxygen with silver catalysts; higher alkenes can only be done using hydrogen peroxide or other stoichiometric oxygen donors.[96] Various catalysts have been investigated, such as solid acid catalysts like titanium silicalite-1, Ti/SiO_2, and titanium silicalite-2; unfortunately, most of them have poor conversions and selectivity toward epoxidation reactions of terminal

alkenes.[98–100] Metallic gold (Au) was believed to be catalytically inactive toward hydrogenation and oxidation reactions for a long time until Haruta et al. reported the use of supported Au on TiO_2 as a catalyst for propylene epoxidation in 1987.[100] It was found that when the Au particle size is brought down to the nanometer regime, it can facilitate rapid chemical transformations with high turnover numbers (TON) due to its large surface-to-volume ratio, exposed active sites, and properties intermediate between those of bulk materials and individual atoms/molecules as Au is virtually inert in the bulk.[102] In the last two decades since Haruta's discovery,[101] Au-based nanocomposites have widely gained attention in the literature and have been found to display exceptional catalytic activity, especially in oxidation reactions.[103,104] Nijhuis et al., for example, reported the use of Au dispersed on titania as a catalyst for the direct epoxidation of propene, in which a 10% conversion and a 90% selectivity for propylene oxide were achieved.[103] Au NPs stabilized in imidazolium-based disulfide IL were also used as catalysts for styrene epoxidation by Luo et al., resulting in a 100% styrene conversion with selectivity up to 90%.[104]

1.4.3 Cycloaddition of CO_2 to Epoxides

Cyclic carbonates have found extensive use as excellent aprotic polar solvents, electrolytes for secondary batteries, precursors for polymeric materials, and intermediates for the production of pharmaceuticals and fine chemicals.[105,106] Industrial cyclic carbonate syntheses typically involve the use of phosgene; however, alternate routes with similar activity and less toxicity have been developed, such as cycloaddition of CO_2 to epoxides (Figure 1.4).

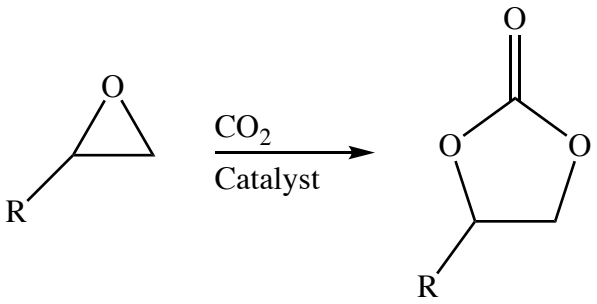

Figure 1.4 Cycloaddition of epoxides to CO_2.

A number of catalysts, such as metal oxides,[107–109] alkali metal halides,[109,110] organic bases,[112–115] zeolite,[116–119] titanosilicates,[120] and metal complexes[121–123] have been investigated and reported in literature for this reaction, though Lewis bases are still the most commonly used catalysts for epoxide activation due to their low cost and high selectivity toward cyclic carbonates.[124] Jagtap et al., for example, reported the use of an alkali metal halide (i.e. NaCl, NaBr, NaI) -supported silica liquid phase as a catalyst for the synthesis of cyclic carbonates, in which the activities of the anions increased in the order of $Cl^- > Br^- > I^-$.[125] Similarly, Zhang et al. employed quaternary ammonium salts as catalysts for ethylene carbonate synthesis, and similar activities of the anions were reported.[126]

ILs have received considerable interest for this reaction as they possess unique advantages such as undetectable vapor pressure, excellent thermal and chemical stabilities, tunable physicochemical properties, and moderate to high solubility of many organic and inorganic materials.[127] Also, CO_2 can dissolve well in many ILs, such as imidazolium-, pyridinium-, and phosphonium-based ILs, making the reactions of CO_2 in ILs feasible and suitable.[128–130] In 2007, a $ZnBr_2$/quaternary phosphonium iodide salts system was reported as the catalyst for the cycloaddition of CO_2 to epoxides, in which the combination of $ZnBr_2$ and PPh_4I showed the highest

TON (>6000).[131] Other combinations such as $ZnCl_2$ and alkyltriphenylphosphonium chloride and bromide salts were also reported in which high conversion and selectivity (>99%) were obtained.[132]

1.4.4 Direct Synthesis of Cyclic Carbonates from Alkenes and CO_2

The production of cyclic carbonates from epoxides and CO_2 is attractive from the viewpoint of Green Chemistry and chemical fixation of CO_2. However, there are still some shortcomings in using commercial epoxides as raw materials since they are more expensive and toxic compared to alkene precursors; hence, a simpler and cheaper approach for the formation of cyclic carbonates would be to start from alkenes and CO_2.

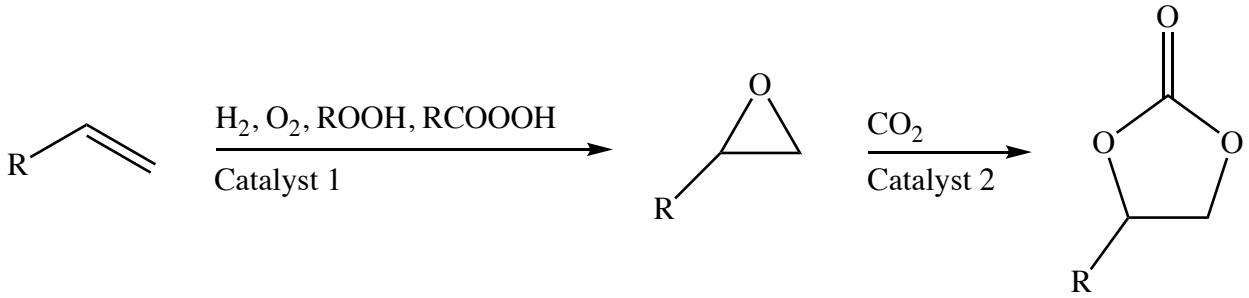

Figure 1.5 Direct synthesis of cyclic carbonates from alkenes and CO_2.

Despite its usefulness, only a few reports are found in the literature for the direct synthesis of cyclic carbonates from CO_2 and alkenes (Figure 1.5).[133–136] For example, a one-pot multistep for the production of styrene carbonates has been described in which methyltrioxorhenium(VII) was used to catalyze the styrene epoxidation reaction and a Zn-contained IL was used for the subsequent ring-opening reaction.[133] Au NPs on silica (Au/SiO_2)[134] and dioxo(tetraphenylporphirinato)ruthenium(VI)[135] were also used as catalysts for the direct synthesis

of cyclic carbonates, although long reaction times were required for these systems. The most recent study was done by Tangestaininejad et al. in which MoO_2(acetylacetonate)$_2$ acts as a catalyst and tert-butyl hydroperoxide functions as an oxidant for the direct synthesis of cyclic carbonates.[136] Although excellent TONs were obtained, and a range of alkenes could be converted in a relatively short reaction time using this catalytic system,[136] it is still essential to keep optimizing the two individual steps to achieve a satisfactory outcome for the overall process.

In this thesis, Au NPs stabilized in a tetraalkylphosphonium IL with strong nucleophilic anions, such as halides, are examined for the synthesis of cyclic carbonates from alkenes and CO_2. Au NPs can act as the catalyst for alkene oxidation, while the IL can function as a solvent for CO_2 and the IL halide anion is a suitable co-catalyst for the cycloaddition of CO_2 to epoxides.

1.5 Research Objectives

Although both alkene epoxidation reactions as well as the ring opening of epoxides to give cyclic carbonate are well-studied in the literature, little to no work have been done on the direct synthesis of cyclic carbonates from alkene precursors. This approach would be more beneficial for industrial applications due to the low-cost and wide availability of the starting material alkenes. The ultimate aim of this work, therefore, is to combine alkene epoxidation and the subsequent cyclic carbonate reactions in the same reaction flask by optimizing the conditions for each reaction. The chosen tetraaklylphosphonium IL for this reaction is trihexyltetradecylphosphonium chloride ([P66614][Cl]) because this IL has been shown to stabilize NPs effectively and has good CO_2 solubility.[51] Also, this is a stable room-temperature IL that can stabilize Au NPs over long period of time.[51] Tert-butyl hydroperoxide (TBHP) is selected as an oxidant as it is known to give higher rates of alkene oxidations compared to O_2. In this thesis, the [P66614][Cl] IL is used to stabilize

Au NPs and this gives a robust and reusable catalytic NP system that avoids the use of organic solvents and secondary stabilizers.

1.6 Organization and Scope

This MSc dissertation, which consists of 5 chapters, describes how Au NPs stabilized in tetraalkylphosphonium halide IL can catalyze the epoxidation of alkenes and the subsequent cyclic carbonate formation (Scheme 1.4). Styrene and propylene as starting materials were chosen to be examined in depth for these two reactions. A synopsis is provided at the beginning of each chapter, along with comments on the relationship between the particular chapter and the overall goal of the research program.

Chapter 1 introduces a promising alternative solvent to conventional organic solvents: ILs, as well as how their unique properties allow them to support metal NPs exceptionally well. This chapter also covers how the novel system of metal NPs in ILs, particularly Au NPs in tetraalkylphosphonium halide ILs, might be able to catalyze both alkene epoxidations followed by cycloaddition of CO_2 to epoxides for cyclic carbonate formations. The synthesis of epoxides from alkenes catalyzed by NP/IL is studied in depth in Chapter 2. Details in the examined reaction conditions, the recovery of Au NPs during the reaction, as well as kinetic studies are also discussed in this chapter. Chapter 3 covers the synthesis of cyclic carbonates in which the IL functions as a solvent for both CO_2 and the epoxides, and the IL halide catalyzes the cycloaddition of CO_2 to the epoxides. Chapter 4 continues this narrative by studying the possibility of a direct synthesis of cyclic carbonates from alkenes, building up from the separate reactions detailed in Chapter 2 and Chapter 3. Additionally, another type of tetraalkylphosphonium-based IL, tetraalkylphosphonium

bis(trifluromethylsulfonyl)imide, was also examined for the same reaction. Finally, in Chapter 5, a summary, an outlook, and possible future work in this field of research are presented.

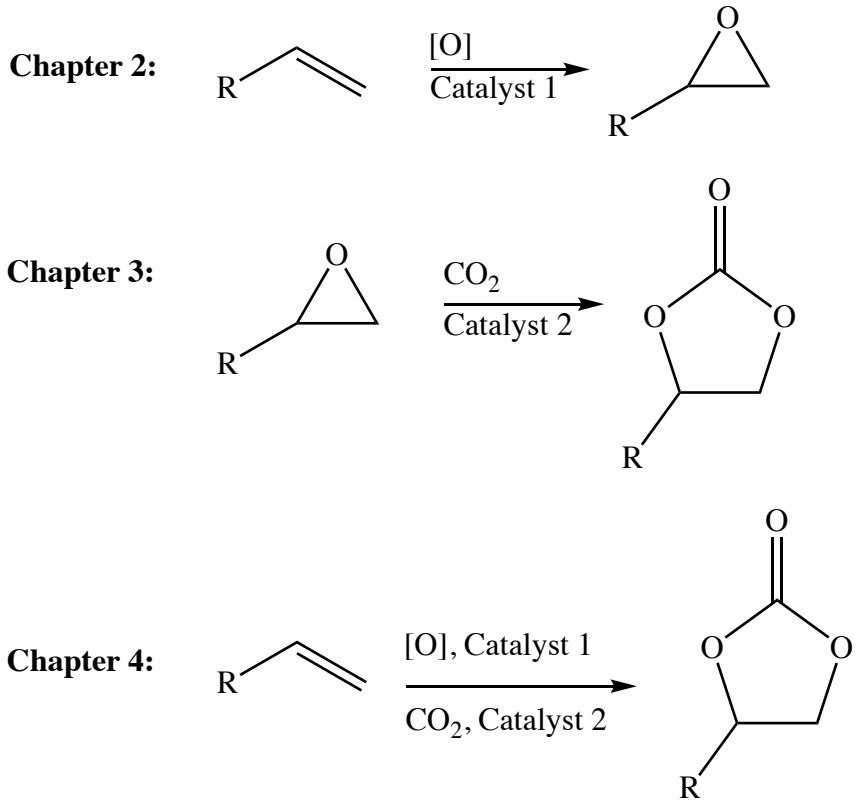

Scheme 1.4 Reactions investigated in this thesis.

1.7 References

(1) Hayes, R.; Warr, G. G.; Atkin, R. *Chem. Rev*. **2015**, *115*, 6357–6426.

(2) Gordon, C. M.; Muldoon, M. J.; Wagner, M.; Hilgers, C.; Davis, J. H.; Wasserscheid, P. Synthesis and Purification. In *Ionic Liquids in Synthesis,* Wasserscheid, P.; Welton, T.*;* Wiley-VCH: Weinheim, Germany, 2008; 37–43.

(3) Sheldon, R. *Chem. Commun.* **2001**, *23*, 2399–2407.

(4) Lee, C. K.; Huang, H. W.; Lin, I. J. B. *Chem. Commun.* **2000**, *19*, 1911–1912.

(5) Varma, R. S.; Namboodiri, V. V. *Chem. Commun.* **2001**, *7*, 643–644.

(6) Gabriel, S.; Weiner, J. *Chem. Ber.* **1888**, *21*, 2669–2679.

(7) Walden, P. *Bull. Russ. Acad. Sci*. **1914**, 405–422.

(8) Atefi, F.; Garcia, M. T.; Singer, R. D.; Scammells, P. J. *Green Chem.* **2009**, *11*, 1595–1604.

(9) Wilkes, J. S.; Zaworotko, M. J. *J. Chem. Soc. Chem. Commun.* **1992**, *13*, 965–967.

(10) Bonhôte, P.; Dias, A.-P.; Papageorgiou, N.; Kalyanasundaram, K.; Grätzel, M. *Inorg. Chem.* **1996**, *35*, 1168–1178.

(11) Ohno, H.; Ito, K. *Chem. Lett*. **1998**, *27*, 751–752.

(12) Ye, C.; Liu, W.; Chen, Y.; Yu, L. *Chem. Commun.* **2001**, *21*, 2244–2245.

(13) Liang, C.; Yuan, C.-Y.; Warmack, R. J.; Barnes, C. E.; Dai, S. *Anal. Chem.* **2002**, *74*, 2172–2176.

(14) Abbott, A. P.; Capper, G.; Davies, D. L.; Rasheed, R. K.; Tambyrajah, V. *Chem. Commun.* **2003**, *1*, 70–71.

(15) Sakaebe, H.; Matsumoto, H. *Electrochem. Commun*. **2003**, *5*, 594–598.

(16) Wang, Q.; Baker, G. A.; Baker, S. N.; Colon, L. A. *Analyst* **2006**, *131*, 1000–1005.

(17) Marták, J.; Schlosser, Š.; Vlčková, S. *J. Membr. Sci*. **2008**, *318*, 298–310.

(18) Tao, F.; Song, H.; Chou, L. *Can. J. Chem*. **2010**, *89*, 83–87.

(19) Van Buu, O. N.; Aupoix, A.; Hong, N. D. T.; Vo-Thanh, G. *New J. Chem.* **2009**, *33*, 2060–2072.

(20) Ho, T. D.; Canestraro, A. J.; Anderson, J. L. *Anal. Chim. Acta.* **2011**, *695*, 18–43.

(21) Hernández-Fernández, F. J.; de los Ríos, A. P.; Lozano-Blanco, L. J.; Godínez, C. *J. Chem. Technol. Biotechnol.* **2010**, *85*, 1423–1435.

(22) Pauliukaite, R.; Doherty, A. P.; Murnaghan, K. D.; Brett, C. M. A. *Electroanalysis* **2008**, *20*, 485–490.

(23) Warke, I. J.; Patil, K. J.; Terdale, S. S. *J. Chem. Thermodyn.* **2016**, *93*, 101–114.

(24) Wang, C.; Luo, H.; Jiang, D.; Li, H.; Dai, S. *Angew. Chem. Int. Ed.* **2010**, *49*, 5978–5981.

(25) Cristiano, R.; Ma, K.; Pottanat, G.; Weiss, R. G. *J. Org. Chem.* **2009**, *74*, 9027–9033.

(26) Fraser, K. J.; MacFarlane, D. R. *Aust. J. Chem.* **2009**, *62*, 309–321.

(27) Rauhut, M. M.; Currier, H. A.; Semsel, A. M.; Wystrach, V. P. *J. Org. Chem.* **1961**, *26*, 5138–5145.

(28) Bradaric, C. J.; Downard, A.; Kennedy, C.; Robertson, A. J.; Zhou, Y. *Green Chem.* **2003**, *5*, 143–152.

(29) Tsurumaki, A.; Tajima, S.; Iwata, T.; Scrosati, B.; Ohno, H. *Electrochimica. Acta.* **2017**, *248*, 556–561.

(30) Yao, T.; Yao, S. *J. Chromatogr. A* **2017**, *1481*, 12–22.

(31) Shirvani, S.; Mallah, M. H.; Moosavian, M. A.; Safdari, *J. Chem. Eng. Res. Des.* **2016**, *109*, 108–115.

(32) Chatzimitakos, T.; Binellas, C.; Maidatsi, K.; Stalikas, C. *Anal. Chim. Acta.* **2016**, *910*, 53–59.

(33) Stoimenovski, J.; MacFarlane, D. R.; Bica, K.; Rogers, R. D. *Pharm. Res.* **2010**, *27*, 521–526.

(34) Ranke, J.; Stolte, S.; Störmann, R.; Arning, J.; Jastorff, B. *Chem. Rev.* **2007**, *107*, 2183–2206.

(35) Cornellas, A.; Perez, L.; Comelles, F.; Ribosa, I.; Manresa, A.; Garcia, M. T. *J. Colloid Interface Sci.* **2011**, *355*, 164–171.

(36) Wood, N.; Stephens, G. *Phys. Chem. Chem. Phys.* **2010**, *12*, 1670–1674.

(37) Sheldon, R. A. *Green Chem.* **2005**, *7*, 267–278.

(38) Breslow, R. A Fifty-Year Perspective on Chemistry in Water. In *Organic Reactions in Water: Principles, Strategies and Application*, Lindström U. M.; Blackwell Publishing Ltd.: Oxford, UK, 2007; 13–17.

(39) Guan, Y., Song. W., Hensen, E. J. M. Gold Clusters and Nanoparticles Stabilized by Nanoshaped Ceria in Catalysis. In *Catalysis by Materials with Well-Defined Structures*, Wu, Z.; Overbury, S. H.; Elsevier Inc.: Amsterdam, Netherlands, 2015, 127–132.

(40) Beyersdorff, T.; Schubert, T. J. S.; Biermann, U.; Pitner, W.; Abbott, A. P.; McKenzie, K. J.; Ryder, K. S. Synthesis of Ionic Liquids. In *Electrodeposition from Ionic Liquids*, Endress, F.; Abbott, A.; MacFarlane, D.; Wiley-VCH: Weinheim, Germany, 2008, 17–29.

(41) Stark, A. Ionic Liquid Structure-Induced Effects on Organic Reactions. In *Ionic Liquids*, Kirchner, B.; Springer: Berlin, Germany, 2010, pp 41-47.

(42) Uphade, B. S.; Akita, T.; Nakamura, T.; Haruta, M. *J. Catal.* **2002**, *209*, 331–340.

(43) Galvan, M.; Selva, M.; Perosa, A.; Noè, M. *Asian J. Org. Chem.* **2014**, *3*, 504–513.

(44) Yoo, K.; Deshpande, A.; Banerjee, S.; Dutta, P. *Electrochimica Acta* **2015**, *176*, 301–310.

(45) Usui, H.; Shimizu, M.; Sakaguchi, H. J. *Power Sources* **2013**, *235*, 29–35.

(46) Chen, X.; Li, Q.; Zhao, J.; Qiu, L.; Zhang, Y.; Sun, B.; Yan, F. *J. Power Sources* **2012**, *207*, 216–221.

(47) Lane, G. H. *Electrochimica. Acta.* **2012**, *83*, 513–528.

(48) Janiak, C. Z. *Für Naturforschung B* **2013**, *68*, 1059-1089.

(49) Hotze, E. M.; Phenrat, T.; Lowry, G. V. *J. Environ. Qual.* **2010**, *39*, 1909–1924.

(50) Luska, K. L.; Moores, A. *ChemCatChem* **2012**, *4*, 1534–1546.

(51) Dupont, J.; Fonseca, G. S.; Umpierre, A. P.; Fichtner, P. F. P.; Teixeira, S. R. *J. Am. Chem. Soc.* **2002**, *124*, 4228–4229.

(52) Luska, K. L.; Moores, A. *Green Chem.* **2012**, *14*, 1736–1742.

(53) Banerjee, A.; Theron, R.; Scott, R. W. J. *ChemSusChem* **2012**, *5*, 109–116.

(54) Richter, K.; Campbell, P. S.; Baecker, T.; Schimitzek, A.; Yaprak, D.; Mudring, A.-V. *Phys. Status Solidi.* **2013**, *250*, 1152–1164.

(55) Zhang, H.; Cui, H. *Langmuir* **2009**, *25*, 2604–2612.

(56) Kaushik, M.; Feng, Y.; Boyce, N.; Moores, A. Fe, Ru, and Os Nanoparticles. In *Nanocatalysis in Ionic Liquids*, Prechtl, M. H. G.; Wiley-VCH: Weinheim, Germany, 2016; 3–10.

(57) Lignier, P. Size Control of Monodisperse Metal Nanocrystals in Ionic Liquids. In *Ionic Liquids (ILs) in Organometallic Catalysis*, Dupont, J.; Kollar, L.; Springer: Berlin, Germany, 2015; 55–58.

(58) Prechtl, M. H. G.; Campbell, P. S.; Scholten, J. D.; Fraser, G. B.; Machado, G.; Santini, C. C.; Dupont, J.; Chauvin, Y. *Nanoscale* **2010**, *2*, 2601–2606.

(59) Migowski, P.; Teixeira, S. R.; Machado, G.; Alves, M. C. M.; Geshev, J.; Dupont, J. *Electron. Spectrosc. Struct. ICESS-10* **2007**, *156*, 195–199.

(60) Migowski, P.; Machado, G.; Texeira, S. R.; Alves, M. C. M.; Morais, J.; Traverse, A.; Dupont, J. *Phys. Chem. Chem. Phys.* **2007**, *9*, 4814–4821.

(61) Scholten, J. D.; Leal, B. C.; Dupont, J. *ACS Catal.* **2012**, *2*, 184–200.

(62) Maclennan, A.; Banerjee, A.; Scott, R. W. *Catal. Today.* **2013**, *207*, 170–179.

(63) Zawartka, W.; Trzeciak, A. M.; Ziółkowski, J. J.; Lis, T.; Ciunik, Z.; Pernak, J. *Adv. Synth. Catal.* **2006**, *348*, 1689–1698.

(64) Ullah, Z.; Man, Z.; Sada Khan, A. *ARPN J. Eng. Appl. Sci.* **2016**, *11*, 1653–1659.

(65) Chauvin, Y.; Mussmann, L.; Olivier, H. *Angew. Chem. Int. Ed. Engl.* **1996**, *34*, 2698–2700.

(66) Vollmer, C.; Redel, E.; Abu-Shandi, K.; Thomann, R.; Manyar, H.; Hardacre, C.; Janiak, C. *Chem. – Eur. J.* **2010**, *16*, 3849–3858.

(67) Yu, Y.; Sun, Q.; Liu, X.; Wu, H.; Zhou, T.; Shi, G. *Chem. – Eur. J.* **2011**, *17*, 11314–11323.

(68) Thanh, N. T. K.; Maclean, N.; Mahiddine, S. *Chem. Rev.* **2014**, *114*, 7610–7630.

(69) Katritzky, A. R.; Kuanar, M.; Stoyanova-Slavova, I. B.; Slavov, S. H.; Dobchev, D. A.; Karelson, M.; Acree, W. E. *J. Chem. Eng. Data* **2008**, *53*, 1085–1092.

(70) Clark, K. D.; Purslow, J. A.; Pierson, S. A.; Nacham, O.; Anderson, J. L. *Anal. Bioanal. Chem.* **2017**, *409*, 4983–4991.

(71) Rosatella, A. A.; Afonso, C. A. M. Metal-Catalyzed Oxidation of C–X (X = S, O) in Ionic Liquids. In *Ionic Liquids (ILs) in Organometallic Catalysis*, Dupont, J.; Kollar, L.; Springer: Berlin, Germany, 2015; 163–184.

(72) Shi, G.; Wang, Z.; Xia, J.; Bi, S.; Li, Y.; Zhang, F.; Xia, L.; Li, Y.; Xia, Y.; Xia, L. *Electrochimica. Acta.* **2014**, *142*, 167–172.

(73) Ding, K.; Liu, L.; Cao, Y.; Yan, X.; Wei, H.; Guo, Z. *Int. J. Hydrog. Energy* **2014**, *39*, 7326–7337.

(74) Restrepo, J.; Lozano, P.; Burguete, M. I.; García-Verdugo, E.; Luis, S. V. *Catal. Today* **2015**, *255*, 97–101.

(75) Migowski, P.; Dupont, J. *Chem. – Eur. J.* **2007**, *13*, 32–39.

(76) Ramalho, H. F.; di Ferreira, K. M. C.; Machado, P. M. A.; Oliveira, R. S.; Silva, L. P.; Prauchner, M. J.; Suarez, P. A. Z. *Ind. Crops Prod.* **2014**, *52*, 211–218.

(77) Bucsi, I.; Mastalir, Á.; Molnár, Á.; Juhász, K. L.; Kunfi, A. *Struct. Chem.* **2017**, *28*, 501–509.

(78) Gyton, M. R.; Cole, M. L.; Harper, J. B. *Chem. Commun.* **2011**, *47*, 9200–9202.

(79) McNulty, J.; Capretta, A.; Wilson, J.; Dyck, J.; Adjabeng, G.; Robertson, A. *Chem. Commun.* **2002**, *17*, 1986–1987.

(80) McLachlan, F.; Mathews, C. J.; Smith, P. J.; Welton, T. *Organometallics* **2003**, *22*, 5350–5357.

(81) Calò, V.; Nacci, A.; Monopoli, A.; Montingelli, F. *J. Org. Chem.* **2005**, *70*, 6040–6044.

(82) Kmentová, I.; Gotov, B.; Gajda, V.; Toma, Š. *Monatsh. Chem.* **2003**, *134*, 545–549.

(83) Bong Park, S.; Alper, H. *Chem. Commun.* **2004**, *11*, 1306–1307.

(84) Geldbach, T. J.; Zhao, D.; Castillo, N. C.; Laurenczy, G.; Weyershausen, B.; Dyson, P. J. *J. Am. Chem. Soc.* **2006**, *128*, 9773–9780.

(85) Zielinski, W.; Kukawka, R.; Maciejewski, H.; Smiglak, M. *Molecules* **2016**, *21*, 1203–1206.

(86) Banerjee, A.; Scott, R. W. J. *Green Chem*. **2015**, *17*, 1597–1604.

(87) Alper, E.; Yuksel Orhan, O. *Petroleum* **2017**, *3*, 109–126.

(88) Cadena, C.; Anthony, J. L.; Shah, J. K.; Morrow, T. I.; Brennecke, J. F.; Maginn, E. J. *J. Am. Chem. Soc.* **2004**, *126*, 5300.

(89) Ramdin, M.; de Loos, T. W.; Vlugt, T. J. H. *Ind. Eng. Chem. Res.* **2012**, *51*, 8149–8177.

(90) Sistla, Y. S.; Khanna, A. J. *Chem. Eng. Data* **2011**, *5*6, 4045–4060.

(91) Maiti, A. *ChemSusChem* **2009**, *2*, 628–631.

(92) Zhang, X.; Liu, Z.; Wang, W. *AIChE J.* **2008**, *54*, 2717–2728.

(93) Almantariotis, D.; Gefflaut, T.; Pádua, A. A. H.; Coxam, J.-Y.; Costa Gomes, M. F. *J. Phys. Chem. B* **2010**, *114*, 3608–3617.

(94) Shimoyama, Y.; Ito, A. *Fifth Mol. Thermodyn. Mol. Simul.* **2010**, *297*, 178–182.

(95) Ramdin, M.; Olasagasti, T. Z.; Vlugt, T. J. H.; de Loos, T. W. J. *Supercrit. Fluids* **2013**, *82*, 41–49.

(96) Modak, J. M. *Resonance* **2002**, *7*, 69–77.

(97) Hughes, M. D.; Xu, Y.-J.; Jenkins, P.; McMorn, P.; Landon, P.; Enache, D. I.; Carley, A. F.; Attard, G. A.; Hutchings, G. J.; King, F.; Stitt, E. H.; Johnston, P.; Griffin, K.; Kiely, C. J. *Nature* **2005**, *437*, 1132–1135.

(98) Fraile, J. M.; García, N.; Herrerías, C. I.; Mayoral, J. A. *Catal. Today* **2011**, *173*, 15–20.

(99) Dumbre, D. K.; Choudhary, V. R.; Patil, N. S.; Uphade, B. S.; Bhargava, S. K. J. *Colloid Interface Sci.* **2014**, *415*, 111–116.

(100) Liu, Y. Gold-Catalyzed Oxidation Reactions: Oxidation of Alkenes. In *Modern Gold Catalyzed Synthesis*, Hashmi, A. S. K., Toste, F. D.; Wiley-VCH: Weinheim, Germany, 2012; 263–272.

(101) Haruta, M.; Yamada, N.; Kobayashi, T.; Iijima, S. *J. Catal.* **1989**, *115*, 301–309.

(102) Quiñonero, D.; Musaev, D. G.; Morokuma, K. *Recent Adv. Theor. Underst. Catal.* **2009**, *903*, 115–122.

(103) Nijhuis, T. A.; Visser, T.; Weckhuysen, B. M. *J. Phys. Chem. B* **2005**, *109*, 19309–19319.

(104) Luo, L.; Yu, N.; Tan, R.; Jin, Y.; Yin, D.; Yin, D. *Catal. Lett.* **2009**, *130*, 489–495.

(105) Weissermel, K.; Arpe, H.-J. *Industrial Organic Chemistry*; Wiley-VCH: Weinheim, Germany, 2008; 59–89.

(106) Shaikh, A.-A. G.; Sivaram, S. *Chem. Rev.* **1996**, *96*, 951–976.

(107) Rana, S. V. S. *Environmental Pollution: Health and Toxicology*; Alpha Science International Ltd.: Oxford, UK, 2006; 171-174.

(108) Bartholomew, C. H. ; Farrauto, R. J. *Fundamentals of Industrial Catalytic Processes*; John Wiley & Sons Inc.: Hoboken, NJ, 2010; 632–634.

(109) Dai, W.; Luo, S.; Yin, S.; Au, C. *Front. Chem. Eng. China* **2010**, *4*, 163–171.

(110) Ramidi, P.; Munshi, P.; Gartia, Y.; Pulla, S.; Biris, A. S.; Paul, A.; Ghosh, A. *Chem. Phys. Lett.* **2011**, *512*, 273–277.

(111) Zhou, X.; Zhang, Y.; Yang, X.; Yao, J.; Wang, G. Chin. *J. Catal.* **2010**, *31*, 765–768.

(112) Darensbourg, D. J.; Lewis, S. J.; Rodgers, J. L.; Yarbrough, J. C. *Inorg. Chem.* **2003**, *42*, 581–589.

(113) Rulev, Y. A.; Larionov, V. A.; Lokutova, A. V.; Moskalenko, M. A.; Lependina, O. L.; Maleev, V. I.; North, M.; Belokon, Y. N. *ChemSusChem* **2016**, *9*, 216–222.

(114) Chen, A.; Chen, C.; Xiu, Y.; Liu, X.; Chen, J.; Guo, L.; Zhang, R.; Hou, Z. *Green Chem.* **2015**, *17*, 1842–1852.

(115) Gomes, C. R.; Ferreira, D. M.; Leopoldo Constantino, C. J.; Pérez González, E. R. *Tetrahedron Lett.* **2008**, *49*, 6879–6881.

(116) Srivastava, R.; Srinivas, D.; Ratnasamy, P. *Appl. Catal. Gen.* **2005**, *289*, 128–134.

(117) Wang, R.; Guo, X.; Wang, X.; Hao, *J. Catal. Lett.* **2003**, *90*, 57–63.

(118) Kinage, A. K.; Gupte, S. P.; Chaturvedi, R. K.; Chaudhari, R. V. *Catal. Commun.* **2008**, *9*, 1649–1655.

(119) Sarmah, B.; Srivastava, R. *Ind. Eng. Chem. Res.* **2017**, *56*, 8202–8215.

(120) Srivastava, R.; Srinivas, D.; Ratnasamy, P. *Catal. Lett.* **2003**, *91*, 133–139.

(121) Zheng, X.; Zhang, Q.; Guo, Y.; Zhan, W.; Guo, Y.; Wang, Y.; Lu, G. *J. Mol. Catal. Chem.* **2012**, *357*, 106–111.

(122) Kathalikkattil, A. C.; Roshan, R.; Tharun, J.; Soek, H.-G.; Ryu, H.-S.; Park, D.-W. *ChemCatChem* **2014**, *6*, 284–292.

(123) Guo, Z.; Liu, B.; Zhang, Q.; Deng, W.; Wang, Y.; Yang, Y. *Chem. Soc. Rev.* **2014**, *43*, 3480–3524.

(124) Fujita, S.-I.; Yoshida, H.; Liu, R.; Arai, M. Catalytic Transformation of CO_2 into Value-Added Organic Chemicals. In *New and future developments in catalysis*: *Activation of carbon dioxide*, Suib, S. L.; Elsivier: Amsterdam, Netherlands, 2013; 163–169.

(125) Jagtap, S. R.; Bhanushali, M. J.; Panda, A. G.; Bhanage, B. M. *Catal. Lett.* **2006**, *112*, 51–55.

(126) Wang, J.-Q.; Dong, K.; Cheng, W.-G.; Sun, J.; Zhang, S.-J. *Catal. Sci. Technol.* **2012**, *2*, 1480–1484.

(127) Zhao, Y.; Yao, C.; Chen, G.; Yuan, Q. *Green Chem***. 2013**, *15*, 446–452.

(128) Khoshro, H.; Zare, H. R.; Namazian, M.; Jafari, A. A.; Gorji, A. *Electrochimica Acta.* **2013**, *113*, 263–268.

(129) Kanakubo, M.; Makino, T.; Umecky, T. *J. Mol. Liq.* **2016**, *217*, 112–119.

(130) Lei, Z.; Dai, C.; Chen, B. *Chem. Rev.* **2014**, *114*, 1289–1326.

(131) Wu, S.-S.; Zhang, X.-W.; Dai, W.-L.; Yin, S.-F.; Li, W.-S.; Ren, Y.-Q.; Au, C.-T. *Appl. Catal. Gen.* **2008**, *341*, 106–111.

(132) Sun, J.; Wang, L.; Zhang, S.; Li, Z.; Zhang, X.; Dai, W.; Mori, R. *J. Mol. Catal. A: Chem.* ***2006,*** 256, 295–300.

(133) Sun, J.; Fujita, S.; Bhanage, B. M.; Arai, M. *Catal. Today* **2004**, *93*, 383–388.

(134) Sun, J.; Fujita, S.; Arai, M. *J. Organomet. Chem.* **2005**, *690*, 3490–3497.

(135) Bai, D.; Jing, H. *Green Chem.* **2010**, *12*, 39–41.

(136) Tangestaninejad, S.; Moghadam, M.; Mirkhani, V.; Mohammadpoor-Baltork, I.; Ghani, K. *Inorg. Chem. Commun.* **2008**, *11*, 270–274.

2.0 Alkene Epoxidation Catalyzed by Gold Nanoparticles Stabilized in Tetraalkylphosphonium Halide Ionic Liquids

Au NPs synthesized in tetraalkylphosphonium halide ILs via $LiBH_4$ reduction were characterized by UV-Vis spectroscopy and TEM microscopy. The NP/IL catalytic system was evaluated as a potential catalyst for alkene epoxidation, in which styrene and propylene act as substrates in this chapter. The influence of the reaction conditions, such as reaction time and temperature, as well as the use of $LiBH_4$ to ensure that the NPs do not get oxidized during the reaction, were examined.

2.1 Introduction

Epoxidation of alkenes is an important chemical reaction as the resultant epoxides are used as raw materials or intermediates for production of commercially valuable flavours, fragrances, paints, polymers, and pharmaceuticals substances.[1] Conventional synthesis of epoxides often involves peracids such as m-chloroperbenzoic acid, peroxybenzoic acid and peroxyacetic acid as oxidants, and acid waste as by-products, making it less environmentally friendly.[2] Also, peracids themselves are expensive, hazardous to handle, and not always completely selective toward epoxidation reactions.[3]

Current research focuses on the development of hydrogen peroxide (H_2O_2) and oxygen (O_2) as oxidants for alkene epoxidation as they can provide high content of active oxygen species and generate only water as a by-product.[4–6] However, neither H_2O_2 nor O_2 epoxidizes alkenes directly; thus, it is essential to find an efficient catalyst to activate these oxidants. Over the last few decades, soluble compounds of transition metals with good catalytic activity and product selectivity have been used to catalyze alkene epoxidations. These include but are not limited to: organometallic compounds and/or nanoparticles of platinum, titanium, palladium, manganese, molybdenum, and gold.[7–10] Among the catalysts tested, noble metal Au NPs catalysts have widely attracted attention as oxidation catalysts due to their resistance to oxidation and their ability to activate oxygen species.

Au was initially believed to be catalytically inactive toward hydrogenation and oxidation reactions for many years. However, after the pioneering work by Haruta and co-workers in which nanoscale Au particles was used toward CO oxidation,[11] it is now well-known that Au NPs below 5 nm in size are capable of catalyzing oxidation reactions efficiently at low temperatures.[12] Au-based catalysts also show high selectivity toward the target products, and are less prone to

over-oxidation and self-poisoning during selective oxidation reactions compared to the Pt- or Pd-based catalysts.[13,14] Metallic Au NPs, however, are thermodynamically unstable with respect to the bulk phase, thus need to be stabilized with supporting additives such as metal oxide and carbon supports.[15] Beside the traditional solid supports, there are also liquid stabilizers with unique physicochemical properties such as polymers, resins, and ionic liquids (ILs).[16,17] Among them, ILs offer outstanding possibilities as media for NP stabilization due to their unique properties such as negligible vapor pressure, high chemical and thermal stability, and easily modified structures to fit any desired task-specific applications.[18]

There are a number of reports in the literature where IL-stabilized Au NPs serve as active catalysts for the selective oxidation of alkenes.[19–21] However, only styrene (C_8H_8) epoxidation to styrene oxide (C_8H_8O), and propylene (C_3H_6) epoxidation to propylene oxide (C_3H_6O), will be covered here as these are the two reactions being studied during the course of this project. Styrene oxide (SO) is an industrially important organic intermediate used for production of fine chemicals and pharmaceuticals such as Flouxetine and Norflouxetine, diluting agents, flavoring agents, and ultraviolet absorbents.[22] Recently, a number of supported Au catalysts have been reported for the epoxidation of styrene using aqueous or anhydrous hydrogen peroxide such as TBHP or pure H_2O_2 adduct as an oxidizing agent.[23,24] Sharma et al., for example, reported the use of Au NPs in dendrimer@resin supports for selective oxidation of styrene that resulted in 95% conversion and 48% SO selectivity.[23] Liu et al. employed carbon nanotube-supported Au NPs as catalysts for styrene epoxidation, in which 78% conversion and 77% SO selectivity were obtained.[24]

Simple epoxides such as ethylene oxide and propylene oxide (PO) have been synthesized since the mid-1800s, but it was not until World War I that their values as chemical intermediates became commercially recognized.[25] Similar to SO, PO is an important and versatile intermediate

used in a large number of valuable consumer products, such as polyurethane, polyols, propylene glycol, cosmetics, and food emulsifiers.[25] The chlorohydrin or the Halcon (hydroperoxide) processes are often used to synthesized PO industrially.[26] The former process, unfortunately, yields environmentally unfriendly chlorinated organic by-products as well as calcium chloride, while the latter process requires heavy capital investment.[26] Supported Au NPs as catalysts for propylene epoxidation have been studied experimentally in the past due to their high selectivity for several oxidation reactions in both the liquid and gas phases; however, the conversions reported are still relatively low.[27–29]

In this chapter, Au NPs were synthesized directly in the trihexyl(tetradecyl)phosphonium chloride ([P66614][Cl]) IL via $LiBH_4$ reduction and in the absence of any organic solvents and external NP stabilizers. [P66614][Cl] was chosen because it is a liquid at room temperature and has been shown to stabilize Au NPs well.[30] The NP/IL catalytic system was used in styrene and propylene epoxidations with TBHP as an oxidant as it is more active toward alkene epoxidation than O_2,[31] and the conditions for the reactions such as reaction time and reaction temperature were examined. Although Au/[P66614][Cl] can catalyze alkene epoxidation, care has to be taken to prevent the oxidation of the Au NPs catalyst, which then lose their catalytic efficiency. Control reactions were also carried out to re-confirm the catalytic activity of Au NPs in IL.

2.2 Experimental

2.2.1 Materials

Hydrogen tetrachloroaurate trihydrate ($HAuCl_4 \cdot 3H_2O$, 99.9% on metal basis, Aldrich) was stored under vacuum and flushed with nitrogen after every use. Tert-butyl hydroperoxide (TBHP, 70 wt% in H_2O, Sigma-Aldrich), lithium borohydride ($LiBH_4$, 2.0 M in THF, Sigma-Aldrich),

styrene (99%, Sigma-Aldrich), tetraoctylammonium bromide (TOAB, ≥98%, Sigma-Aldrich), silver nitrate ($AgNO_3$, ≥99%, Sigma-Aldrich) were used as received. Propylene (C_3H_5, 99.5%) was purchased from Praxair and used as received. Commercial samples of the [P66614][Cl] IL were obtained from Cytec Industries Ltd. and used as received. Deuterated chloroform solvent was purchased from Cambridge Isotope Laboratories and used as received.

2.2.2 Synthesis of Gold Nanoparticles in Ionic Liquids

20.0 mg of $HAuCl_4 \cdot 3H_2O$ (equivalent to 0.0508 mmol of Au) was added to a 10.0 mL sample of [P66614][Cl] at 80 °C to give a pale golden yellow solution. The solution was cooled to 60 °C, and a stoichiometric excess of $LiBH_4$ reagent (1.5 mL, 2.0 M in THF) was injected drop-wise over a period of 5 mins (Scheme 2.1). The solution turned a dark purple colour then dark wine-red later upon the complete addition of $LiBH_4$, indicating formation of the Au NPs. The synthesized Au NPs solution was stored under nitrogen in capped vials until use.

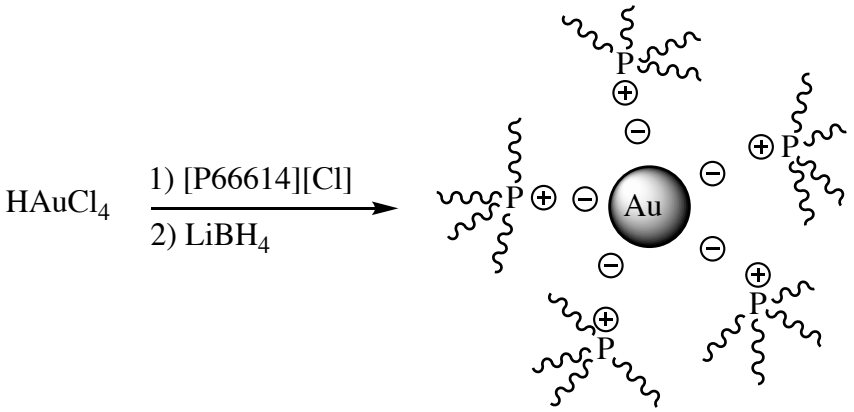

Scheme 2.1 Au NPs synthesized in [P66614][Cl].

2.2.3 Synthesis of Gold(I) Salts

The synthesis of (TOA)($AuCl_2$) was carried out via a two-step reaction by Goulet and Lennox,[32] in which (TOA)($AuCl_4$) was synthesized and used as starting material for the synthesis of the desired product (TOA)($AuCl_2$).

To synthesize (TOA)($AuCl_4$), anhydrous ethanol (500 mL) was used to dissolve a stoichiometric amount of $HAuCl_4$ (3.000 g) and TOAB (2.952 g). The solution was stirred for 30 mins and stored in the freezer overnight. The orange precipitate that formed, (TOA)($AuCl_4$), was recrystallized, filtered, washed with ice-cold ethanol, and dried under vacuum the next day. 2.000 g of (TOA)($AuCl_4$) was then partially dissolved in 20 mL anhydrous ethanol and heated to 70 ºC while stirring. Acetone (2.0 mL) was then added to this solution, with stirring, until the solution became colorless. The solution was allowed to cool slowly then stored in a freezer overnight. The white precipitate that formed, (TOA)($AuCl_2$), was recrystallized, filtered, washed with ice-cold ethanol, and dried under vacuum the next day. The metal salts were stored under vacuumed and flushed with nitrogen after every use.

2.2.4 Synthesis of Silver Nanoparticles in Ionic Liquids

8.5 mg of $AgNO_3$ (0.050 mmol) was added to a 10 mL sample of [P66614][Cl] under nitrogen at 80 ºC, with vigorous stirring until all the $AgNO_3$ dissolved. The solution was cooled to 50 ºC, and a stoichiometric excess of $LiBH_4$ reagent (1.5 mL, 2.0 M in THF) was injected drop-wise over a period of 5 mins. A brisk effervescence followed, and the entire solution turned deep yellowish-brown, indicating formation of the Ag NPs. After the addition of $LiBH_4$, volatile impurities were removed by vacuum-stripping the system at 80 ºC (Scheme 2.2). The synthesis

procedure above resulted in a 5.0 mM solution of Ag NPs in [P66614][Cl], and the obtained NP/IL composite was stored under nitrogen in capped vials wrapped with foil until use.

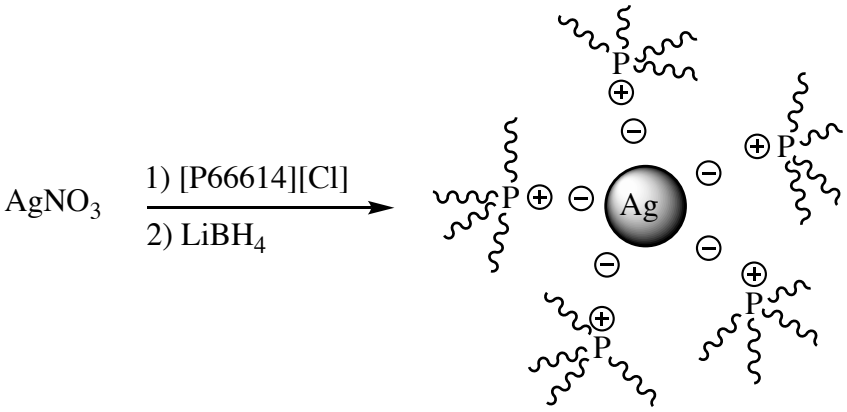

Scheme 2.2 Ag NPs synthesized in [P66614][Cl].

2.2.5 Synthesis of Styrene Oxide

The synthesis of SO from styrene and TBHP was done by following the procedure of Song et al. with a few modifications.[4] A mixture of styrene (0.6 mL, 5.24 mmol) and TBHP (1.9 mL, 19.7 mmol) were added into a stirred solution of 2.0 mL [P66614][Cl] containing 5.08 mM Au NPs at 80 °C to give a substrate:catalyst ratio of 514:1. After 15–30 mins, the original wine-red solution turned a pale yellow colour. The reaction was run for 4 h, and the final solution had a pale-yellow color. One drop of the solution was placed in deuterated chloroform for ^{1}H NMR characterization. Conversion and product distribution were determined using relative quantification of distinct ^{1}H NMR peaks. To ensure reproducibility, each reaction was performed at least three times, in which the conversion and product distribution for every reaction were found to vary by no more than ± 3–4%; and the reported values were an average of all reproducible trials. Figure 2.1 shows the individual peak assignment for styrene epoxidation catalyzed by Au NPs in [P66614][Cl]. **Styrene**: ^{1}H NMR (500 MHz, $CDCl_3$): 5.19 (d, 1H), 5.70 (d, 1H), 6.67 (m, 1H),

7.50–7.10 (m, 5H). **Styrene oxide**: ^{1}H NMR (500 MHz, $CDCl_3$): 2.76 (m, 1H), 3.10 (m, 1H), 3.82 (m, 1H), 7.29–7.35 (m, 5H). **Benzaldehyde**: ^{1}H NMR (500 MHz, $CDCl_3$): 7.99–8.01 (m, 5H), 9.97 (s, 1H). **Benzoic acid**: ^{1}H NMR (500 MHz, $CDCl_3$): 7.45–8.12 (m, 5H), 9.51 (s, broad, 1H). **Polystyrene**: ^{1}H NMR (500MHz, $CDCl_3$), δ ppm: 6.95–7.21 (broad, 3H), 4.87–5.45 (broad, 2H), 1.63–1.85 (broad, 1H), 0.93–1.25 (broad, 2H).

2.2.6 Attempted Synthesis of Propylene Oxide

1.63 mL of Au NPs in [P66614][Cl] (5.08 mM) was added to a 25.0 mL three-neck round bottom flask. One of the necks was connected to a reflux condenser, one was connected to a pressure meter and the other was connected to the propylene gas tank. Air was removed from the flask first by injecting a needle at the top of the reflux condenser and passing propylene through the flask for 1 min. The needle was removed, and the pressure was raised until it reached 0.5 MPa before closing the valve to obtain a closed system. The differential pressure was constant at this stage, indicating the absence of leaks. 1.54 mL of TBHP was then added slowly into the reaction flask over a period of 10 mins. The reaction was stirred vigorously for 4 h and the reaction was monitored using an Extech 407910 Heavy Duty Differential Pressure Manometer. Control studies were done without the oxidant/catalyst and the pressure stayed the same over an hour.

2.2.7 Characterization

UV-Vis spectra were obtained using a Varian Cary 50 Bio UV-Vis spectrometer with a scan range of 300–800 nm and an optical path length of 1.0 cm. TEM analysis of the synthesized Au NPs was conducted using a Hitachi HT7700 operating at 100 kV. The samples were prepared by ultrasonication of a 1% NP/IL solution in deuterated chloroform for 5 mins, followed by drop

casting onto a carbon-coated copper TEM grid (Electron Microscopy Sciences, Hatfield, PA). To determine the average particle size, a minimum of 100 particles were manually measured from several TEM images of the same sample using ImageJ. The standard deviation was calculated using the formula shown below:

$$Stdev = \sqrt{\frac{1}{N}\sum_{i=1}^{N}(x_i - \mu)^2}$$

where x_i is the individual particle size value, μ is the mean of all measured particle sizes, and N is the number of values used. ^{1}H NMR spectra were obtained using a Brüker Avance 500 MHz spectrometer, and the chemical shifts were referenced to the residual protons of the deuterated solvent.

2.2.8 Example Spectra for Conversion, Selectivity and TON Calculation

A

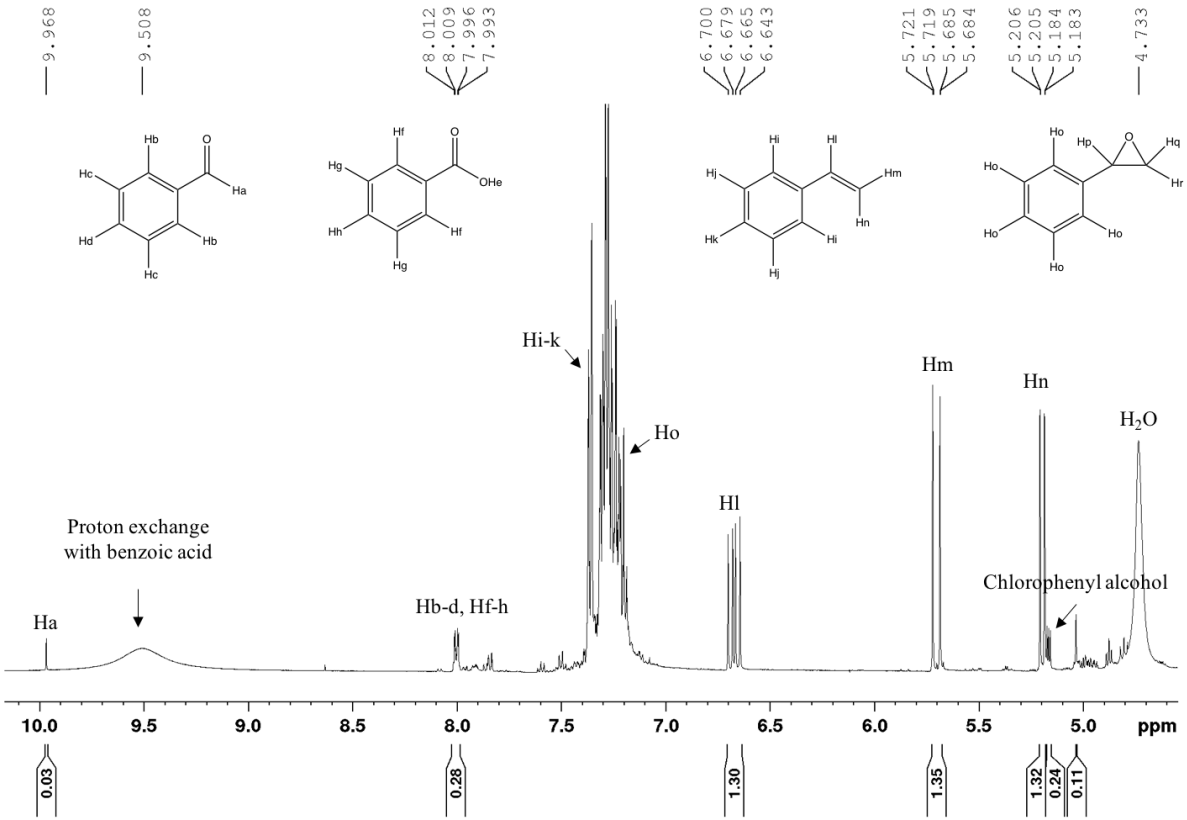

B

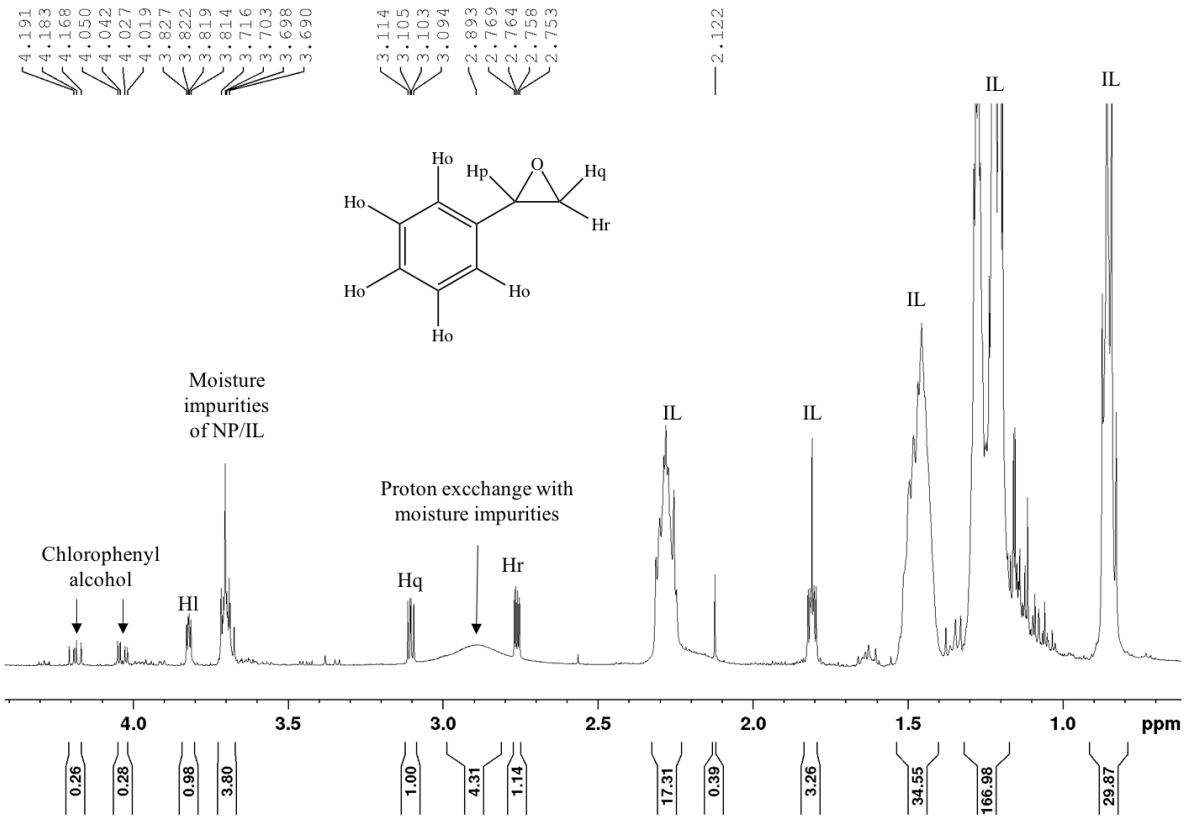

Figure 2.1 (a), (b) Styrene epoxidation catalyzed by Au/[P66614][Cl] with individual peak assignment. Reaction conditions used: styrene:Au mmol ratio of 5.24:0.0102, 0.1 MPa, 80 ºC and with re-addition of LiBH4 after 3 h during the 4 h of the reaction.

The conversions were calculated via relative quantization from the peak areas of individual, well-separated reactant and product peaks from ^{1}H NMR spectra. Sample calculations for SO conversion and selectivity are shown below. We believe that the peaks at 5.14, 4.15, and 4.01 ppm belong to 2-chloro-1-phenylethanol or an associated chlorophenyl alcohol compound as a result of the nucleophilic attack of SO by the IL chloride anions. For the purpose of conversion and selectivity calculations, all of the peaks were assigned to 1H which is consistent with the integrated area under the peaks.

$$\%\ \text{Conversion}$$

$$= \frac{\text{All products}}{\text{All products} + \text{all leftover reactants}}$$

$$= \frac{\text{Benzylaldehyde H} + \text{Benzoic acid H} + \text{SO H} + \text{Unk H}}{\text{Styrene H} + \text{Benzylaldehyde H} + \text{Benzoic Acid H} + \text{SO H} + \text{Unk H}} \times 100\%$$

$$= \frac{0.03 + 0.03 + 1.15 + 0.22}{0.99 + 0.03 + 0.03 + 1.15 + 0.22} \times 100\%$$

$$= 59\ \%$$

$$\text{Selectivity} = \frac{\text{Desired product}}{\text{All products}} \times 100\%$$

$$\text{TON} = \frac{\text{mmol SO}}{\text{mmol Au}} = \frac{\text{mmol of styrene} \times \%\ \text{conversion}}{\text{mmol Au}}$$

2.3 Results & Discussion

This study explored the effect of temperature on the formation of epoxides and the efficiency of the reaction when the oxidized Au NPs catalysts were recovered upon re-addition of a reducing agent $LiBH_4$. Control reactions were also carried out to re-confirm the catalytic activity of the Au NPs synthesized in the [P66614][Cl] IL.

2.3.1 Characterization of Gold Nanoparticles in [P66614][Cl]

Au NPs of the size range from 2–4 nm were found to be effective catalysts for the epoxidation of various alkenes such as propene, octane, and styrene.[12] The [P66614][Cl] IL, on the other hand, is well known to stabilize metal NPs dispersion and facilitate their synthesis in the size range of 3–5 nm.[33] Last but not least, the resulting colloidal NPs have found to be stable ranging from days to months previously in our group.[30]

Au NPs were formed in ILs upon reducing the Au salts with $LiBH_4$, without the involvement of any organic solvents or secondary stabilizers. Since the [P66614][Cl] IL is moderately viscous at room temperature, cooling the product led to highly viscous system; however, the viscosity was found to reduce drastically upon heating. To confirm the formation of Au NPs and determine the NP size, the colloidal NP/IL solution was examined using UV-Vis absorbance spectroscopy and TEM. Figure 2.2a and Figure 2.2b show the UV-Vis spectra and TEM image of the synthesized Au NPs respectively. The absorbance peak in the UV-Vis spectra, also known as the surface plasmon resonance peak, was recorded at λ = 520 nm. This was in agreement with TEM results, in which the average size of NPs was found to be 4.1 ± 0.2 nm (Figure 2.2c). The synthesized NPs were found to be in the same size range as seen in previous work by our group.[30]

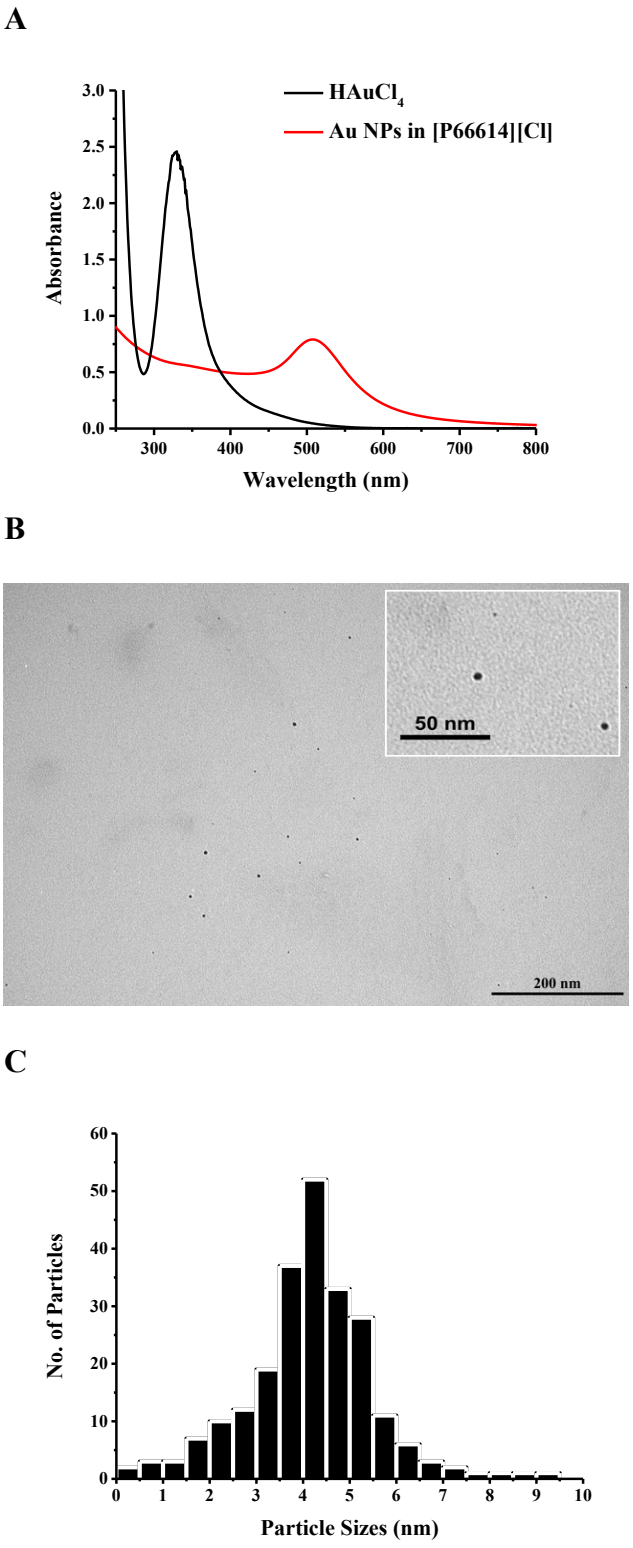

Figure 2.2 (a) UV-Vis spectra; (b) TEM image and (c) Size distribution of Au NPs synthesized in [P66614][Cl].

2.3.2 Styrene Epoxidation

Oxidation of styrene **(1)** in Au/[P66614][Cl] using anhydrous TBHP as an oxidant yielded SO **(2)** as a major product in every case, along with benzaldehyde (BA1) **(3)** and benzoic acid (BA2) **(4)** as by-products (Scheme 2.3). This reaction also yielded a racemic product (i.e. (S)-SO and (R)-SO) due to the chiral α-carbon of styrene. The NP/IL catalyst tested from different batches presented minor variations in conversion and product selectivity.

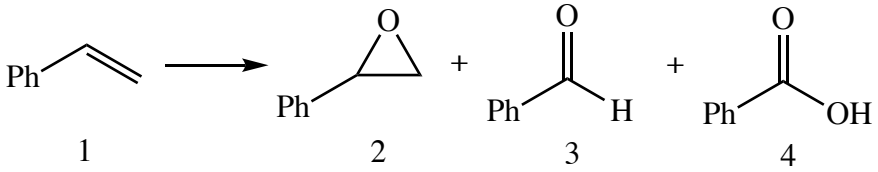

Scheme 2.3 Potential Products for Styrene Epoxidation.

When there is an excess amount of chloride ions presented in the solution, a nucleophilic attack of SO by the IL chloride anion can occur, and a by-product that could be either 2-chloro-1-phenylethanol or an associated chlorophenyl alcohol is formed. There was evidence in the ^{1}H NMR spectra for this. In particular, the peaks at 5.14, 4.15, and 4.01 ppm in ^{1}H NMR spectra have chemical shifts and splitting patterns consistent with this assignment. The boiling point of 2-chloro-1-phenylethanol is about 110−112 °C, which is consistent with the fact that this product remained in the product flask after vacuum stripping at 100 ºC. GC-MS showed molecular ion peaks at 105 and 77 m/z, which are very similar to the 107 and 77 m/z molecular ion peaks of the hypothesized 2-chloro-1-phenylethanol. No alternative by-products we could think of or those reported in literature fitted well with the obtained data.

2.3.2.1 Effect of Temperature

Since the [P66614][Cl] IL is used as the solvent for styrene epoxidation, it is very desirable to heat up the reaction to reduce the high viscosity of the IL itself, thus minimizing possible mass-transfer issues. The reaction was tested at 40 °C initially by following the procedure outline by Song et al.;[4] however, there was little to no epoxide formed even after 10 h. Hence, the reaction temperature was decided to raise in 10 °C increments. Table 2.1 shows the conversion, product distributions, and TON values of Au NPs in [P66614][Cl] at atmospheric pressure from 40 °C to 90 °C in 4 h. As the temperature increased, the conversion of styrene also started to rise to 45% and 50% at 70 °C and 80 °C, respectively, which work out to TON values of 233 and 258. At 80 °C, the reaction reached the highest conversion and was remained roughly constant from 80 °C to 90 °C.

Table 2.1 Styrene epoxidation catalyzed by Au NPs in [P66614][Cl] over 4 h.

Entry[a]	Temp.	Conversion[b] (%)	Selectivity (%)[b]					TON[b]
			SO	BA1	BA2	Chlorophenyl-OH	PS	
1	70 °C	45	70	5	4	21	0	233
2	80 °C	50	75	2	2	21	0	258
3	90 °C	50	70	2	2	21	5	258

[a] Reaction conditions: 5.24 mmol styrene: 0.0102 mmol Au:19.7 mmol TBHP, 0.1 MPa pressure.

[b] Conversion, product selectivity, TON (see Experimental 2.2.5 for reproducibility discussion Experimental 2.2.8 for sample calculation).

A side reaction, however, was found to occur when the reaction temperature went above 80 °C as a white crystalline solid was formed at the bottom of the reaction flask, which later on was determined to be polystyrene (PS) (Figure 2.3). In conclusion, 80 °C was the optimized temperature for the styrene epoxidation reaction and increasing the reaction temperature has a pronounced positive effect on the reaction conversion, resulting in an increase of catalytic activity. Also, this temperature was found to work well for the same reaction using Au_{25} clusters on SiO_2 calcined at 250 °C (TON = 3000).[34]

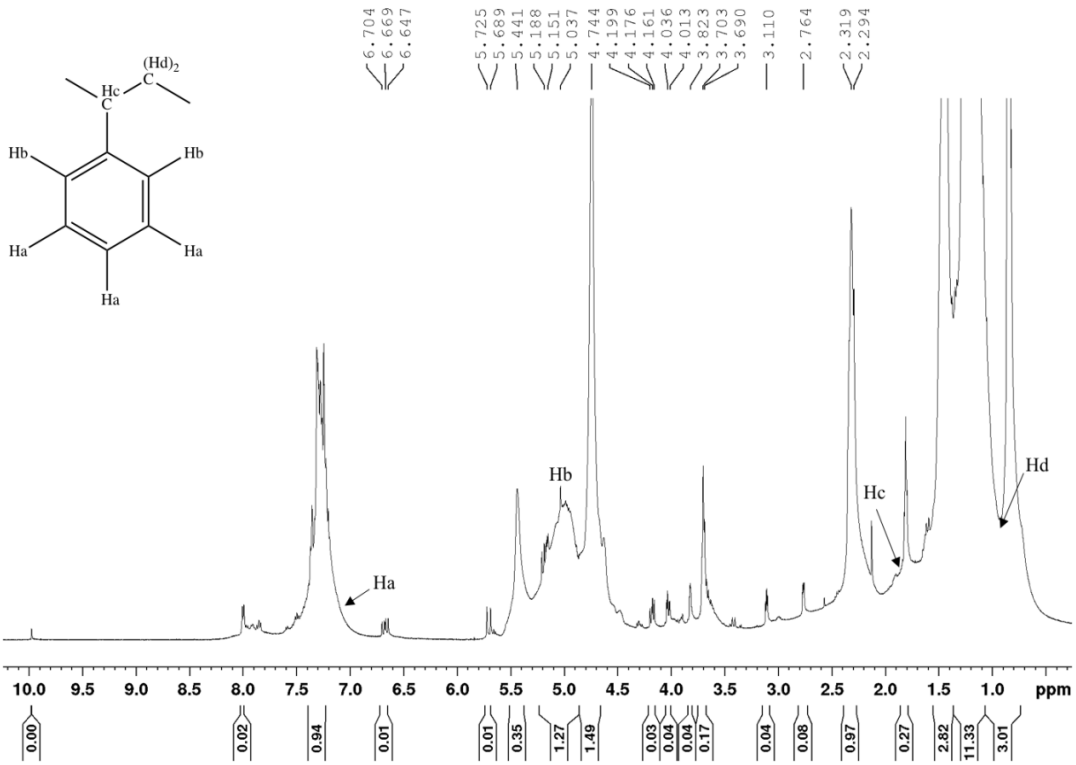

Figure 2.3 ^{1}H NMR spectra of PS as a side-product for styrene epoxidation. Please note that only polystyrene is being labelled here, other peaks are due to styrene, SO, BA1, BA2, chlorophenyl alcohol, and [P66614][Cl].

2.3.2.2 Effect of Lithium Borohydride on Gold Nanoparticles Recovery

Under air and at elevated temperature, Au NPs in [P66614][Cl] shows a very slow aerial oxidation as the red Au(0) system turned colourless, then pale yellow. This is likely due to oxidative etching of gold assisted by halide absorption on the surface, leading to the formation of Au(I) and Au(III) salts.[30] To avoid this, $LiBH_4$ was re-added to the reaction flask to re-reduce the oxidized Au NPs during the reaction. Table 2.2 shows the obtained conversions and TON values of styrene to SO with re-addition of $LiBH_4$ at various points: after 1 h, 2 h, and 3 h during the 4 h reaction. These values were also compared with the results above in which no attempt was made to re-reduce the oxidized Au catalyst, and re-addition of $LiBH_4$ after 3 h of the reaction produced the highest TON for this reaction. This shows that the Au NPs oxidation is a slow process, and that enhanced TONs for this reaction can be achieved by re-reducing the catalyst during the reaction.

Table 2.2 Styrene epoxidation catalyzed by NP/IL with re-addition of $LiBH_4$.

Entry[a]	Re-addition of $LiBH_4$	Conversion (%)[b]	Selectivity (%)[b]				TON[b]
			SO	BA1	BA2	Chlorophenyl-OH	
1	No $LiBH_4$	50	75	2	2	21	258
2	After 1 h	53	76	2	2	20	274
3	After 2 h	57	78	2	2	18	295
4	After 3 h	60	80	2	2	16	310
5	After 3.5 h	60	80	2	2	16	310

[a] Reaction conditions: 5.24 mmol substrate: 0.0102 mmol Au; 0.1 MPa, 80 ºC, and 4 h.

[b] Conversion, product selectivity, and TON (see Experimental 2.2.5 for reproducibility discussion and Experimental 2.2.8 for sample calculation).

2.3.2.3 Control Reaction with Gold(I) Salts

Au(I) salts were prepared via a two-step reaction. The first step involved an ion exchange between $HAuCl_4$ and the stabilizing agent TOAB, giving $(TOA)(AuCl_4)$ as the product. $(TOA)(AuCl_4)$ was then dried, purified, and re-dissolved for the subsequent reduction step, from $(TOA)(AuCl_4)$ to $(TOA)(AuCl_2)$ in which acetone functioned as a reducing agent. The reduction of Au^{3+} to Au^{1+} was confirmed by monitoring the disappearance of the 340 nm peak absorption band of the Au^{3+}, with the solution going from intense orange to colourless (Figure 2.4).

Control reactions were carried out with just the substrates to further confirm the role of Au NPs as catalysts for styrene epoxidation: TBHP and styrene only; TBHP, styrene and $LiBH_4$ in the presence and absence of Au(III) salts, or TBHP, styrene and Au(I) salts. Among the tested reactants, only the Au(III) salts in IL showed SO formation, though the conversion was significantly lower (5.0%). This may be due to the formation of Au NPs in situ during the reaction.

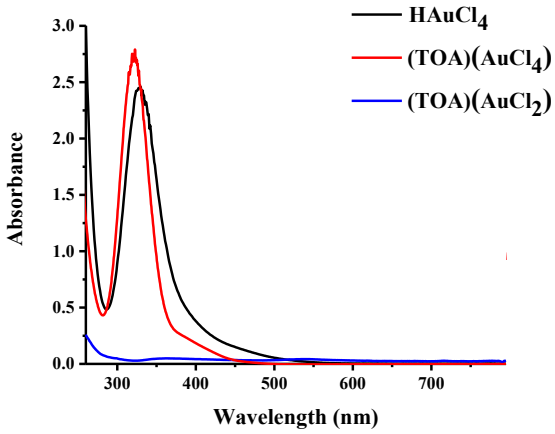

Figure 2.4 UV-Vis absorbance spectrum of $HAuCl_4$, $(TOA)(AuCl_4)$, and $(TOA)(AuCl_2)$.

2.3.3 Propylene Epoxidation

Since the Au/[P66614][Cl] system worked well as the catalyst for styrene epoxidation, it was then examined for propylene epoxidation with the hope that it would help the reaction to reach the commonly accepted standard for economic sustainability: 70% PO selectivity and 10% propylene conversion (i.e. 7% PO yield).[35]

Unlike styrene epoxidation where styrene is already in its liquid state, propylene is in gas state at room temperature. Also, the desired product PO is colorless, highly flammable and has a low boiling point (34 ºC),[36] thus making the reaction set-up more difficult compared to styrene epoxidation.

2.3.3.1 Effect of Pressure

A closed system for propylene epoxidation was constructed and the reaction was monitored using a pressure meter. When the reaction was run under atmospheric pressure, no product was obtained; thus, a pressure of 0.5 MPa was applied as this is the highest pressure the 25 mL three-neck round bottom flask is able to withstand. The ideal gas law was used to calculate the amount of propylene in the flask (Equation 2.1). From there, a stoichiometric amount of TBHP and NP/IL were determined.

$$n_{PO} = \frac{V_{PO} \times P}{RT} = \frac{(25.0\ \text{L})(0.5\ \text{MPa})}{(8.31 \text{cm}^3 \text{MPa K}^{-1}\text{mol}^{-1})(353.15\text{K})} = 4.24 \times 10^{-3} \text{mol} \qquad (2.1)$$

The pressure of propylene decreased over the 4 h of the reaction, indicating the possible reaction of propylene with TBHP over the Au NPs in ILs (Figure 2.5). However, upon checking the ^{1}H NMR spectra, there was no peaks corresponding to PO found, which might be due to the low boiling point of PO (34 ºC). The final solution, therefore, was cooled down with an ice bath but no product was obtained upon checking the ^{1}H NMR spectra. The reaction was then set up in

a way so that the products were condensed in a product flask using a dry ice/acetone bath and later on a liquid nitrogen trap was employed to produce a larger temperature difference (80 ºC for reaction flask vs -78 ºC for the product flask). Unfortunately, no PO or other product peaks were seen upon analyzing ^{1}H NMR spectra. Despite the absence of the recoverable products, we are still uncertain why a pressure decay was seen in the flask.

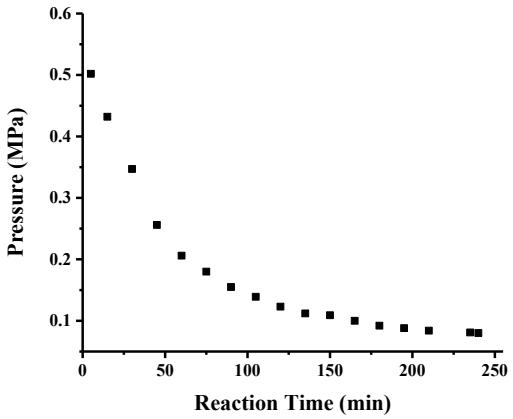

Figure 2.5 Reduction in pressure over time for propylene epoxidation.

2.3.3.2 Silver Nanoparticles in [P66614][Cl] as Catalysts

Ag NPs in [P66614][Cl] was also examined as catalysts for the propylene epoxidation reaction since Ag-based catalysts are known to be successful toward ethylene epoxidation to ethylene oxide.[37] Although several groups have reported optimistic results, low PO selectivity with potential combustion due to the propylene allylic hydrogen abstraction by an adsorbed neighboring oxygen on the Ag surface was also reported.[38,39] Wang et al. used Ag supported on titanium silicalite zeolite as catalysts for propylene epoxidation in the presence of oxygen and hydrogen, resulting in 1.0% conversion and 91% selectivity toward PO.[38] Zheng et al. reported the use of

bimetallic catalytic system of supported Ag_{95}–$Cu_5/BaCO_3$ with a conversion of 3.6% and a selectivity of 55% toward PO.[39]

Ag NPs were synthesized directly in [P66614][Cl] using the previously established procedure in our group (Figure 2.6),[40] and the reaction was done under the tested conditions for styrene epoxidation. No ^{1}H NMR peaks corresponding to PO were seen, even when the reaction was allowed to run for a longer period of time (i.e. 6 and 8 h instead of just 4 h). This might be because the pressure was not high enough for substantial amounts of the propylene gas to dissolve into the liquid phase (i.e. a mass-transfer problem); and therefore, less propylene molecules are available for reaction over the Au or Ag NP catalyst surfaces. At this stage, we decided to stop going toward this direction due to safety considerations: we did not want to have a flammable reagent, propylene, and an oxidizing reagent, TBHP, in the same reactor under even higher pressures and temperatures.

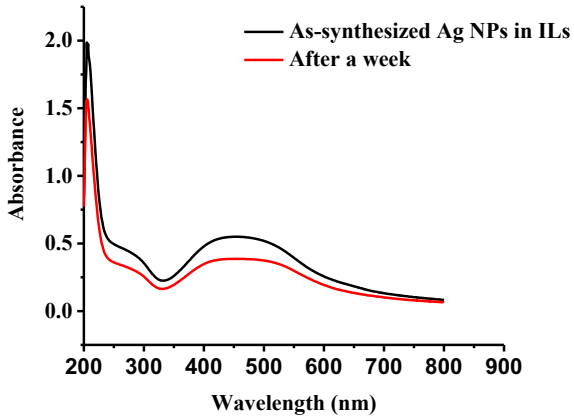

Figure 2.6 UV-Vis spectra of the synthesized Ag NPs in ILs.

2.4 Conclusions

Au NPs in [P66614][Cl] were successfully synthesized and characterized by UV-Vis absorption and TEM. UV-Vis absorbance spectra showed an absorbance peak at 520 nm, which was in agreement with an average size of 4.1 ± 0.2 nm obtained from the TEM images. The Au/[P66614][Cl] system was then used for styrene epoxidation with TBHP as an oxidant, and SO was yielded as a major product in every case. The reaction was tested at 5.24 mmol styrene:0.0102 mmol Au, 0.1 MPa, and from 40–90 ºC for 4 h. It was discovered that heating up the reaction to 80 ºC produced the highest conversion, while polystyrene as a side-product started to form when the temperature went above 80 ºC. The TON values increased sharply from 233 to 258 with an increase in temperature from 70 to 80 ºC and remained roughly the same after that. This suggests an increase in reaction temperature results in a positive effect on the reaction conversion and the catalytic activity of the catalyst. Control reactions were also carried out, and only Au(III) salt reactions showed minimal styrene oxide formation. After optimizing the temperature for styrene epoxidation, recovery of oxidized Au NPs was attempted by re-addition of $LiBH_4$ after an h, 2 h, 3 h, and 3.5 h during the 4 h of the reaction. The conversions were improved and re-addition of $LiBH_4$ after 3 h during the 4 h reaction showed the highest overall conversion (60%) as the Au oxidation is a very slow process.

Although these reaction conditions worked very well for styrene epoxidation, they did not work when propylene was used as the starting material. Modifications of the reaction conditions were attempted such as raising the reaction pressure, lengthening the reaction time, and condensing the product using either an ice bath, a dry ice/acetone bath or a liquid nitrogen trap to capture the desired product PO. Unfortunately, no PO peaks were observed by ^1H NMR. Ag NPs catalysts were also examined, and no PO was found using that catalytic system either.

2.5 References

(1) Mohammed, M. L.; Patel, D.; Mbeleck, R.; Niyogi, D.; Sherrington, D. C.; Saha, B. *Appl. Catal. Gen.* **2013**, *466*, 142–152.

(2) Dumbre, D. K.; Choudhary, V. R.; Patil, N. S.; Uphade, B. S.; Bhargava, S. K. *J. Colloid Interface Sci.* **2014**, *415*, 111–116.

(3) Ranieri, B.; Escofet, I.; Echavarren, A. M. *Org. Biomol. Chem.* **2015**, *13*, 7103–7118.

(4) Song, J.; Zhang, Z.; Jiang, T.; Hu, S.; Li, W.; Xie, Y.; Han, B. *J. Mol. Catal. Chem.* **2008**, *279*, 235–238.

(5) Calvente, R. M.; Campos-Martin, J. M.; Fierro, J. L. G. *Catal. Commun.* **2002**, *3*, 247–251.

(6) Kotov, St. V.; Balbolov, E. *J. Mol. Catal. Chem.* **2001**, *176*, 41–48.

(7) Quiñonero, D.; Musaev, D. G.; Morokuma, K. *Recent Adv. Theor. Underst. Catal.* **2009**, *903*, 115–122.

(8) Irina P Beletskaya. *Russ. Chem. Rev.* **2010**, *79*, 441–461.

(9) Liu, Y.; Tsunoyama, H.; Akita, T.; Tsukuda, T. *Chem. Commun.* **2010**, *46*, 550–552.

(10) Zhang, H.; Cui, H. *Langmuir* **2009**, *25*, 2604–2612.

(11) Haruta, M.; Yamada, N.; Kobayashi, T.; Iijima, S. *J. Catal.* **1989**, *115*, 301–309.

(12) Della Pina, C.; Falletta, E.; Prati, L.; Rossi, M. *Chem. Soc. Rev.* **2008**, *37*, 2077–2095.

(13) Bawaked, S.; He, Q.; Dummer, N. F.; Carley, A. F.; Knight, D. W.; Bethell, D.; Kiely, C. J.; Hutchings, G. J. *Catal. Sci. Technol.* **2011**, *1*, 747.

(14) Shi, G.; Wang, Z.; Xia, J.; Bi, S.; Li, Y.; Zhang, F.; Xia, L.; Li, Y.; Xia, Y.; Xia, L. *Electrochimica. Acta.* **2014**, *142*, 167–172.

(15) Banerjee, A.; Theron, R.; Scott, R. W. J. *Chem. Commun.* **2013**, *49*, 3227–3229.

(16) Sinha, A. K.; Seelan, S.; Tsubota, S.; Haruta, M. *Angew. Chem. Int. Ed.* **2004**, *43*, 1546–1548.

(17) Mu, X.; Meng, J.; Li, Z.-C.; Kou, Y. *J. Am. Chem. Soc.* **2005**, *127*, 9694–9695.

(18) Ameta, S.; Ameta, R. *Green Chemistry: Fundamentals and Applications*; Apple Academic Press Inc.: New York, 2013; 45–49.

(19) Tsuda, T.; Kondo, K.; Tomioka, T.; Takahashi, Y.; Matsumoto, H.; Kuwabata, S.; Hussey, C. L. *Angew. Chem. Int. Ed.* **2011**, *50*, 1310–1313.

(20) Bravo-Suárez, J. J.; Bando, K. K.; Lu, J.; Fujitani, T.; Oyama, S. T. *J. Catal.* **2008**, *255*, 114–126.

(21) Restrepo, J.; Lozano, P.; Burguete, M. I.; García-Verdugo, E.; Luis, S. V. *Cat. Today* **2015**, *255*, 97–101.

(22) Kathalikkattil, A. C.; Roshan, R.; Tharun, J.; Soek, H.-G.; Ryu, H.-S.; Park, D.-W. *ChemCatChem* **2014**, *6*, 284–292.

(23) Sharma, A. S.; Shah, D.; Kaur, H. *RSC Adv.* **2015**, *5*, 42935–42941.

(24) Liu, J.; Wang, F.; Xu, T.; Gu, Z. *Catal. Lett.* **2010**, *134*, 51–55.

(25) Seubsai, A.; Kahn, M.; Senkan, S. *ChemCatChem* **2011**, *3*, 174–179.

(26) Turner, C. H.; Ji, J.; Lu, Z.; Lei, Y. *Chem. Eng. Sci.* **2017**, *174*, 229–237.

(27) Zhu, W.; Zhang, Q.; Wang, Y. *J. Phys. Chem. C* **2008**, *112*, 7731–7734.

(28) Su, W.; Wang, S.; Ying, P.; Feng, Z.; Li, C. *J. Catal.* **2009**, *268*, 165–174.

(29) Zohour, B.; Noon, D.; Seubsai, A.; Senkan, S. *Ind. Eng. Chem. Res.* **2014**, *53*, 6243–6248.

(30) Banerjee, A.; Theron, R.; Scott, R. W. J. *ChemSusChem* **2012**, *5*, 109–116.

(31) Guo, Z.; Liu, B.; Zhang, Q.; Deng, W.; Wang, Y.; Yang, Y. *Chem. Soc. Rev.* **2014**, *43*, 3480–3524.

(32) Goulet, P. J. G.; Lennox, R. B. *J. Am. Chem. Soc.* **2010**, *132*, 9582–9584.

(33) Uphade, B. S.; Akita, T.; Nakamura, T.; Haruta, M. *J. Catal.* **2002**, *209*, 331–340.

(34) Sudheeshkumar, V.; Shivhare, A.; Scott, R. W. J. *Catal Sci Technol* **2017**, *7*, 272–280.

(35) Phon-in, P.; Seubsai, A.; Chukeaw, T.; Charoen, K.; Donphai, W.; Prapainainar, P.; Chareonpanich, M.; Noon, D.; Zohour, B.; Senkan, S. *Catal. Commun.* **2016**, *86*, 143–147.

(36) Bedolla-Pantoja, M. Investigation of Silver Catalyst for Propylene Epoxidation: Promotion and Reaction Mechanism. MSc Thesis, University of Delaware, 2010.

(37) Ozbek, M. O.; Onal, I.; van Santen, R. A. *Mol. Approach Heterog. Catal.* **2011**, *284*, 230–235.

(38) Wang, R.; Guo, X.; Wang, X.; Hao, J. *Catal. Lett.* **2003**, *90*, 57–63.

(39) Zheng, X.; Zhang, Q.; Guo, Y.; Zhan, W.; Guo, Y.; Wang, Y.; Lu, G. *J. Mol. Catal. Chem.* **2012**, *357*, 106–111.

(40) Banerjee, A.; Theron, R.; Scott, R. W. J. *J Mol. Catal. A: Chem.* **2014**, *393*, 105–111.

3.0 Cycloaddition of CO_2 to Epoxides Catalyzed by Ionic Liquid Halide Anions

Following Chapter 2 work, the reaction conditions of the subsequent reaction, cycloaddition of CO_2 to epoxides, in which tetraalkylphosphonium halide ILs function as the catalyst (via the halide nucleophile) was examined. It was found that the reaction followed pseudo-first order kinetics with respect to CO_2, and increasing in pressure led to an increase in the reaction conversions and rates. Also, stirring the system at 600 rpm helped to take the reaction out of the mass-transfer limiting range.

3.1 Introduction

As the annual consumption of fossil fuels continues to rise as a result of increasing in market demand, more CO_2 is being produced, thus making global warming one of the most difficult challenges facing the human race in the 21st century.[1] Hence, it is highly desirable to develop carbon capture and storage techniques that can mitigate CO_2 emissions. Conventional methods involve concentrating/compressing CO_2 to store it either in disused oil/gas wells or in the ocean; however, these methods are often labour intensive and time consuming.[2] An alternative way to store CO_2 is to use it as the building block for commercially-significant chemicals, such as cyclic carbonates.[3,4]

Cyclic carbonates are manufactured industrially by an interfacial phosgene process, which is not an environmentally benign method as phosgene is poisonous in its gas state.[5] Producing cyclic carbonates by incorporating CO_2 to epoxides, therefore, is a more promising route as CO_2 is a renewable, abundant, and cheap resource. However, a high energetic barrier needs to be overcome for CO_2 to be successfully activated as CO_2 is thermodynamically and kinetically stable due to the high oxidation state of the carbon (C^{4+}).[6] High temperatures are often required to overcome the activation barrier and endothermic reactions, while high pressures are used to increase CO_2 saturation within the reaction media by increasing the solubility of the CO_2 to the liquid phase.[7] Unfortunately, the higher the temperature, the lower the CO_2 solubility in the reaction media according to Henry's law;[8] hence, catalysts are needed for CO_2 conversion to limit the temperatures required for the reaction.[9] Nucleophilic catalysts, for example, are often used for cyclic carbonate formation at high pressures ranging from 1.1 MPa to 2.5 MPa CO_2.[10] Only a few papers report cyclic carbonate formation at atmospheric pressure.[11]

CO_2 capture by absorption in ionic liquids (ILs) -based solvents have been widely studied in literature, making them a suitable media for the cycloaddition of CO_2 to epoxides (Figure 3.1).[12] Generally, it is the anions that are modulated to increase CO_2 absorption.[13] Fluorinated anions, for example, are especially adept at increasing CO_2 solubility compared to non-fluorinated anions.[13] The nature of the cations, on the other hand, also play a part in CO_2 solubility, though it was found to be a secondary factor compared to the impact of the anion.[13] Carvalho and Coutinho reported that the solubility of CO_2 in phosphonium ILs can be substantially larger than in imidazolium-based ILs.[14] Gomes et al. later on noted that CO_2 was more soluble in phosphonium- and pyrrolidium-based ILs compared to ethane and nitrogen gases when the anion was held constant as tris(pentafluoroethyl)trifluorophoshate.[15] Increasing the molecular weight of the ILs by increasing the alkyl chain length on the cation was found to improve CO_2 absorption as well.[16]

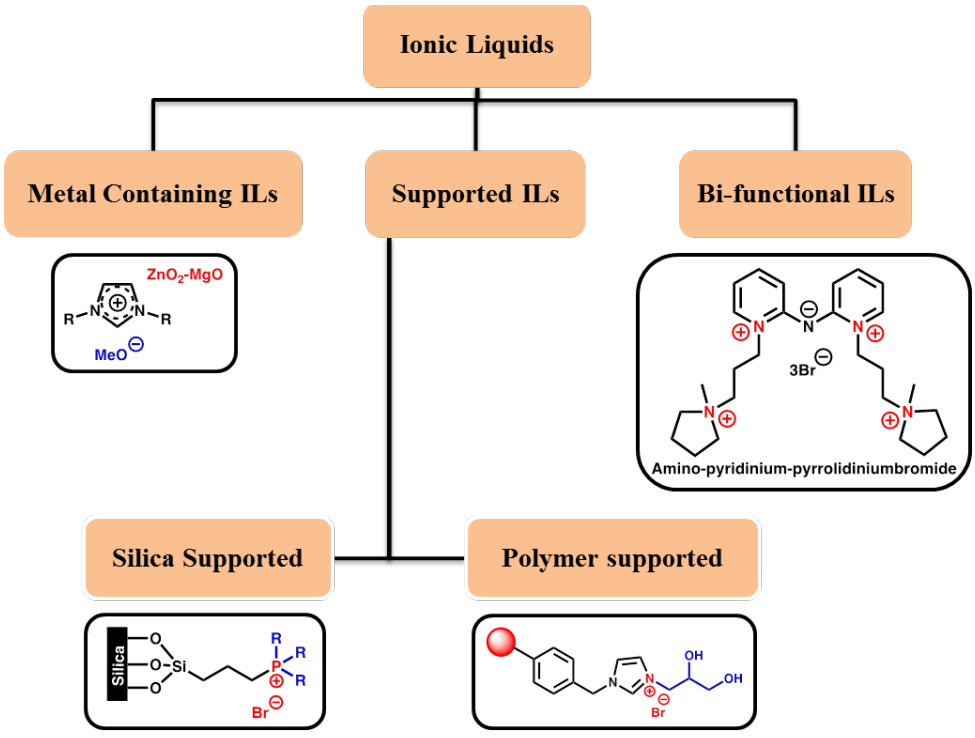

Figure 3.1 ILs used in the cycloaddition of CO_2 to epoxides. Reprinted with permission from reference (12). Copyright © 2017 Elsevier.

The high solubility of CO_2 in ILs has led to a whole field of CO_2-related chemistry in which ILs have an active functional role, especially in carbon capture and sequestration.[17–19] ILs have also been used as a solvent and/or a catalyst for cyclic carbonate formation.[20,21] Peng and Deng, for instance, employed [BMIm][BF_4] IL (BMIm = 1-butyl-3-methylimidazolium) as a catalyst for the propylene carbonate reaction, resulting in 90% conversion and TON value of 450.[20] Li et al., on the other hand, studied the use of $ZnCl_2$/[BMIm][Br] as catalysts for propylene carbonate and styrene carbonate reactions, yielding conversions of 98% and 86% respectively.[21]

It was hypothesized that [P66614][Cl] with a strong nucleophilic anion could function as a solvent for CO_2, and also as a catalyst for the cycloaddition reaction of epoxides and CO_2. Here we employed a long chain IL for the cycloaddition of epoxides and CO_2 in this work: [$P66614^+$] cations. Chloride anions were chosen as our group found that they can facilitate the ring-opening of epoxides well compared to other nucleophiles such as bromine, iodine, and p-toluenesulfonate anions under mild conditions and atmospheric pressures.[22] Also, this IL possesses higher CO_2 absorption capacities than most organic solvents at ambient temperature.[23]

The effectiveness of the catalyst was further studied at elevated pressures for cyclic carbonate formation. The two model reactions used for this study were the cycloaddition of CO_2 to propylene oxide (PO) and styrene oxide (SO). Three reasons accounted for this choice: first, the [P66614][Cl] IL had already shown great potential in aiding Au NPs to catalyze the styrene epoxidation reaction (Chapter 2) and the IL halide anions can be used to catalyze the cycloaddition of CO_2 to epoxides. Second, if this catalytic system works well for both the epoxidation of alkenes and cycloaddition of epoxides and CO_2, it would be a useful system to study for the direct synthesis of cyclic carbonates from alkenes and CO_2. Third, if this IL catalyst able to activate poor

electrophiles such as SO, it should also be able to catalyze the addition of CO_2 to other more active epoxides.

3.2 Experimental

3.2.1 Materials

Styrene oxide (C_8H_8O, 99%, Sigma-Aldrich) and propylene oxide (C_3H_6O, 99%, Sigma-Aldrich) were purchased and used as received. Carbon dioxide (CO_2, 99.99%, Praxair) was purchased and used as received. Commercial samples of the [P66614][Cl] IL were obtained from Cytec Industries Ltd. and used as received. Deuterated chloroform solvent was purchased from Cambridge Isotope Laboratories and used as received.

3.2.2 Synthesis of Propylene Carbonate

The reaction was carried out in a hermetically sealed stainless-steel Parr high-pressure reactor equipped with a temperature control system, a mechanical magnetic stirrer, and a pressure meter (Parr 4560) (Figure 3.2a). A mixture of [P66614][Cl] (5.0 mL, 8.49 mmol) and PO (2.0 mL, 28.6 mmol) were added to the Teflon liner inside the reactor, flushed with CO_2 at moderate pressure to remove any remaining oxygen gas, then pressurized with CO_2 until the desired pressure was reached (Figure 3.2b). The reaction was sealed off, and heated to 33 °C at 0.1–2.4 MPa CO_2 for 1–4 h. After the reaction, the solution was cooled to ambient temperature and the products were characterized by ^{1}H NMR in which 1 drop of the solution and 1 drop of the internal standard acetic acid were added to deuterated chloroform. To ensure reproducibility, each reaction was repeated for at least three times, in which the conversion was found to vary no more than ± 1–2%; and the reported values were an average of all reproducible trials. Figure 3.3 shows example spectra for

propylene carbonate reaction with individual peak assignment. **Propylene oxide**: ^{1}H NMR (500 MHz, $CDCl_3$): 1.31 (m, 3H), 2.45 (m, 1H), 2.74 (m, 1H), 2.97 (m, 1H). **Propylene carbonate**: ^{1}H NMR (500 MHz, $CDCl_3$): 1.50 (m, 3H), 4.02 (m, 1H), 4.56 (m, 1H), 4.85 (m, 1H).

A

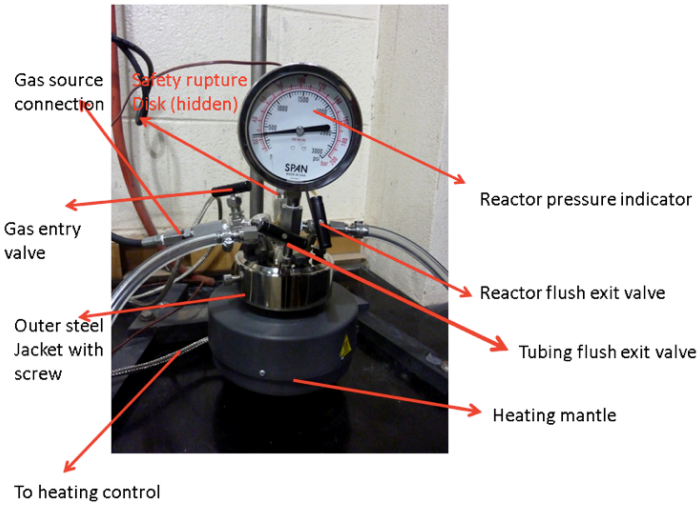

B

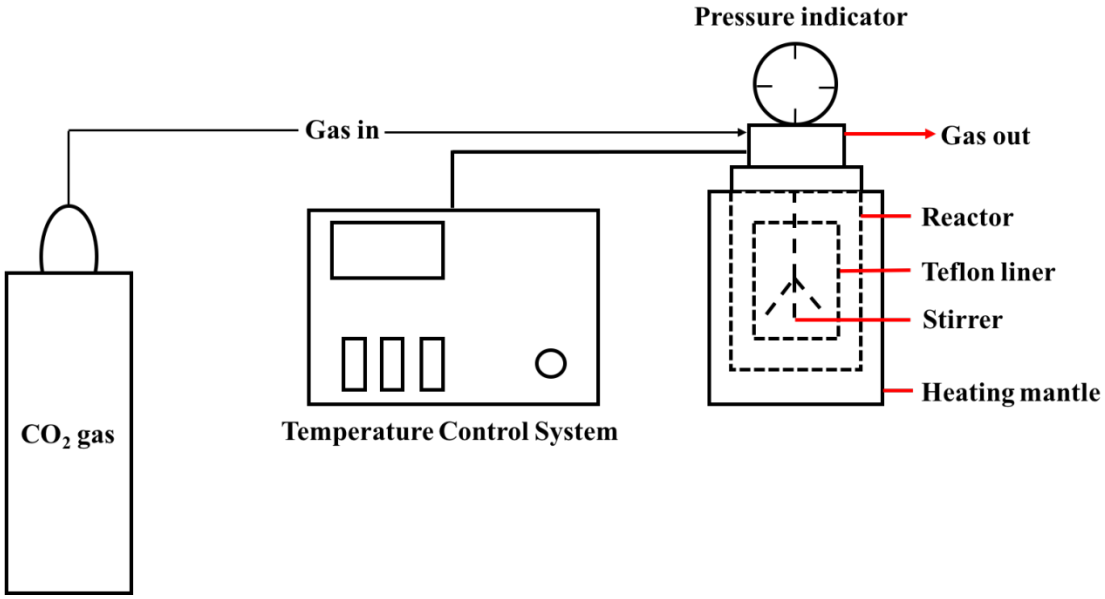

Figure 3.2 (a) Parr 4560 high pressure reactor; (b) Reaction set-up illustration.

3.2.3 Synthesis of Styrene Carbonate

The set-up for styrene carbonate formation was very similar to the propylene carbonate procedure detailed in the last section. This reaction was also carried out in a hermetically sealed stainless-steel Parr high-pressure reactor equipped with a temperature control system. [P66614][Cl] (1.0 mL, 8.49 mmol) and SO (3.26 mL, 28.6 mmol) were added to the Teflon reaction liner inside the reactor, and was sealed after the desired CO_2 pressure reached. The reaction was heated to 55 °C at 0.1-2.4 MPa CO_2 for 1-7 h. The solution was allowed to cool to ambient temperature after the reaction and the products were characterized by ^{1}H NMR in which 1 drop of the solution and 1 drop of the internal standard acetic acid were added to deuterated chloroform. To ensure reproducibility, each reaction was repeated for at least three times, in which the conversion was found to vary no more than ±1–2%; and he reported values were an average of all reproducible trials. Figure 3.4 shows example spectra with individual peak assignment for styrene carbonate reaction. **Styrene oxide**: ^{1}H NMR (500 MHz, $CDCl_3$): 2.76 (m, 1H), 3.10 (m, 1H), 3.82 (m, 1H), 7.29–7.35 (m, 5H). **Styrene carbonate**: ^{1}H NMR (500 MHz, $CDCl_3$): 4.33 (t, 1H), 4.79 (t, 1H), 5.67 (t, 1H), 7.34–7.43 (m, 5H).

3.2.4 Example Spectra for Conversion Calculation

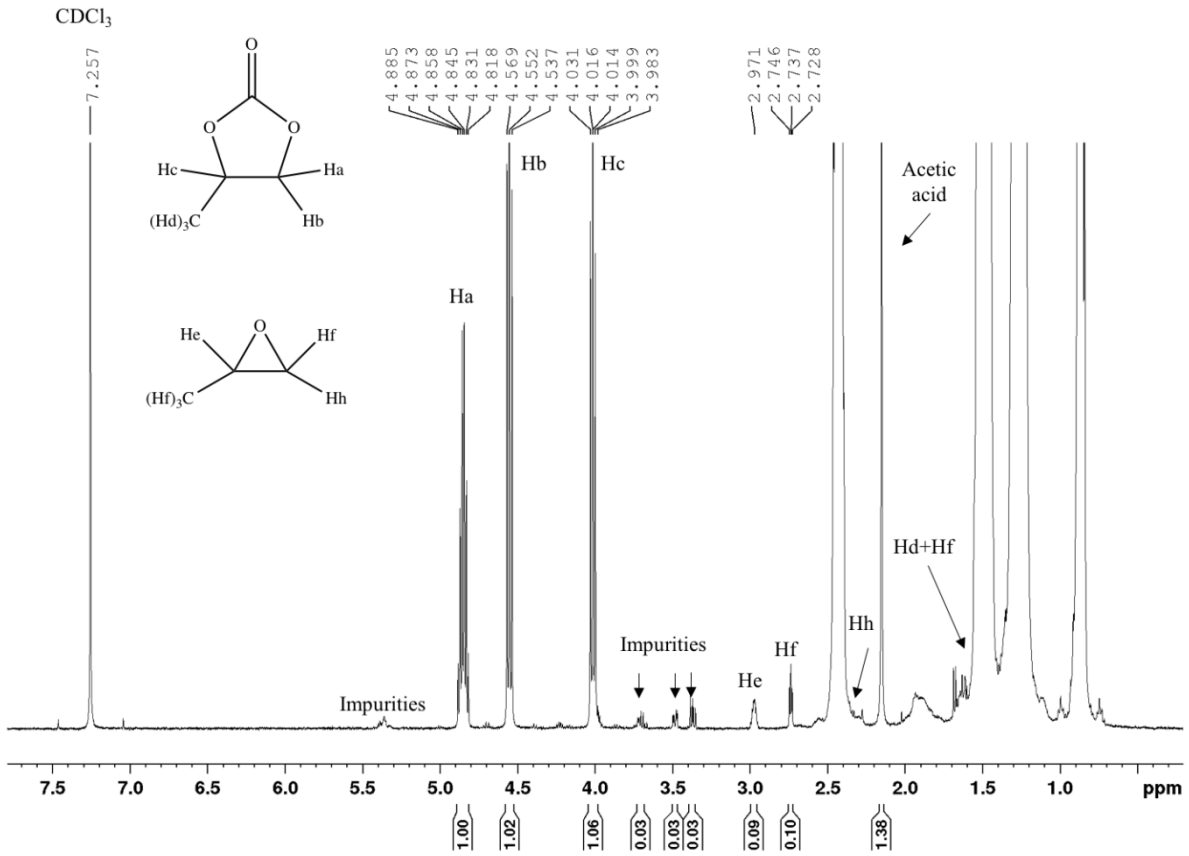

Figure 3.3 Example spectra for propylene carbonate reaction with individual peak assignment. Reaction conditions used: substrate:catalyst mmol ratio of 8.49:28.6, 2.4 MPa, 3 h, 33 ºC, and 600 rpm.

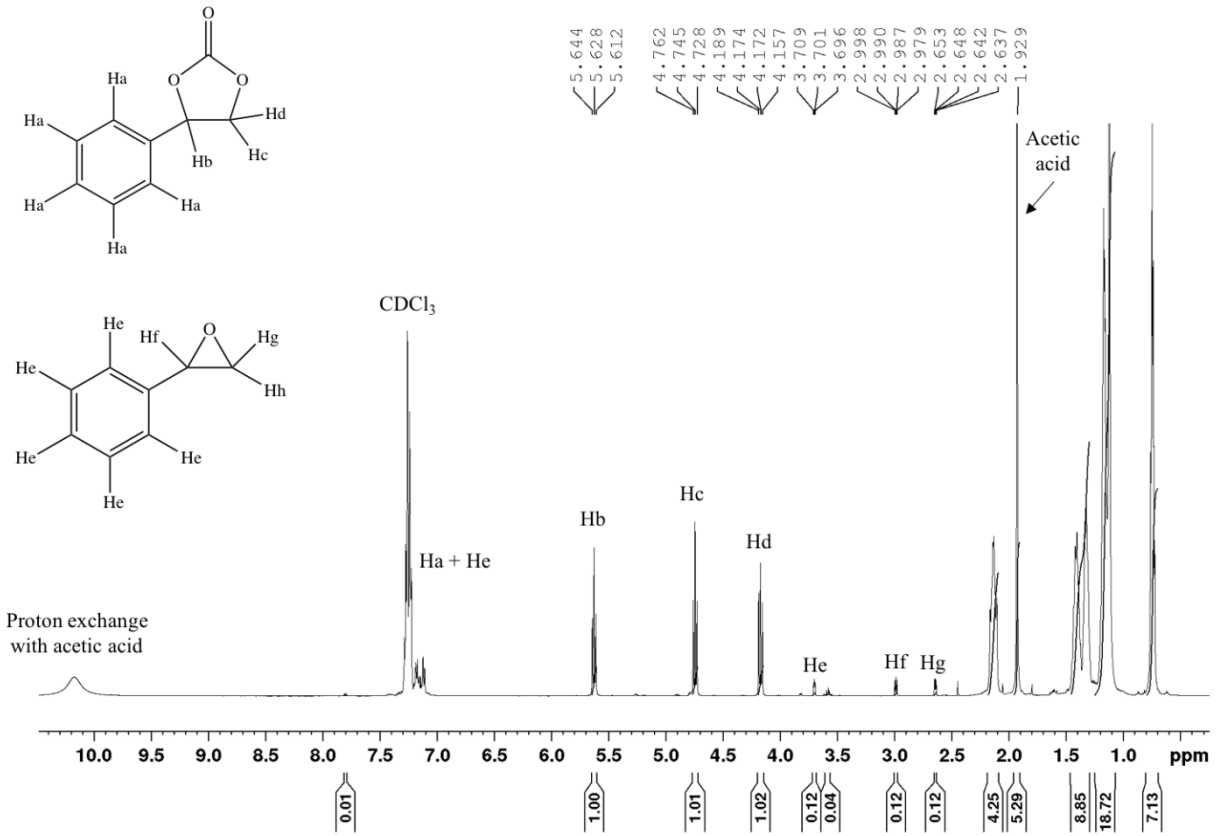

Figure 3.4 Example spectra for propylene carbonate reaction with individual peak assignment. Reaction conditions used: substrate:catalyst mmol ratio of 8.49:28.6, 2.4 MPa, 3 h, 33 ºC, and 600 rpm.

Conversions were calculated via relative quantization from the peak areas of individual, well-separated reactant and product peaks from ^{1}H NMR spectra. Please note that the calculated conversion derived from the internal standard acetic acid was found to be similar to the one shown above. Also, the observed impurities (the peaks from 3.3–3.7 ppm) in the NMR spectra for propylene carbonate reaction were believed to be propylene glycol due to propylene carbonate hydrolysis catalyzed by the internal standard acetic acid.[26] ^{1}H NMR characterization was done without the use of the internal standard and no changes in the conversion as well as the product selectivity was seen (Figure A-1)

$$\%\ \text{Conversion}$$

$$= \frac{\text{All products}}{\text{All products} + \text{all leftover reactants}}$$

$$= \frac{\text{Propylene Carbonate H}}{\text{Propylene Carbonate H} + \text{PO H}} \times 100\%$$

$$= \frac{1.00}{1.00 + 0.10} \times 100\%$$

$$= 91\ \%$$

$$\%\ \text{Conversion}$$

$$= \frac{\text{All products}}{\text{All products} + \text{all left} - \text{over reactants}}$$

$$= \frac{\text{Styrene Carbonate H}}{\text{Styrene Carbonate H} + \text{SO H}} \times 100\%$$

$$= \frac{1.00}{1.00 + 0.12}$$

$$= 89\%$$

3.3 Results & Discussion

The synthesis of propylene carbonate was performed under mild conditions (33 °C and at atmospheric pressure) in our lab in the past. A conversion of 71% for cycloaddition of PO and CO_2 was obtained after 30 h at a slow rate with no by-products. However, it was hypothesized that this reaction could be accelerated under high pressures as CO_2 solubility would be enhanced in the IL phase. Since typical reactions in the literature range from 1.1–3.5 MPa of CO_2,[13] the reaction was decided to run at 1.4 MPa instead of 0.1 MPa, and a relatively similar conversion was recorded for the cyclic carbonate reaction with PO as substrate in 1 h (Table 3.1). The reaction parameters for the synthesis of propylene carbonate, therefore, have been investigated in detail to maximize the reaction conversion. Acetic acid was used as an internal standard to re-confirm the calculated conversions. Under various reaction conditions, only propylene carbonate was formed, and no by-products were observed. The determined reaction conditions for propylene carbonate formation were then applied to the styrene carbonate reaction.

Table 3.1 Comparison between low- and high-pressure reactions of PO or SO with CO_2.

	PO results[a]	**SO results**[a]
[22]Low-pressure reaction: P = 0.1 MPa, t = 30 h	Conversion = 71%	Conversion = 24%
High-pressure reaction: P =1.4 MPa, t = 1 h	Conversion = 62%	Conversion = 19%

[a] Reaction conditions used: substrate:IL mmol ratio of 8.49:28.6, 33 °C, and without stirring.

3.3.1 Synthesis of Propylene Carbonate

PO was used as the model substrate to evaluate the catalytic performance of the [P66614][Cl] IL in the cycloaddition reaction of CO_2 and PO to form PC (Scheme 3.1). Control studies showed that the reaction could not proceed without a catalyst.

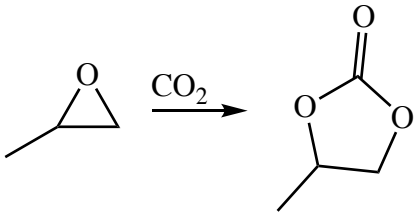

Scheme 3.1 Cycloaddition of CO_2 to PO.

3.3.1.1 Mechanism

Steric effects play an important role in the cyclic carbonate reaction. Particularly, the bulkier the substrate, the more steric hindrance it would be; thus, the lower the reaction rates and conversions. Under mild conditions, a three-step proposed mechanism involves catalysis by the anion halide in tetraalkylphosphonium ILs (Scheme 3.2).[23–25] The first step is the ring-opening of PO, followed by CO_2 insertion then intramolecular cyclization.

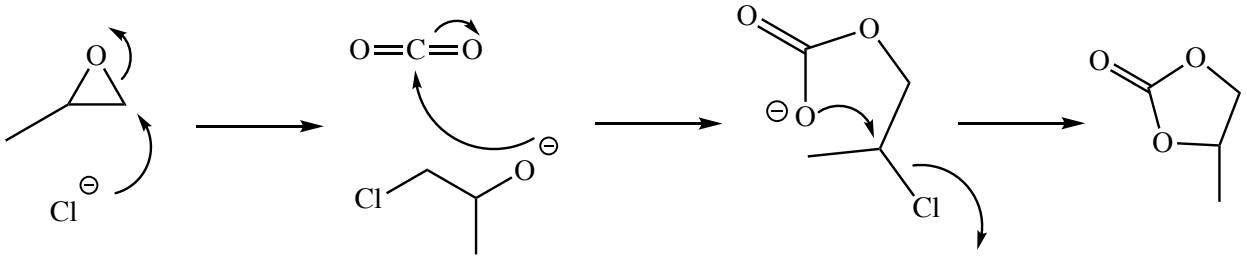

Scheme 3.2 Proposed mechanism for propylene carbonate formation from PO and CO_2.

The chloride anion is a strong enough nucleophile for the first ring-opening step to occur and is also a good enough leaving group for the subsequent cyclization step. Different nucleophiles, such as bromide, chloride, iodide, phenolate, tosylate anions, were tested in the past by our group and it was found that a very strong nucleophile could slow down the last step of the mechanism, leading to polymerization.[22] Also, when a weak nucleophile such as tosylate anion

was employed, the reaction progressed more slowly compared to when halide anions were used, and has no conversion at moderate temperatures but did show low conversions at higher temperatures.[22] If the use of an IL was eliminated and the anion was employed in an aqueous solution only such as NaCl, it was found that while the [Cl^-] anion catalyzed the reaction, side reactions still occurred in water to give products such as chlorinated alcohols.[26] Therefore, full selectivity of PO to propylene carbonate is limited in water, which further confirms the need for non-aqueous systems.

The importance of the tetraalkylphosphonium cation can also be seen by comparing experimental CO_2 solubility data using various single ILs at ambient temperature and atmospheric pressure.[27] Among the single-component ILs tested, phosphonium ILs were found to have the lowest Henry's law constant; thus, the highest CO_2 solubility compared to imidazolium- and pyridinium-based ILs.[27] For example, Henry's law constant for $[N1444]^+$ is twice as high as that for [$P66614^+$] when [Tf_2N^-] anions were used.[27] Furthermore, the chloride anion in phosphonium ILs was found to be crucial in the stability of nanoparticles (NPs) due to its large surface charge density and its capability for excellent electrostatic protection of the NP surface, thus enhancing the catalytic abilities of the NPs dispersed in chloride-bearing ILs.[28]

3.3.1.2 Effect of Reaction Time and Pressure

A pressure of 1.4 MPa CO_2 was employed for initial testing and a conversion of 62% was recorded after 1 h. Figure 3.5a shows the effect of CO_2 pressure from 0.1−2.4 MPa on the first order reaction rate constant, k, for the propylene carbonate reaction in [P66614][Cl] after 1 h, 33 °C, substrate:catalyst mmol ratio of 8.49:28.6, and without stirring. Catalyst concentration was not varied as the catalyst also acts as the solvent in this case. Kinetic studies of the reaction were

then examined, and the reaction was found to have pseudo-first order rate as described in Equation 3.1:

$$\frac{\mathrm{d[Propylene\ carbonate]}}{\mathrm{dt}} - \frac{\mathrm{d[PO]}}{\mathrm{dt}} = \mathrm{k[PO]} \tag{3.1}$$

where k is the observed pseudo-first order rate constant.

Integrating Equation 3.1 gave Equation 3.2:

$$\ln \frac{[\mathrm{PO}]_0}{[\mathrm{PO}]} = \mathrm{kt} \tag{3.2}$$

Defining $[\mathrm{PO}] = [\mathrm{PO}]_0(1 - \mathrm{C})$, where C represents the reaction conversion, yields Equation 3.3:

$$\ln \frac{1}{1-\mathrm{C}} = \mathrm{kt} \tag{3.3}$$

Treatment as a pseudo-first order reaction assumes the amount of CO_2 in solution is significantly higher than PO at elevated pressures; thus, the concentration of CO_2 should not appreciably change during the reaction. Nonetheless, it was found that increasing the CO_2 pressure had a positive effect on the reaction rate. Major mass-transfer issues were observed for low pressure reactions, and the reaction rate increased remarkably from 0.1−1.4 MPa CO_2 pressure as not enough CO_2 can dissolve into the IL at low pressures, thus limiting the reaction kinetics (Figure 3.5a). Kinetically-limited reactions were seen from 1.4−2.4 MPa CO_2 pressure as there were only minor changes further seen in the reaction rate constant. Another reaction was run for a longer time (3 h) at 2.4 MPa CO_2 pressure, in which the temperature and the substrate:catalyst mmol ratio were kept the same at 33 °C and 8.49:28.6 respectively. The time dependence of ln $(\frac{1}{1-C})$ was plotted in Figure 3.5b. Since the ln $(\frac{1}{1-C})$ vs. t plot was linear, it further confirmed the validity of the pseudo-first order reaction hypothesis.

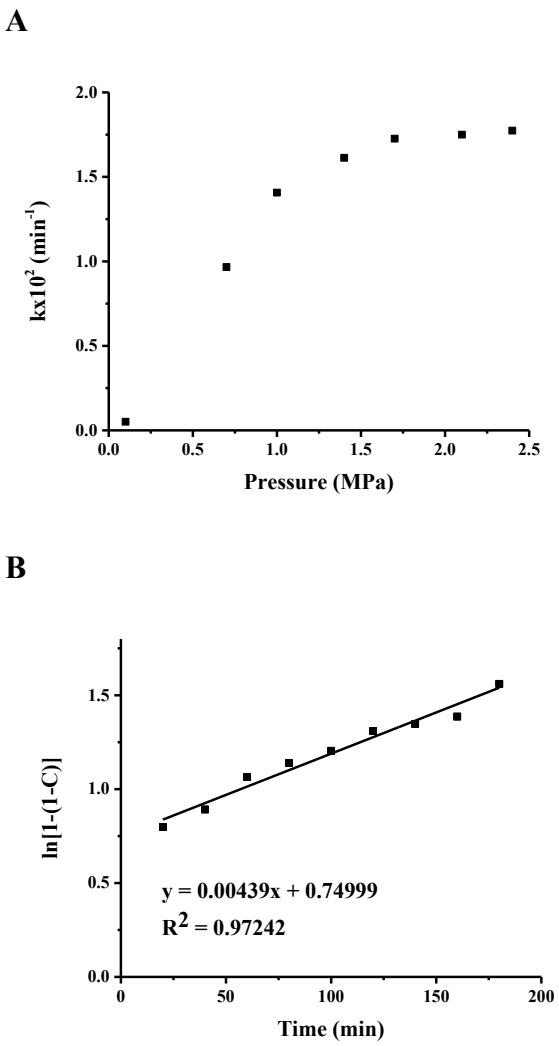

Figure 3.5 (a) Effect of pressure from 0.1−2.4 MPa on the rate constant of the reaction after 1 h of the reaction; (b) Pseudo-first order plot of $\ln(\frac{1}{1-C})$ over 3 h. Reaction conditions: substrate:catalyst mmol ratio of 8.49:28.6, 33 ºC, 2.4 MPa CO_2, and with no stirring (please refer to Experimental 3.2.2 for reproducibility discussion).

3.3.1.3 Influence of Stirring on Mass Transfer and Reaction Rate

The effect of mass transfer was further examined as the results in the last section showed mass transfer of CO_2 into the ILs could limit the reaction rates. This was tested by comparing the

reaction constant for reactions with and without stirring (Table 3.2). The point where the rate switches from being mass transfer-limited to being truly kinetically limited would be at a point where stirring no longer influences the kinetics of the reaction. No stirring produced a slightly slower rate constant ($4.4x10^{-3}$ min^{-1}) than stirring the reaction at our highest rate of 600rpm ($5.3x10^{-3}$ min^{-1}), which corresponded to conversions of 79% and 91%, respectively. This indicated that there are some mass transfer issues for this reaction in the absence of stirring. Also, no significant difference was noted in the rate constant of the reaction at high stirring speeds. In conclusion, stirring the reaction at 600 rpm helps to take the system out of mass-transfer limited range.

Table 3.2 Rate constant for cycloaddition of PO and CO_2 at different stirring speeds.

Entry[a]	Stirring rate	Pseudo-first order reaction rate constant[b]
1	No stirring	$4.4x10^{-3}$ min^{-1}
2	100 rpm	$4.7x10^{-3}$ min^{-1}
3	200 rpm	$4.8x10^{-3}$ min^{-1}
4	300 rpm	$5.0x10^{-3}$ min^{-1}
5	400 rpm	$5.1x10^{-3}$ min^{-1}
6	500 rpm	$5.2x10^{-3}$ min^{-1}
7	600 rpm	$5.3x10^{-3}$ min^{-1}

[a] Reaction conditions were 8.49 mmol PO: 28.6 mmol IL, 33°C, 2.4 MPa CO_2, and 3 h.

[b] Pseudo-first order rate constant was calculated using Equation 3.3.

3.3.2 Synthesis of Styrene Carbonate

The overall conversion and the product distribution depend strongly on the conditions used as described in the following sections for the cycloaddition of CO_2 into SO. Styrene carbonate was yielded as a major product in every cases and no by-product were observed (Scheme 3.3).

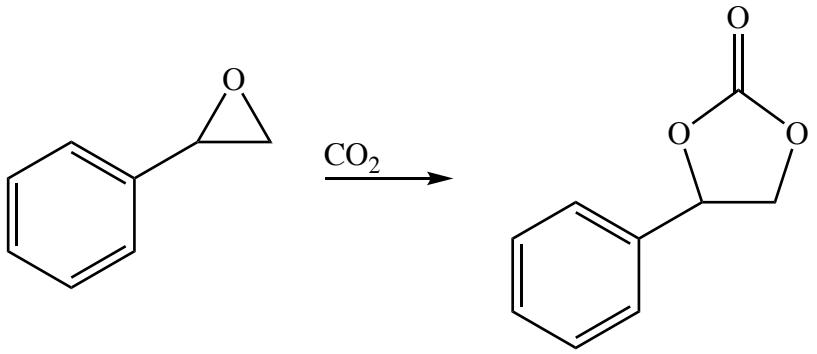

Scheme 3.3 Cycloaddition of CO_2 to SO.

The mechanism of cycloaddition of CO_2 to SO is very similar to that of PO: it starts with the ring-opening of SO in which the halide anion attacks the less hindered carbon position, followed by CO_2 insertion, and then intramolecular cyclization (Scheme 3.4). However, SO is generally more difficult to react compared to PO due to the bulky phenyl group.[29]

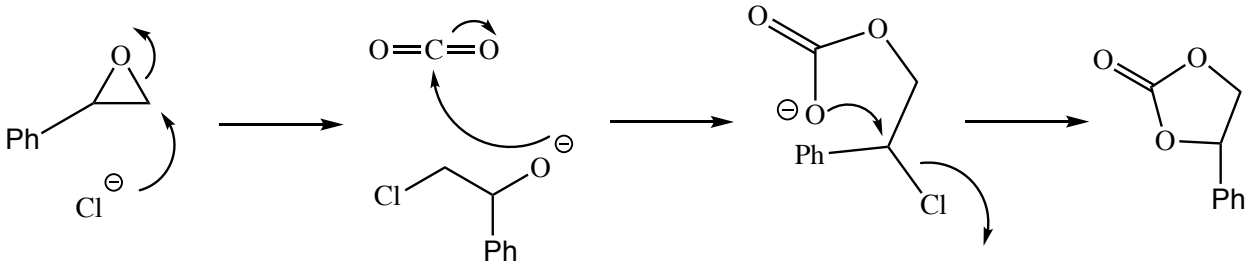

Scheme 3.4 Proposed mechanism of styrene carbonate formation from SO and CO_2.

3.3.2.1 Effect of Reaction Temperature

The influence of reaction temperature from 30–65 ºC on the cycloaddition of SO was evaluated at 2.4 MPa pressure for 1 h, with a substrate:catalyst mmol ratio of 8.49:28.6 (Table 3.3). The reaction temperature was shown to have a positive influence on the catalytic activity. In a relatively low temperature range, the conversion was drastically increased from 35% to 82% as the temperature increased from 30−55 ºC. Further increase in reaction temperature (to 65 ºC) did not exhibit any significant change in the conversion, which might be due to reducing of CO_2 solubility in the IL at higher temperatures.[30,31] The optimized temperature for the synthesis of styrene carbonate, therefore, was 55ºC.

Table 3.3 Effect of temperature on the conversion of the styrene carbonates reaction.

Entry[a]	Temperature (ºC)	Conversion (%)[b]
1	30 ºC	35
2	35 ºC	46
3	40 ºC	57
4	45 ºC	64
5	50 ºC	75
6	55 ºC	82
7	60 ºC	82
8	65 ºC	82

[a] Reaction conditions were used at 8.49mmol SO:28.6mmol IL, 2.4 MPa CO_2, 1 h, and 600 rpm.

[b] Conversion (see Experiment 3.2.3 for reproducibility discussion and Experimental 3.2.4 for sample calculation).

Similar to the propylene carbonate reaction, the rate constants for styrene carbonate reaction were determined using a pseudo-first-order reaction (Equation 3.4):

$$\frac{\mathrm{d[Styrene\ carbonate]}}{\mathrm{dt}} - \frac{\mathrm{d[SO]}}{\mathrm{dt}} = \mathrm{k[SO]} \qquad (3.4)$$

where k is the observed pseudo-first order rate constant. Integrating Equation 3.4, and defining [SO] as $[\mathrm{SO}]_0 = (1 - \mathrm{C})$ where C is the reaction conversion gave Equation 3.5:

$$\ln \frac{1}{1-\mathrm{C}} = \mathrm{kt} \qquad (3.5)$$

The validity of the pseudo-first order reaction hypothesis was confirmed as the $\ln\left(\frac{1}{1-C}\right)$ vs. t plot was linear (Figure 3.6).

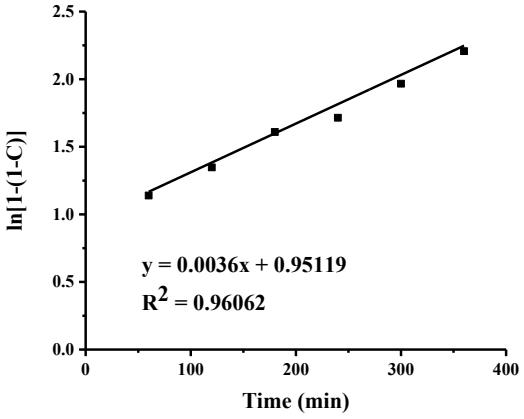

Figure 3.6 Pseudo-first order plot of $\ln\left(\frac{1}{1-C}\right)$ with respect to time. Reaction conditions used: 8.49mmol SO:28.6mmol IL, 55 ºC, 2.4 MPa CO_2, and 600 rpm. Please refer to Experimental 3.2.3 for reproducibility discussion.

The activation energy for the reaction was then calculated using the Arrhenius equation (Equation 3.6):

$$\mathrm{k} = \mathrm{Ae}^{-\mathrm{E_a}/(\mathrm{RT})} \qquad (3.6)$$

where A and E_a are the pre-exponential factor (min^{-1}) and the activation energy ($kJmol^{-1}$), respectively. R is the universal gas constant (8.314 $Jmol^{-1}K^{-1}$), and T is the absolute temperature (K). Taking the natural logarithm of Equation 3.6 gave Equation 3.7:

$$\ln k = \ln A - \frac{E_a}{RT} \tag{3.7}$$

The activation energy for the styrene carbonate reaction was determined over the range of 30−55 ºC by fitting the data of ln(k) and $\frac{1}{T}$ to Equation 3.7 (Figure 3.7). The value of the activation energy E_a was found to be 50 $kJmol^{-1}$, which was comparable to the know published data for the reaction of styrene carbonate (Table 3.4).

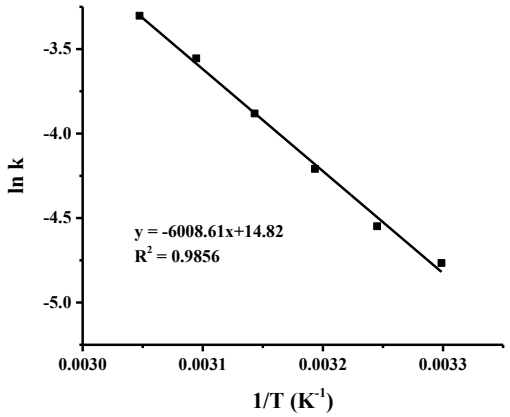

Figure 3.7 Arrhenius plot for the determination of the activation energy for the styrene carbonate reaction catalyzed by the [P66614][Cl] IL. Reaction conditions: substrate:catalyst mmol ratio of 8.49:28.6, 2.4MPa CO_2, 1 h, and 600 rpm. Please refer to Experimental 3.2.3 for reproducibility discussion.

Table 3.4 Comparison of activation energy between various catalytic systems.

Catalyst type	Activation Energy ($kJmol^{-1}$)
[32]Without catalyst	209–251
[33]Al1cat/TBAB	23
[33]Al1cat	34
This work: [P66614][Cl]	50

Al1cat/TBAB = non-symmetrial aluminium salen-acac hybdrid complex with tetrabutylammonium bromide as co-catalyst.

3.3.2.2 Effect of Reaction Time

The reaction conversions for the synthesis of styrene carbonate at various reaction times are presented in Table 3.5. The conversion, however, was found to increase remarkably in the region of 1–5 h, from 82% to 89%, and reached its maximum at 6 h (90% conversion) (Table 3.5).

Table 3.5 Effect of reaction time on the reaction conversion of styrene carbonate reaction.

Entry[a]	Time (h)	Conversion (%)[b]
1	1	82
2	2	84
3	3	86
4	4	87
5	5	88
6	6	89
7	7	89

[a] Reaction conditions used: 8.49 mmol SO:28.6 mmol IL, 55ºC, 2.4 MPa CO_2, and 600 rpm.

[b] Conversion (see Experimental 3.2.3 for reproducibility discussion and Experimental 3.2.4 for sample calculation).

3.4 Conclusion

The reaction conditions for cyclic carbonate reactions with PO and SO were studied. Particularly, a higher CO_2 pressure was employed, and it was found that the higher the pressure, the higher the conversion obtained, thus indicating the reaction is mass-transfer limited at low pressures. Kinetic studies of the PO reaction with CO_2 was done by varying the CO_2 pressure and showed pseudo-first order kinetics, and the effect of mass transfer of CO_2 into the IL was studied by comparing the reaction rate constant at various stirring rates to find the point where the rate limiting step switches from being mass transfer-limited to being kinetically limited. Increasing in stirring rates at 600 rpm helped to take the system out of the mass transfer limiting range.

The optimized conditions for cycloaddition of PO and CO_2 were then applied for the SO reaction with CO_2. Room temperature reaction conditions, unfortunately, did not work well, which might due to the steric hindrance of the phenyl group. The reaction, therefore, was run at elevated temperatures between 30−65 ºC. Increasing in temperature showed positive effects on the catalytic activity, in which the conversion increased drastically from 35% to 82% when the temperature was increased from 30 ºC to 55ºC respectively. Increasing in the reaction time also led to higher conversions, in which the conversion increased from 82% to 89% when the reaction was run from 1–6 h. Further increasing in reaction temperature (to 65ºC) or reaction time (to 7 h), however, did not show any significant change in the conversions. Kinetic studies of the cycloaddition of CO_2 to SO showed a pseudo-first order rate behaviour. The activation energy of the reaction was found using an Arrhenius plot, and a value of 50 $kJmol^{-1}$ was acquired. Since the Arrhenius plot was relatively linear, it was further concluded that there were no major mass-transfer issues existing at the optimized reaction conditions.

3.5 References

(1) Xiaoding, X.; Moulijn, J. A. *Energy Fuels* **1996**, *10*, 305–325.

(2) Wong, C. S.; Chan, Y.-H.; Page, J. S.; Bellegay, R. D.; Pettit, K. G. J. *Geophys. Res. Atmospheres* **1984**, *89*, 9527–9539.

(3) Choudhary, V. R.; Dumbre, D. K. *Top. Catal.* **2009**, *52*, 1677–1687.

(4) He, Q.; O'Brien, J. W.; Kitselman, K. A.; Tompkins, L. E.; Curtis, G. C. T.; Kerton, F. M. *Catal. Sci. Technol.* **2014**, *4*, 1513.

(5) Woo, B.-G.; Choi, K. Y.; Song, K. H.; Lee, S. H. *J. Appl. Polym. Sci.* **2001**, *80*, 1253–1266.

(6) Song, Q.-W.; Zhou, Z.-H.; He, L.-N. *Green Chem*. **2017**, *19*, 3707–3728.

(7) Fujita, S.; Nishiura, M.; Arai, M. *Catal. Lett.* **2010**, *135*, 263–268.

(8) Galvan, M.; Selva, M.; Perosa, A.; Noè, M. *Asian J. Org. Chem.* **2014**, *3*, 504–513.

(9) Butera, V.; Russo, N.; Cosentino, U.; Greco, C.; Moro, G.; Pitea, D.; Sicilia, E. *ChemCatChem* **2016**, *8*, 1167–1175.

(10) Dai, W.; Luo, S.; Yin, S.; Au, C. *Front. Chem. Eng. China* **2010**, *4*, 163–171.

(11) Caló, V.; Nacci, A.; Monopoli, A.; Fanizzi, A. Org. Lett. **2002**, 4, 2561–2563.

(12) Chaugule, A. A.; Tamboli, A. H.; Kim, H. *Fuel* **2017**, *200*, 316–332.

(13) Klähn, M.; Seduraman, A. *J. Phys. Chem. B* **2015**, *119*, 10066–10078.

(14) Carvalho, P. J.; Coutinho, J. A. P. *J. Phys. Chem. Lett.* **2010**, *1*, 774–780.

(15) Costa Gomes, M. F. J; Stevanovic, S.. *Chem. Thermodyn*. **2013**, *59*, 65–71.

(16) Steinbauer, J.; Spannenberg, A.; Werner, T. *Green Chem.* **2017**, *19*, 3769–3779.

(17) Ohno, H. Physical Properties of Ionic Liquids for Electrochemical Applications. In *Electrodeposition from Ionic Liquids,* Endress, F.; Abbott, A.; MacFarlane, D.; Wiley-VCH: Weinheim, Germany, 2017; 26–35.

(18) Boot-Handford, M. E.; Abanades, J. C.; Anthony, E. J.; Blunt, M. J.; Brandani, S.; Mac Dowell, N.; Fernandez, J. R.; Ferrari, M.-C.; Gross, R.; Hallett, J. P.; Haszeldine, R. S.; Heptonstall, P.; Lyngfelt, A.; Makuch, Z.; Mangano, E.; Porter, R. T. J.; Pourkashanian, M.; Rochelle, G. T.; Shah, N.; Yao, J. G.; Fennell, P. S. *Energy Environ. Sci.* **2014**, *7*, 130–189.

(19) Wang, C.; Luo, H.; Jiang, D.; Li, H.; Dai, S. *Angew. Chem. Int. Ed.* **2010**, *49*, 5978–5981.

(20) Peng, J.; Deng, Y. *New J. Chem.* **2001**, *25*, 639–641.

(21) Li, F.; Xiao, L.; Xia, C.; Hu, B. *Tetrahedron Lett.* **2004**, *45*, 8307–8310.

(22) Theron, R. Activation and Conversion of Carbon Dioxide in Tetraalkylphosphonium Ionic Liquids. 4th year report. University of Saskatchewan, 2013.

(23) Dauner, B. R.; Pringle, D. L. *J. Chem. Educ.* **2014**, *91*, 743–746.

(24) Zhu, J.; Diao, T.; Wang, W.; Xu, X.; Sun, X.; Carabineiro, S. A. C.; Zhao, Z. *Appl. Catal. B Environ.* **2017**, *219*, 92–100.

(25) Wang, Q.; Guo, C.-H.; Jia, J.; Wu, H.-S. *J. Mol. Model.* **2015**, *21*, 179.

(26) Khoshro, H.; Zare, H. R.; Namazian, M.; Jafari, A. A.; Gorji, A. *Electrochimica. Acta.* **2013**, *113*, 263–268.

(27) Adam, F.; Appaturi, J. N.; Ng, E.-P. *J. Mol. Catal. Chem.* **2014**, *386*, 42–48.

(28) Banerjee, A.; Theron, R.; Scott, R. W. J. *Chem. Commun.* **2013**, *49*, 3227–3229.

(29) Wang, T.; Wang, W.; Lyu, Y.; Chen, X.; Li, C.; Zhang, Y.; Song, X.; Ding, Y. *RSC Adv.* **2017**, *7*, 2836–2841.

(30) Manic, M. S.; Macedo, E. A.; Najdanovic- Visak, V. *Fluid Phase Equilibria* **2012**, *324*, 8–12.

(31) Manic, M. S.; Queimada, A. J.; Macedo, E. A.; Najdanovic-Visak, V. J. *Supercrit. Fluids* **2012**, *65,* 1–10.

(32) Comerford, J. W.; Ingram, I. D. V.; North, M.; Wu, X. *Green Chem***. 2015**, *17*, 1966–1987.

(33) Supasitmongkol, S.; Styring, P. *Catal. Sci. Technol*. **2014**, *4*, 1622–1630.

4.0 Direct Synthesis of Styrene Carbonate from Styrene and CO_2 Catalyzed by Tetraalkylphosphonium Ionic Liquid-Stabilized Gold Nanoparticles

The reaction conditions for styrene epoxidation, and cycloaddition of CO_2 to styrene oxide have been studied in detail in Chapter 2 and 3, respectively. Hence, it was essential for us to combine the two reactions as synthesizing styrene carbonate from styrene and CO_2 would be more beneficial from an economic standpoint. Moderate conversions and selectivity were obtained when Au NPs synthesized in [P66614][Cl] function as catalysts. Also, another catalytic system, Au NPs stabilized in a non-halide IL, [P66614][NTf_2], was tested for the same reaction.

4.1 Introduction

SC, along with other organic carbonates such as propylene carbonate, ethylene carbonate, dimethyl carbonate and diphenyl carbonate, are important reagents in industry as they are used in polycarbonates and polyurethanes syntheses, which are among the most extensively used plastics, as well as in Li-ion batteries as aprotic polar solvents.[1] The direct synthesis of SC from styrene and CO_2 instead of styrene oxide (SO) consists of two sequential reactions: epoxidation of styrene, and CO_2 cycloaddition of CO_2 to SO to form SC. This is an appealing industrial process as the reaction uses readily available and low-priced chemical alkenes as the substrate, while avoiding preliminary synthesis and separation of epoxides. Also, this facile synthetic approach would make the cyclic carbonate synthesis simpler and even cheaper from both economic and environmental points of view.

Despite the usefulness of SC, only a few studies have been done on the direct synthesis of SC from styrene and CO_2 catalyzed by either homogeneous or heterogeneous catalysts.[2–5] For example, Aresta and Dibenedetto carried out the one-pot synthesis of SC from styrene with homogeneous rhodium (I) complex catalysts at 40 °C, 5.1 MPa CO_2, and 0.3 MPa O_2.[2] A 30% selectivity toward SC was seen, along with benzaldehyde, benzoic acid, acetophenone and phenylacetaldehyde as by-products.[2] In 2003, Srinivas et al. reported on a heterogeneous catalytic system of titanosilicate coupled with N, N-dimethylaminopyridine for the synthesis of SC in a single reactor, resulting in a conversion of 50% and a selectivity of 26% toward SC.[3] The first example of 100% selectivity was reported by Bai and Jing in which a dioxo(tetraphenylporphyrinato)ruthenium complex coupled with quaternary onium salt were used as co-catalyst to initiate the cyclic carbonate formation from alkenes, O_2 and CO_2 at ambient temperature and elevated pressure.[4] Supported gold nanoparticles (Au NPs) on a basic resin, in

which the functional group was polystyryl-methyl-trimethylammonium hydroxide, was employed as catalysts for cyclic carbonate formation, resulting in a conversion of 83% and selectivity of 90% toward SC.[5] Although homogeneous catalytic systems have shown good catalytic activity, short catalyst life times and complexity involved in separation and recycling of the catalysts are the main drawbacks for their use. Heterogeneous catalytic systems, on the other hand, are often more stable, easy to separate and handle, and can be right away used after product recovery, though high production costs and long reaction times limit them from industrial applications. An effective catalyst system with high selectivity and easy recyclability, therefore, is still being sought for the direct synthesis of cyclic carbonates from alkenes and CO_2.

Recent research has focused on quasi-homogeneous nanocatalysis, i.e. NPs dispersed in ILs as an interesting catalytic system for the cyclic carbonate formation as this system combines the benefits of both homogeneous and heterogeneous catalysis and can be readily used after product recovery.[6,7] NPs, especially noble-metal Au NPs, are known to have excellent catalytic activity for alkene epoxidations.[8] ILs, on the other hand, have gained considerable attention as strong candidates for the cycloaddition of CO_2 to epoxides due to their high CO_2 solubility, which are mainly governed by the alkyl-side chain length of the IL cations and/or the nature of the IL anions.[9] The effect of the cation type on CO_2 absorption ability was studied by Stevanovic and Costa Gomes, and the trihexyl(tetradecyl)phosphonium [$P66614^+$] cation was found to have the highest CO_2 solubility compared to imidazolium and pyrimidine cations when the anion was held constant as tris(pentafluroethyl)trifluorophosphate.[10]

This chapter couples the two reactions, styrene epoxidation and cycloaddition of CO_2 to SO, which were studied in detail in Chapter 2 and 3, respectively, for the direct synthesis of SC from styrene and CO_2 as this is a better approach from both economic and environmental points

of view (Scheme 4.1). Gold nanoparticles (Au NPs) synthesized in tetraalkylphosphonium ILs with highly coordinating anions such as chlorides [Cl^-] and bis(trifluoromethylsulfonyl)imide [NTf_2^-] were evaluated as potential catalysts for the direct synthesis of styrene carbonate (SC) from styrene and CO_2. From preliminary studies, Au NPs dispersed in the trihexyl(tetradecyl)phosphonium chloride ([P66614][Cl]) IL emerged as a catalyst system of choice for its high catalytic activity toward SC formation. Au NPs synthesized in [P66614][NTf_2] IL were chosen to compare with the catalytic system Au/[P66614][Cl] IL for the same reaction. The [NTf_2^-] anion was chosen due to its high CO_2 absorption ability among the non-halide anions[11,12] and strong electrosteric protection of NP surfaces,[13] thus could improve the catalytic activities of the NPs in the IL solvent. In addition, [P66614][NTf_2] and [P66614][Cl] were found to dissolve as much as 0.81 and 0.77 mole fractions of CO_2, respectively, at 8.16 MPa and 40 °C.[14,15] The Au NPs were synthesized similarly via reduction of the gold salts by lithium borohydride ($LiBH_4$) in the IL media. UV-Vis spectroscopy and TEM were used to examine the NP size distribution and stability.

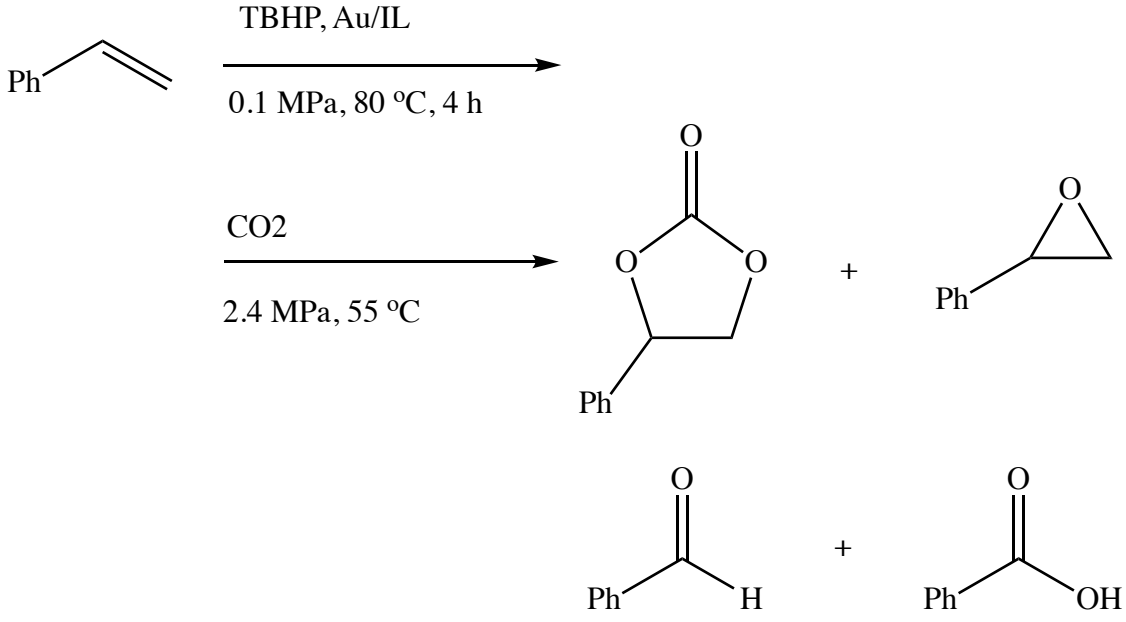

Scheme 4.1 Direct synthesis of styrene to styrene carbonate catalyzed by Au/IL.

4.2 Experimental

4.2.1 Materials

Hydrogen tetrachloroaurate trihydrate ($HAuCl_4 \cdot 3H_2O$, 99.9% on metal basis, Aldrich) was stored under vacuum and flushed with nitrogen after every use. Tert-butyl hydroperoxide (TBHP, 70 wt% in H_2O, Sigma-Aldrich), lithium borohydride ($LiBH_4$, 2.0 M in THF, Sigma-Aldrich), and styrene (contains 4-tert-butylcatechol as stabilizer, ≥99%, Sigma-Aldrich) were used as received. Carbon dioxide (CO_2, 99.99%) was purchased from Praxair and used as received. Commercial samples of the [P66614][Cl] and [P66614][NTf_2] ILs were obtained from Cytec Industries Ltd. and used as received. Deuterated chloroform solvent was purchased from Cambridge Isotope Laboratories and used as received.

4.2.2 Synthesis of Gold Nanoparticles

20.0 mg of $HAuCl_4 \cdot 3H_2O$ (equivalent to 0.0508 mmol of Au) was dissolved in 10.0 mL [P66614][Cl] (or [P66614][NTf_2]) at 80 °C, resulting in a pale golden yellow solution. The solution was cooled to 60 °C, and a stoichiometric excess of $LiBH_4$ reagent (1.5 mL, 2.0 M in THF) was injected drop-wise over a period of 5 mins. Upon addition of $LiBH_4$, the solution turned a dark purple colour, and eventually dark wine-red colour upon complete addition of $LiBH_4$, indicating the formation of Au NPs. The synthesized NP solution was stored under nitrogen in capped vials until use.

4.2.3 Synthesis of Styrene Carbonate

A mixture of styrene (0.6 mL, 5.24 mmol) and TBHP (1.9 mL, 19.7 mmol) were added into a solution of 2.0 mL [P66614][Cl] (or [P66614][NTf_2]) containing 5.08 mM Au NPs while

stirring at 80 °C. The original wine-red solution turned a pale yellow colour after 15 minutes for Au/[P66614][Cl] and after 10 minutes for Au/[P66614][NTf_2]. After 3 hours of the reaction, 1 drop of $LiBH_4$ (2.0 M in THF) was added to recover any oxidized Au NPs, and 2 drops of TBHP were added after the colour of the reaction turned back to wine red colour. The reaction was run for another hour, and the resulting solution had a pale yellow colour.

The solution was then transferred into a Teflon liner placed inside a sealed stainless-steel Parr high-pressure reactor equipped with a temperature control system, a mechanical magnetic stirrer, and a pressure meter (Parr 4560). CO_2 was flushed into the system at moderate pressure to remove any remained oxygen, and the reactor was heated to 55 °C under 2.4 MPa CO_2 while stirring at 600 rpm from 1–8 h. After the reaction, the mixture was allowed to cool to ambient temperature and the pressured was reduced to 0.1 MPa before characterization took place. One drop of the solution was placed in deuterated chloroform for ^{1}H NMR characterization. To ensure reproducibility, each reaction was repeated for at least three times, in which the conversions and product selectivity were found to vary no more than ± 3–4%; and the reported values were an average of all reproducible trials. Figure 4.1 and Figure 4.2 show the individual peak assignment for the direct synthesis of SC catalyzed by Au/[P66614][Cl] and Au/[P66614][NTf_2], respectively. **Styrene**: ^{1}H NMR (500 MHz, $CDCl_3$): 5.19 (d, 1H), 5.70 (d, 1H), 6.67 (m, 1H), 7.50–7.10 (m, 5H). **Styrene oxide**: ^{1}H NMR (500 MHz, $CDCl_3$): 2.76 (m, 1H), 3.10 (m, 1H), 3.82 (m, 1H), 7.29 – 7.35 (m, 5H). **Benzaldehyde**: ^{1}H NMR (500 MHz, $CDCl_3$): 7.99–8.01 (m, 5H), 9.97 (s, 1H). **Benzoic acid**: ^{1}H NMR (500 MHz, $CDCl_3$): 7.45–8.12 (m, 5H), 9.51 (s, broad, 1H). **Styrene carbonate**: ^{1}H NMR (500 MHz, $CDCl_3$): 4.33 (t, 1H), 4.79 (t, 1H), 5.67 (t, 1H), 7.34– 7.43 (m, 5H).

4.2.4 Characterization

UV-Vis spectra were obtained using a Varian Cary 50 Bio UV-Vis spectrometer with a scan range of 300–800 nm and an optical length of 1.0 cm. TEM analysis of the Au NPs was conducted using a Hitachi HT7700 operating at 100 kV. The samples were prepared by ultrasonicating a 1% NP/IL solution in deuterated chloroform for 15 minutes, followed by drop casting onto a carbon-coated copper TEM grid (Electron Microscopy Sciences, Hatfield, PA). To determine the average particle size, an average of 100 particles was manually measured from several different TEM images of the same sample using ImageJ. The standard deviation was calculated using the equation shown below:

$$Stdev = \sqrt{\frac{1}{N}\sum_{i=1}^{N}(x_i - \mu)^2}$$

where x_i is the individual particle size value, μ is the mean of all measured particle sizes, and N is the number of values used. ^{1}H NMR spectra were obtained using a Brüker Avance 500 MHz spectrometer and the chemical shifts were referenced to the residual protons of the deuterated solvent. For characterization regarding the synthesized Au NPs in [P66614][Cl], please refer to section 2.3.1 for detail.

4.2.5 Example Spectra for Conversion and Selectivity Calculation

A

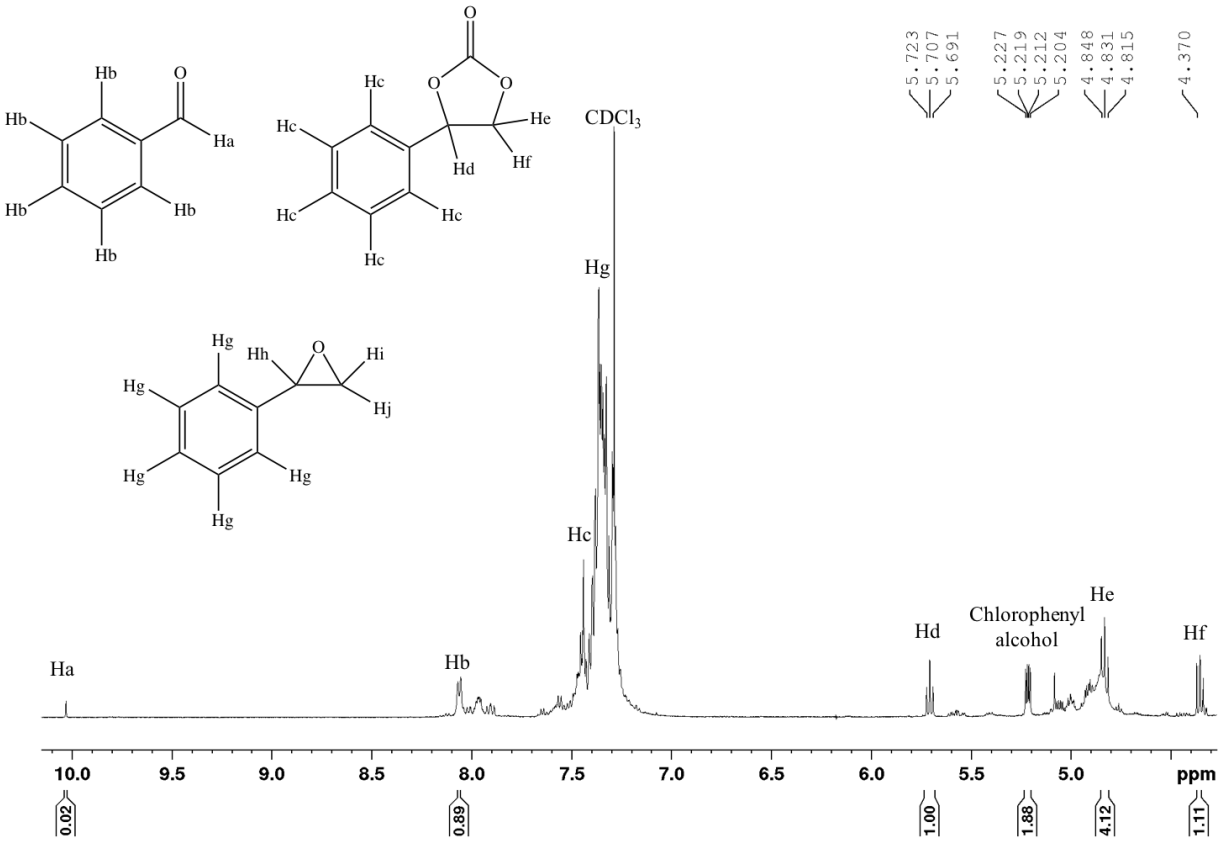

B

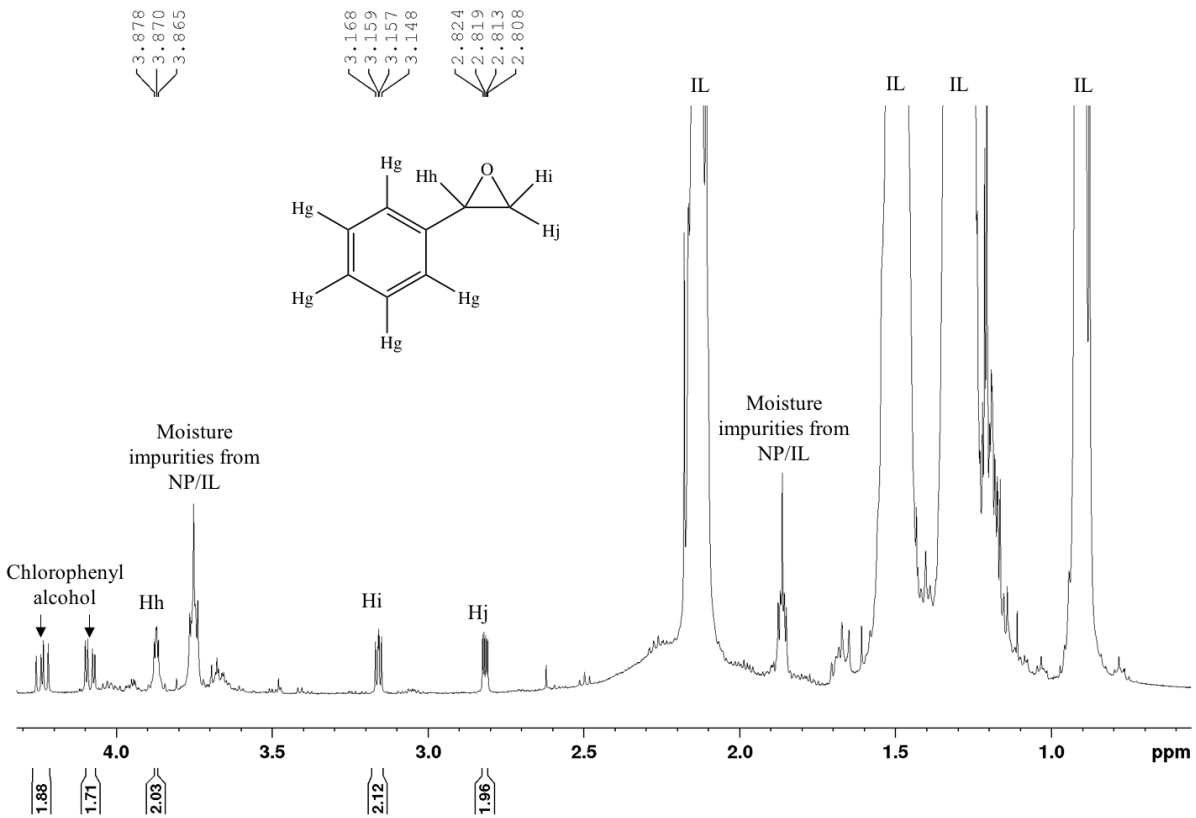

Figure 4.1 (a), (b) Direct synthesis of SC catalyzed by Au/[P66614][Cl] with individual peak assignment. Styrene epoxidation: 5.24 mmol styrene:0.0102 mmol Au:3.40 mmol IL:19.7mmol TBHP, 0.1 MPa, and 80 °C for 4 h. A drop of $LiBH_4$ followed by 2 drops of TBHP were added into the reaction mixture after 3 h during the 4 h reaction. Cycloaddition of CO_2 to SO: the solution was transferred to a high-pressure reactor and was run at 2.4 MPa, 55°C, 6 h and 600 rpm.

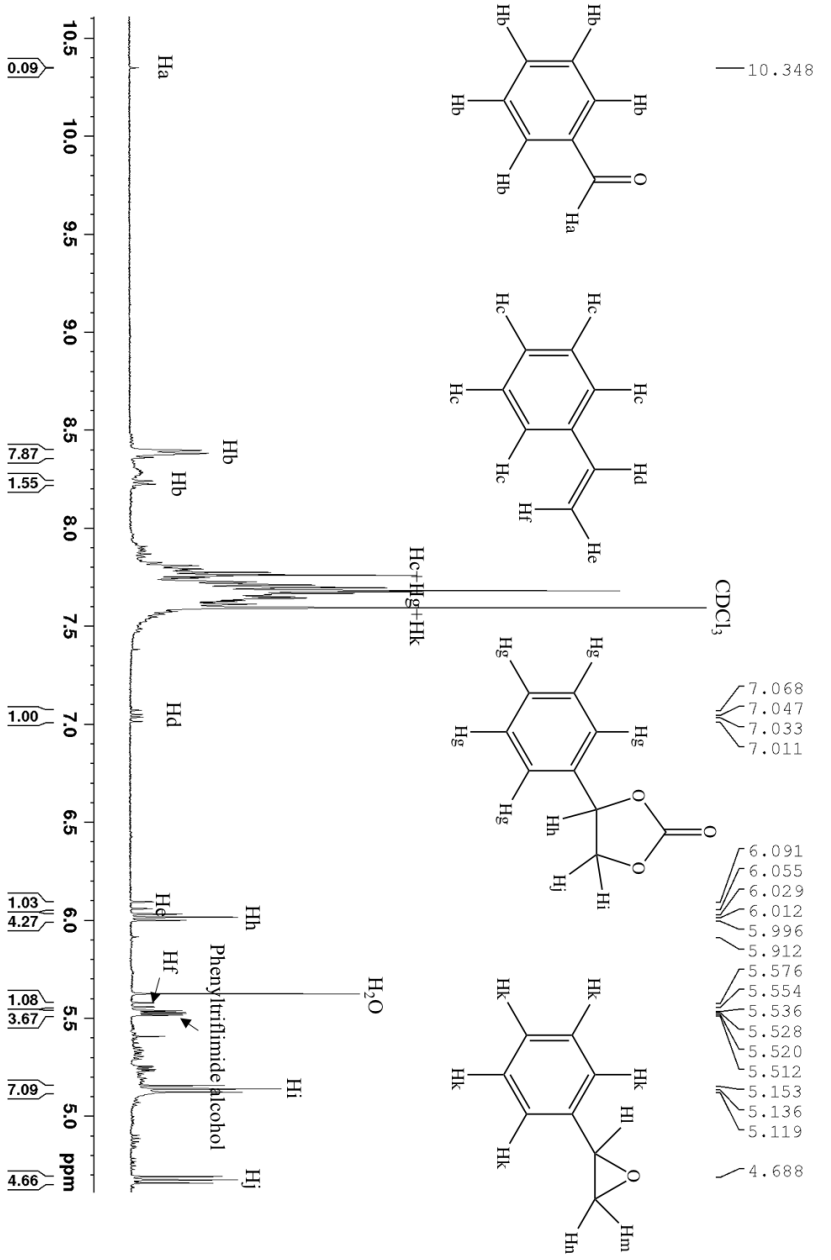
10.348
7.068
7.047
7.033
7.011
6.091
6.055
6.029
6.012
5.996
5.912
5.576
5.554
5.536
5.528
5.520
5.512
5.153
5.136
5.119
4.688
CDCl3
H2O
Ha
Hb
Hc+Hg+Hk
Hd
Hc
Hh
Hf
Phenyltriflimide
alcohol
Hi
Hj
0.09
7.87
1.55
1.00
1.03
4.27
1.08
3.67
7.09
4.66
ppm

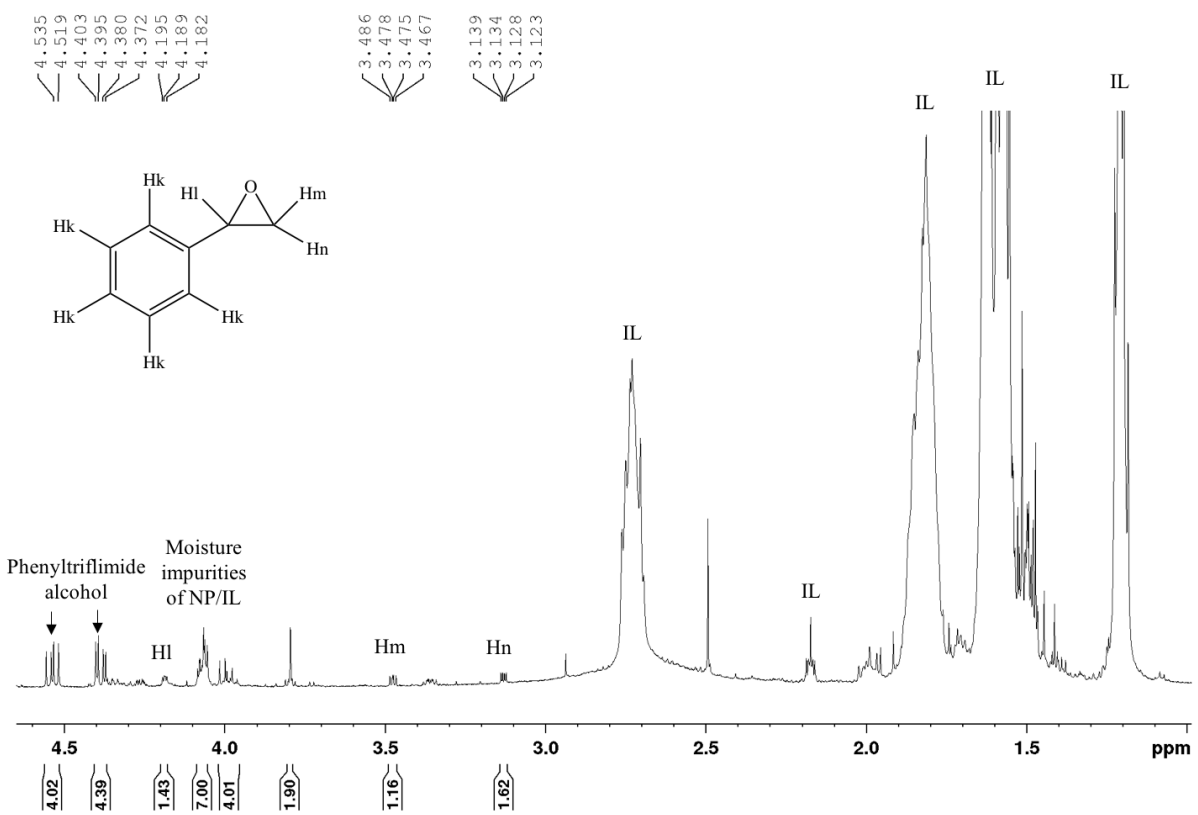

Figure 4.2 (a), (b) Direct synthesis of SC catalyzed by Au/[P66614][NTf_2] with individual peak assignment. Styrene epoxidation: 5.24 mmol styrene:0.0102 mmol Au:3.40 mmol ILs:19.7mmol TBHP, 0.1 MPa, and 80 °C for 4 h. A drop of $LiBH_4$ followed by 2 drops of TBHP were added into the reaction mixture after 3 h during the 4 h reaction. Cycloaddition of CO_2 to SO: the solution was transferred to a high-pressure reactor and was run at 2.4 MPa, 55°C, 7 h and 600 rpm.

Conversions were calculated via relative quantization from the peak areas of individual, well-separated reactant and product peaks from ^{1}H NMR spectra. BA1 stands for benzaldehyde and BA2 stands for benzoic acid. Also, please note that although the conversion for the direct synthesis of SC reported in this chapter are higher than the conversion of styrene epoxidation in Chapter 2, there is a significant amount of intermediate SO present in the resulting solution (Table 4.4).

Conversion for the direct synthesis of SC catalyzed by Au/[P66614][Cl]

$$= \frac{All\ products}{All\ products + all\ left - over\ reactants}$$

$$= \frac{\text{SC H} + \text{SO H} + \text{BA1 H} + \text{BA2 H} + \text{Chlorophenyl} - \text{OH H}}{\text{Styrene H} + \text{SC H} + \text{SO H} + \text{BA1 H} + \text{BA2 H} + \text{Chlorophenyl} - \text{OH H}} \times 100\%$$

$$= \frac{1.00 + 2.03 + 0.02 + 0.00 + 1.88}{0.00 + 1.00 + 2.03 + 0.02 + 0.00 + 1.88}$$

$$= 100\%$$

Conversion for the direct synthesis of SC catalyzed by Au/[P66614][NTf_2]

$$= \frac{All\ products}{All\ products + all\ left - over\ reactants}$$

$$= \frac{\text{SC H} + \text{SO H} + \text{BA1 H} + \text{Phenyltriflimide} - \text{OH}}{\text{Styrene H} + \text{SC H} + \text{SO H} + \text{BA1 H} + \text{Phenyltriflimide} - \text{OH}} \times 100\%$$

$$= \frac{4.27 + 1.16 + 0.09 + 4.02}{1.00 + 4.27 + 1.16 + 0.09 + 4.02}$$

$$= 90\%$$

$$\text{Selectivity} = \frac{\text{Desired product}}{\text{All products formed}}$$

4.3 Results & Discussion

4.3.1 Gold Nanoparticles in [P66614][Cl] as Catalysts

The direct synthesis of SC from styrene and CO_2 was prepared using the previously established reaction conditions in Chapter 2 and 3. SC and SO were formed along with other by-products such as benzaldehyde (BA1), benzoic acid (BA2) and an unknown substance that we believe to be an associated of chlorophenyl alcohol. Similar to what was seen in Chapter 2, styrene epoxidation was effectively catalyzed by Au/[P66614][Cl], resulting in 60% conversion and 80% selectivity of SO after 4 h of reaction at 80 °C. The solution was then transferred to a sealed reactor for the cycloaddition of CO_2 to SO in which the [P66614][Cl] IL acts as both a solvent and a catalyst (via the chloride nucleophile). Table 4.1 summarizes the progress for SC reaction inside the sealed reactor using a time-dependent measurement of the conversions. It was expected that the conversions of SO increased with increasing in reaction time based on Chapter 3 results, and this was true up to 6 h. After 6 h, the conversion reached a maximum of 100% and the selectivity for SC was found to be at 20% with a significant amount of the intermediate SO present. Further increasing in reaction time, however, lowered the SC selectivity. Two possible reasons for the reduced activity with longer reaction times are the ring-opening of epoxides by the IL chloride anion to give chlorophenyl alcohol, and the decomposition of SC to SO with long reaction time.[16,17]

Table 4.1 Effect of reaction time on the direct synthesis of SC catalyzed by Au/[P66614][Cl].

Entry[a]	Time[b] (h)	Conversion[c] (%)	Selectivity[d] (%)				
			SC	SO	BA1	BA2	Chlorophenyl-OH
1	1	85	2	80	1	1	16
2	2	87	3	79	1	1	16
3	3	89	8	69	1	1	21
4	4	92	12	61	1	1	25
5	5	96	15	49	0	0	36
6	6	100	20	41	0	0	39
7	7	100	17	43	0	0	40

[a] Styrene epoxidation: 5.24 mmol styrene:0.0102 mmol Au:19.7mmol TBHP, 0.1 MPa, 4 h. A drop of $LiBH_4$ followed by 2 drops of TBHP were added into the reaction mixture after 3 h during the 4 h reaction. Cycloaddition of CO_2 to SO: The solution was transferred to a high-pressure reactor and was run at 2.4 MPa, 55ºC, 600 rpm for 1-7 h.

[b] Reaction time for the cycloaddition of CO_2 to SO only

[c, d] Conversion and Selectivity (see Experimental 4.2.3 for reproducibility discussion and Experimental 4.2.5 for sample calculation).

4.3.2 Gold Nanoparticles in [P66614][NTf_2] as Catalysts

A non-halide IL, [P66614][NTf_2], was used to compare with the halide IL, [P66614][Cl] for the direct synthesis of SC from styrene and CO_2. Similar to [P66614][Cl], Au NPs were synthesized in [P66614][NTf_2] via in situ $LiBH_4$ reduction without any organic solvents or secondary stabilizers. Although the [NTf_2^-] anion has a weaker coordinating ability comparing to

the [Cl^-] anion, it still produces stable dispersions of Au NPs, thus ensuring the Au NPs are catalytically active for styrene epoxidation.[18]

4.3.2.1 Characterization

Au NPs were found to be stable in [P66614][NTf_2] and this IL is considerably viscous, although the viscosity can be lowered upon heating. The UV-Vis absorbance spectra and TEM images of the Au NPs synthesized in [P66614][NTf_2] are shown in Figure 4.3a and 4.3b respectively. The obtained Au NPs were mostly uniform in size, with an average size of 4.2 ± 0.5 nm (Figure 4.3c). This is in agreement with the UV-Vis spectra, in which the plasmon peak for the Au NPs was recorded at $\lambda \sim 525$ nm for Au/[P66614][NTf_2] vs. $\lambda \sim 520$ nm for the Au/[P66614][Cl] system. The Au NPs synthesized in [P66614][NTf_2] were found to show a lower uniformity (standard deviation = 0.1 for [P66614][Cl] vs. 0.5 for [P66614][NTf_2]), which is likely due to the weaker coordinating ability of [NTf_2^-] anions with the Au surfaces.

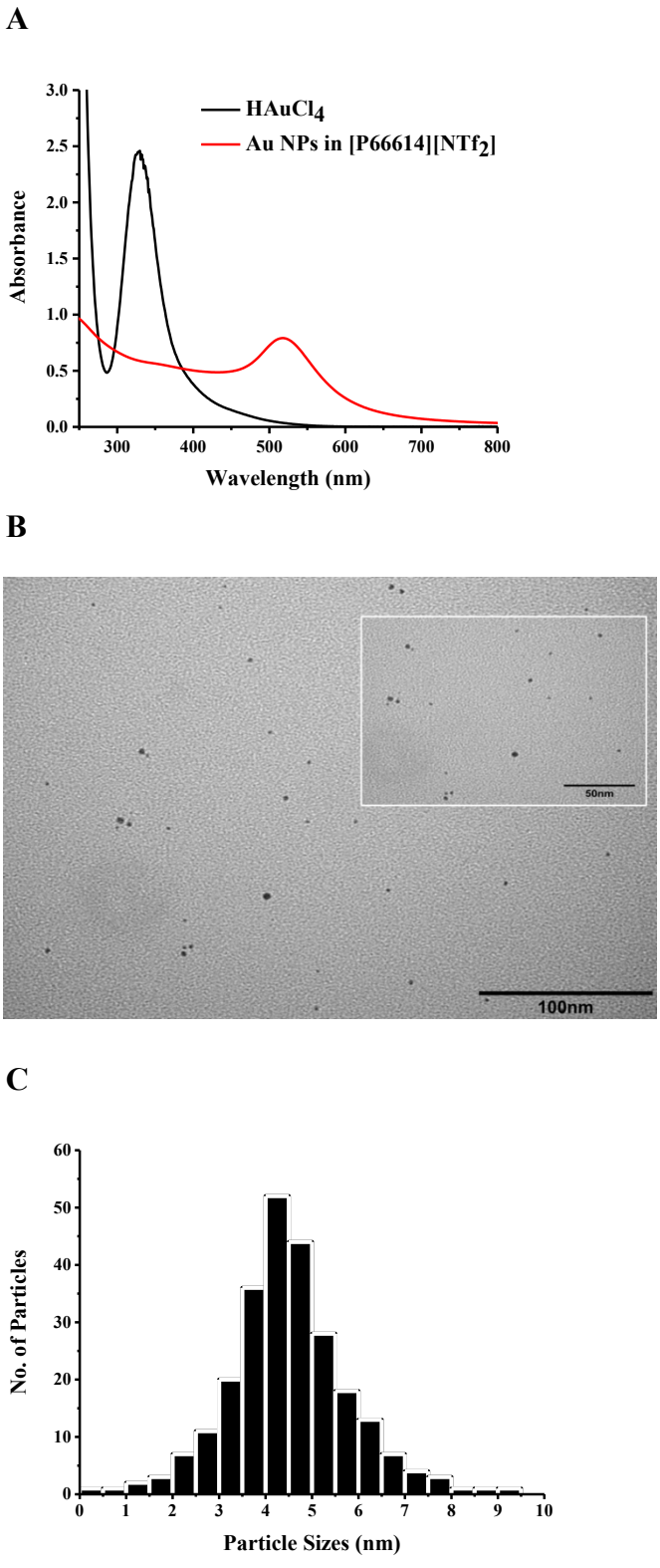

Figure 4.3 (a) UV-Vis spectra, (b) TEM images and (c) Size distribution of Au NPs synthesized in [P66614][NTf_2].

4.3.2.2 Styrene Epoxidation

The reaction conditions studied in Chapter 2 were again applied for the styrene epoxidation catalyzed by Au NPs in [P66614][NTf_2] (Figure A.2). Table 4.2 compares the conversion and product selectivity when Au NPs in [P66614][Cl] and [P66614][NTf_2] were used as catalysts. It was found that higher conversion was achieved with Au NPs in [P66614][NTf_2] compared to [P66614][Cl], which probably because the NPs are less prone toward oxidation in the presence of [NTf_2] anions. Increasing in conversion with Au/[P66614][NTf_2] can also be explained by how the NPs are being stabilized by the anionic species in the IL: although the [NTf_2^-] anion has a larger size, thus a smaller surface charge density compared to the [Cl^-] anion; it is sterically hindered, thus offering better electrosteric stabilization for the Au NPs. Similar to Au/[P66614][Cl], reactions in the Au/[P66614][NTf_2] also produces phenyltriflimide alcohol as a by-product due to the excess amount of [NTf_2^-] anions present in the solution. There was evidence in the ^{1}H NMR spectra for this, in which the peaks at 5.22, 4.51, and 4.37 ppm have chemical shifts and splitting patterns consistent with this assignment. No alternative by-products reported in literature fitted well with the obtained data. Selectivity toward SO formation was very similar between the two catalytic systems (both resulted in 80% SO selectivity); however, Au NPs in [P66614][NTf_2] is still a better choice as it produces slightly less by-products.

Table 4.2 Comparison between Au NPs in [P66614][Cl] and Au NPs in [P66614][NTf_2] as catalysts for styrene epoxidation.

Catalyst[a]	Conversion[b] (%)	Selectivity[c] (%)			
		SO	BA1	BA2	Unk[d]
Au NPs in [P66614][NTf_2]	70	80	2	0	18
Au NPs in [P66614][Cl]	60	80	2	2	16

[a] Reaction conditions: 5.24 mmol styrene:0.01012 mmol Au:19.7 mmol TBHP, 0.1 MPa, 80°C, 4 h. 1 drop of $LiBH_4$ followed by 2 drops of TBHP were added after 3 h during the 4 h reaction.

[b, c] Conversion and Selectivity (see Experimental 4.2.3 for reproducibility discussion and Experimental 4.2.5 for sample calculation).

[d] The unknown is phenyltrifimide alcohol and chlorophenyl alcohol for Au/[P66614][NTf_2] and Au/[P66614][Cl], respectively.

4.3.2.3 Effect of Reaction Time on Cycloaddition of SO and CO_2

The reaction conditions established in Chapter 3 were applied for the cycloaddition of CO_2 to SO in which [P66614][NTf_2] functions as a solvent for CO_2 and a catalyst via the [NTf_2^-] nucleophile (Figure A.3). Table 4.3 shows the influence of reaction time on conversion and selectivity. Similar to results seen for [P66614][Cl], the reaction time also acts as a favourable factor for the ring-opening of SO in the [NTf_2^-] system as the conversion increased from 1 to 7 h (i.e. 48% to 68%). The conversion reached its maximum of 68% after 7 h and further increases in reaction time did not improve the conversion. Comparing to [Cl^-] anions, [NTf_2^-] anions resulted in a lower conversion, mainly because [NTf_2^-] is a poorer nucleophile. Control studies with Au NPs in IL were also carried out and no changes in conversion or/and selectivity were observed.

Table 4.3 Effect of reaction time on the ring-opening of SO catalyzed by [P66614][NTf_2].

Entry[a]	Time (h)	Conversion (%)[b]
1	1	48
2	2	52
3	3	55
4	4	58
5	5	60
6	6	65
7	7	68
8	8	68

[a] Reaction conditions used: 8.49mmol SO:28.6mmol IL, 55ºC, 2.4 MPa, and 600 rpm.

[b] Conversion (see Experimental 4.2.3 for reproducibility discussion and Experimental 4.2.5 for sample calculation).

4.3.2.4 Direct Synthesis of Styrene Carbonate

Table 4.4 shows the conversion and selectivity toward SC formation for the direct synthesis of SC catalyzed by Au NPs in [P66614][NTf_2]. Increasing the reaction time has a positive effect on the CO_2 coupling reaction with SO and complete conversion was achieved at 7 h, though there was still a significant amount of the intermediate SO present in the solution. The selectivity of SC, however, decreased over time, indicating that the epoxide reacts toward by-products, such as chlorophenyl alcohol.

Table 4.4 Effect of reaction time on the direct synthesis of SC catalyzed by Au/[P66614][NTf_2].

Entry[a]	Time[b] (h)	Conversion[c] (%)	Selectivity[d] (%)			
			SC	SO	BA	Phenyltriflimide-OH
1	1	72	22	51	1	26
2	2	75	25	45	1	29
3	3	77	27	40	1	32
4	4	80	30	34	1	35
5	5	84	36	29	1	34
6	6	87	39	22	1	38
7	7	90	45	12	1	42
8	8	90	42	15	1	42

[a] Styrene epoxidation: mmol ratio of 5.24 styrene:0.0102 Au:19.7 TBHP, 0.1 MPa, and 4 h. A drop of $LiBH_4$ followed by 2 drops of TBHP were added to the reaction after 3 h during the 4 h reaction. Cycloaddition of CO_2 to SO: 2.4 MPa, 55 ºC, 600 rpm for 1-8 h.

[b] Reaction time is for the cycloaddition of CO_2 to SO only.

[c, d] Conversion and Selectivity (see Experimental 4.2.3 for reproducibility discussion and Experimental 4.2.5 for sample calculation).

Kinetic studies for the direct synthesis of styrene carbonates catalyzed by Au NPs synthesized in [P66614][NTf_2] also showed pseudo-first order kinetics by varying CO_2 pressure without changing the catalyst concentration as the catalyst is also the solvent in this case (Figure 4.4). The kinetic reaction constant, k, matched favorably with the generated conversion data from NMR spectra.

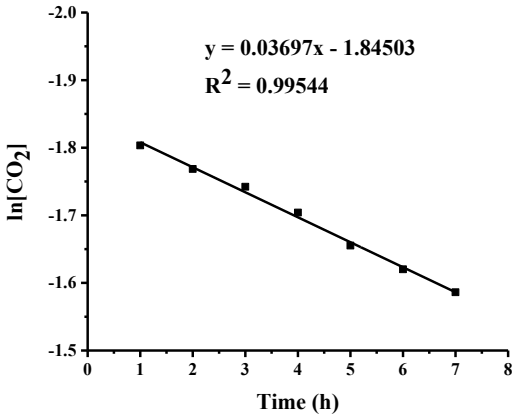

Figure 4.4 Pseudo-first-order plotted SC formation rate for Au NPs in [P66614][NTf_2] over 7 h. Reaction conditions used: 5.24 mmol styrene:0.0102 mmol Au:19.7 mmol TBHP, 0.1 MPa, and 4 h. A drop of $LiBH_4$ followed by 2 drops of TBHP were added to the reaction after 3 h during the 4 h reaction. The solution was then transferred to a high-pressure reactor and was run at 2.4 MPa, 55 ºC, 600 rpm for 1-7 h. Please refer to Experimental 4.2.3 for reproducibility discussion.

4.4 Conclusion

The catalytic systems Au NPs in [P66614][Cl] and [P66614][NTf2] were investigated for the direct synthesis of SC from styrene and CO_2 at elevated temperatures and pressures. The following conclusions were drawn from the study:

1. The studied reaction conditions for styrene epoxidation and cycloaddition CO_2 to SO in Chapter 2 and 3 were applied for the direct synthesis of SC. Complete conversion with low selectivity toward SC was achieved for the Au/[P66614][Cl] catalytic system due to a significant amount of the intermediate SO present in the solution.

2. Both Au NPs in [P66614][Cl] and [P66614][NTf_2] can catalyze the direct synthesis of SC at elevated temperatures and under high pressures; however, Au/[P66614][NTf2] resulted in a higher SC selectivity.

3. Higher conversions were observed for the styrene epoxidation when Au/[P66614][NTf_2] was used (70% for Au/[P66614][NTf_2] vs. 60% for Au/[P66614][Cl]). Selectivity toward SO was similar between the two catalytic systems.

4. Higher conversions were observed for the cycloaddition of CO_2 to SO when [P66614][Cl] was used, mainly because the [Cl] anion is a stronger nucleophile. Both yielded SC as the only product.

5. The optimized reaction conditions for the direct synthesis of SC from styrene and CO_2 when Au NPs synthesized in [P66614][Cl] (and [P66614][NTf_2]) was as follows:

- For styrene epoxidation: 5.24 mmol styrene:0.0102 mmol Au:19.7 mmol TBHP, 0.1 MPa and 4 h. A drop of $LiBH_4$ followed by 2 drops of TBHP were added into the reaction mixture after 3 h during the 4 h reaction.
- For the cycloaddition of CO_2 to SO: the reaction solution was transferred to a high-pressure reactor and was run at 2.4 MPa, 55 ºC, 600 rpm for 6 h for Au/[P66614][Cl] (7 h for Au/[P66614][NTf_2]).

4.5 References

(1) Fujita, S.-I.; Yoshida, H.; Liu, R.; Arai, M. Catalytic Transformation of CO_2 into Value-Added Organic Chemicals. In *New and future developments in catalysis*: *Activation of carbon dioxide*, Suib, S. L.; Elsivier: Amsterdam, Netherlands, 2013; 163–169.

(2) Aresta, M.; Dibenedetto, A. *J. Mol. Catal. Chem.* **2002**, *182*, 399–409.

(3) Srivastava, R.; Srinivas, D.; Ratnasamy, P. *Catal. Lett.* **2003**, *91*, 133–139.

(4) Bai, D.; Jing, H. *Green Chem***. 2010**, *12*, 39–41.

(5) Du, Z.; Shao, Z. *Chem. Soc. Rev.* **2013**, *42*, 1337–1378.

(6) Sun, J.; Liang, L.; Sun, J.; Jiang, Y.; Lin, K.; Xu, X.; Wang, R. *Catal. Surv. Asia* **2011**, *15*, 49–54.

(7) Jasiak, K.; Krawczyk, T.; Pawlyta, M.; Jakóbik-Kolon, A.; Baj, S. *Catal. Lett.* **2016**, *146*, 893–901.

(8) Della Pina, C.; Falletta, E.; Prati, L.; Rossi, M. *Chem. Soc. Rev.* **2008**, *37*, 2077–2095.

(9) Wilkes, J. S. Ion. Liq. Promis. Altern. *Media Org. Synth. Catal.* **2004**, *214*, 11–17.

(10) Stevanovic, S.; Costa Gomes, M. F. J. *Chem. Thermodyn.* **2013**, *59*, 65–71.

(11) Ramdin, M.; de Loos, T. W.; Vlugt, T. J. H. *Ind. Eng. Chem. Res.* **2012**, *51*, 8149–8177.

(12) Yu, C.-H.; Chih-Hung, H.; Tan, C.-S. *Aerosol Air Qual. Res*. **2012**, *12*, 745–769.

(13) Boot-Handford, M. E.; Abanades, J. C.; Anthony, E. J.; Blunt, M. J.; Brandani, S.; Mac Dowell, N.; Fernandez, J. R.; Ferrari, M.-C.; Gross, R.; Hallett, J. P.; Haszeldine, R. S.; Heptonstall, P.; Lyngfelt, A.; Makuch, Z.; Mangano, E.; Porter, R. T. J.; Pourkashanian, M.; Rochelle, G. T.; Shah, N.; Yao, J. G.; Fennell, P. S. *Energy Environ. Sci.* **2014**, *7*, 130–189.

(14) Manic, M. S.; Macedo, E. A.; Najdanovic- Visak, V. *Fluid Ph. Equilibria* **2012**, 324, 8–12.

(15) Manic, M. S.; Queimada, A. J.; Macedo, E. A.; Najdanovic-Visak, V. J. *Supercrit. Fluids* **2012**, *65*, 1–10.

(16) Bhanage, B. M.; Fujita, S.; Ikushima, Y.; Torii, K.; Arai, M. *Green Chem*. **2003**, *5*, 71–75.

(17) Paul, S.; Zhu, Y.; Romain, C.; Brooks, R.; Saini, P. K.; Williams, C. K. *Chem. Commun.* **2015**, *51*, 6459–6479.

(18) Banerjee, A.; Scott, R. W. J. *Green Chem***. 2015**, *17*, 1597–1604.

5.0 Conclusions and Future Work

5.1 Conclusions and Discussion

This dissertation examined the catalytic activity of Au NPs stabilized in tetraalkylphosphonium halide IL for the direct synthesis of cyclic carbonates from alkenes and CO_2. The individual steps of the reaction, alkene epoxidation and cycloaddition of CO_2 into epoxides, were studied in detail, and the reaction conditions were optimized. The established reaction conditions were then combined and employed for cyclic carbonate formation, in which halide and non-halide tetraalkylphosphonium ILs were used as catalysts.

In **Chapter 2**, the synthesis and characterization of the Au NPs in [P66614][Cl] was reported. The synthesized NPs were found to be in 4.1 ± 0.2 nm size range, which is consistent with previous work by our group.[1] The catalytic behavior of the synthesized Au NPs was then explored for alkene epoxidation, in which styrene and propylene acted as substrates and tert-butyl hydroperoxide functioned as an oxidant. For styrene epoxidation, styrene oxide was the major product in every case. The effect of reaction temperature, from 40–90 °C, was studied at a substrate:catalyst mmol ratio of 5.24:0.01012 and 0.1 MPa pressure for 4 h. Highest conversions were obtained when the temperature was at 80 °C, and polymerization of styrene was found to occur when the temperature went above 80 °C. TON values increased from 233 to 258, with an increase in temperature from 70–80 °C, suggesting increasing in temperature results in a positive effect on the reaction conversion as well as the catalytic activity of the catalyst. Recovery of the oxidized Au NPs was also attempted by re-addition of $LiBH_4$ at various point during the reaction.

The highest overall conversion was achieved when $LiBH_4$ was re-added into the reaction mixture after 3 h during the 4 h reaction. The established reaction conditions for styrene epoxidation, however, proved to be challenging when propylene acted as the substrate, mainly due to mass-transfer issues in which not enough propylene gas can dissolve into the liquid phase of the reaction. Modifications of the reaction, such as raising the reaction pressure, lengthening the reaction time, and cooling the product to capture the desired product propylene oxide, were attempted but did not yield any propylene oxide product.

The subsequent reaction, cycloaddition of CO_2 into propylene/styrene oxide, was studied in detail in **Chapter 3**. It was found that both of the reactions are mass-transfer limited at low pressure and the higher the CO_2 pressure, thus the higher the CO_2 concentration, the higher the conversion obtained. Kinetic studies were also done, and pseudo-first order kinetics was observed at higher pressures for this reaction. Increasing stirring rate to 600 rpm helped to take the system out of the mass transfer limiting region. Styrene carbonate reactions, however, required a higher reaction temperature compared to propylene carbonate reactions, mainly due to the sterically bulky phenyl group. The activation energy for styrene carbonate formation was found using an Arrhenius plot, and a value of 50 $kJmol^{-1}$ was acquired.

The previously established reaction conditions were then combined for the direct synthesis of cyclic carbonates from alkenes and CO_2 in **Chapter 4** at elevated temperatures and pressures, in which Au NPs stabilized in the [P66614][Cl] and [P66614][NTf_2] ILs functioned as catalysts. It was found that higher overall conversions were obtained when Au/[P66614][Cl] acted as the catalyst but lower selectivity toward SC formation was seen. Particularly, Au/[P66614][NTf_2] showed higher conversions for styrene epoxidation but lower conversions for the ring-opening of

epoxides, while Au/[P66614][Cl] showed the opposite behaviour. Selectivity toward SO was similar for the two catalysts (both resulted in 80% selectivity toward SO formation).

While the use of metal NPs synthesized in ILs has distinct advantages, there are also some challenges associated with these systems. The presence of a significant amount of the intermediates, for example, can potentially limit the utility of this catalytic system for industrial applications. However, a comparison of reaction conversion and selectivity toward SC in the direct synthesis of SC from CO_2 and styrene at elevated pressures and temperature, catalyzed by Au NPs and/or ILs, shows that NP/IL as catalysts lead to conversion and selectivity comparable to other previously studied catalytic system (Table 5.1). Increasing CO_2 pressure instead of temperature might further improve the catalytic activity as the cycloaddition reaction of epoxides and CO_2 are already highly exothermic.[2] However, high pressures pose greater safety concerns as well as challenges for reactor design, thus might not be suitable for industrial applications. Recyclability of the NP/IL catalytic system can also be difficult to achieve in practice, mainly due to NP sintering, aggregation, or oxidation under reaction conditions, thus limiting the utility of these catalytic system for further reactions. Furthermore, the cost associated with moderate and high degree of purity IL manufacture is much greater compared to traditional organic solvents, though the commercial availability of these ILs has improved considerably over the last few years and prices have already gone down significantly.[3] Still, if the ILs can be recycled and its lifetime proved to be long enough, its price will probably not matter when its cost has to be weighed against current available chemicals or catalysts.

Table 5.1 Comparison of the current catalytic system with other previous ones for the direct synthesis of SC.

Catalysts	Oxidant	CO_2 (MPa)	Temp. (°C)	Time (h)	Con. (%)	Sel. (%)
[4]MTO/Zn[emim]$_2$Br$_4$/[bmim]BF_4	UHP	3	110	4	>99	83
[5]Au/SiO_2-$ZnBr_2$/Bu_4NBr	CHP	1	80	4	76	40
[6]Au/$Fe(OH)_3$–$ZnBr_2$/Bu_4NBr	TBHP	4	80	10	95	53
[7]Au/CNT/[bmim][Br-$ZnBr_2$]	TBHP	1.2	80, 120	4	75	60
This work: Au/[P66614][Cl]	TBHP	2.4	80, 55	4, 6	100	20
This work: Au/[P66614][NTf_2]	TBHP	2.4	80, 55	4,7	90	45

MTO = methyltrioxorhenium, emim = 1-ethyl-3-methylimidazolium ion, bmim = 1-Butyl-3-methylimidazolium, UHP = urea hydrogen peroxide, CHP = cymene hydroperoxide, CNT = multi-walled-carbon nanotubes.

5.2 Future Work

Au NPs synthesized in tetraalkylphosphonium ILs have proven their use as catalysts for the direct synthesis of cyclic carbonates from alkenes and CO_2. In the following sections, recycling of the NP/IL catalytic system for cyclic carbonate formation, and modifications for stereo-selective cyclic carbonate formation are discussed in some detail.

5.2.1 Products extraction and catalyst recycling in cyclic carbonate reaction

The application of the NP/IL catalytic system for industrial cyclic carbonate reactions is limited by the NP oxidation, growth and/or aggregation in tetraalkylphosphonium ILs during

alkene epoxidation, and separation of any unreacted substrates and/or products after the cycloaddition of CO_2 to epoxides. Hence, it is necessary to find a protocol for effective product extraction from the reaction mixture and catalyst reutilization.

The removal of the desired products from the IL phase for both alkene epoxidation and the cycloaddition of CO_2 into epoxides have been investigated experimentally under reduced pressure or via distillation due to the negligible volatility and high thermal stability of the ILs.[8,9] Alvaro et al., for example, removed the leftover substrate and the products by liquid-liquid extraction using volatile organic solvents for the styrene oxide and CO_2 reaction, in which the chromium salen complex/[1-butyl-3-methylimidazolium][PF_6] IL function as catalysts.[8] The catalysts were then recovered and reused; however, catalytic activity was found to decrease over time due to leaching of the chromium catalyst to the organic solvent used in the extraction.[8] Similarly, Paninho et al. employed the use of supercritical CO_2 to extract the final product of propylene carbonate reaction catalyzed by Zn(II) complexes in tetrabutylammonium bromide IL by slowly depressurizing the reaction reactor (from 11.5 MPa to 0.1 MPa) and capturing the product in a glass trap immersed in an ice bath over 3 h.[8] Due to the difference in volatility, propylene carbonate was filtered from the glass trap, whereas the highly volatile propylene oxide was removed with CO_2 out of the system.[9] This procedure allowed for catalyst reutilization for 3 catalytic cycles, without loss of activity and with good reproducibility.[9]

Although the NP/IL catalytic system can be recyclable and used readily after product recovery,[10–12] the catalytically active NPs begin to grow after a finite number of catalytic cycles, resulting in subsequent loss of surface area and catalytic activity even in the presence of capping agents or stabilizers that protect them from agglomeration and sintering.[13] A number of reports have examined the recovery and re-dispersion of the Au NPs, such as treating the NPs with an

oxidant (i.e. O_2, H_2O_2), followed by a reductant (i.e. $LiBH_4$ and $LiAlBH_4$),[14] or using a methyl iodide treatment at moderate to high temperature.[15] In situ laser radiation of the NPs dispersed in IL has also been employed, and the colloidal solution was found to be stable for weeks without any change in their size.[16]

5.2.2 Stereo-selective synthesis of cyclic carbonates

While the NP/IL catalytic system has been used extensively in cyclic carbonate syntheses from various epoxides, less focus has been directed toward stereo-controlled cyclic carbonate reactions, particularly the enantioselective syntheses. Synthesis of enantiopure cyclic carbonates are often prepared by coupling enantiopure epoxides with CO_2 with metal complex supported on IL act as catalysts.[17,18] Buonerba et al. developed a bifunctional Fe(III) complex with bromide ligands for the epoxidation of (R)-styrene oxide and CO_2, yielding 72% ee of cyclic carbonates.[17] Duan et al. reported the use of cobalt salen complexes in imidazolium-based ILs for catalytic asymmetric coupling of epoxides with CO_2 at moderate reaction conditions, in which cyclic carbonates in moderate ee was collected up to 57% (Figure 5.1).[18]

Chiral ILs, often consist of alkyl imidazole cations and amino acid-derived chiral anions, have also been investigated as co-catalyst along with Co(III) salen complexes for the stereo-selective cycloaddition of CO_2 into epoxides.[19-22] Zhang et al. reported the use of Co(III) salen complex coupled with [tertbutylammonium][L-proline amino acid] IL as catalysts for the propylene carbonate and styrene carbonate reactions with CO_2, resulting in 74.6% ee value of (S)-propylene carbonate and 72% ee value of (S)-styrene carbonate, respectively.[19] Although most of the chiral moieties built into the IL structure have been explored for imidazolium-based ILs,[20,21] there is no reason why this cannot be done for tetraalkylphosphonium ILs as well. Indeed,

Fukumoto et al. synthesized chiral ILs with tetrabutylphosphonium cations and a number of amino acid-derived anions.[22]

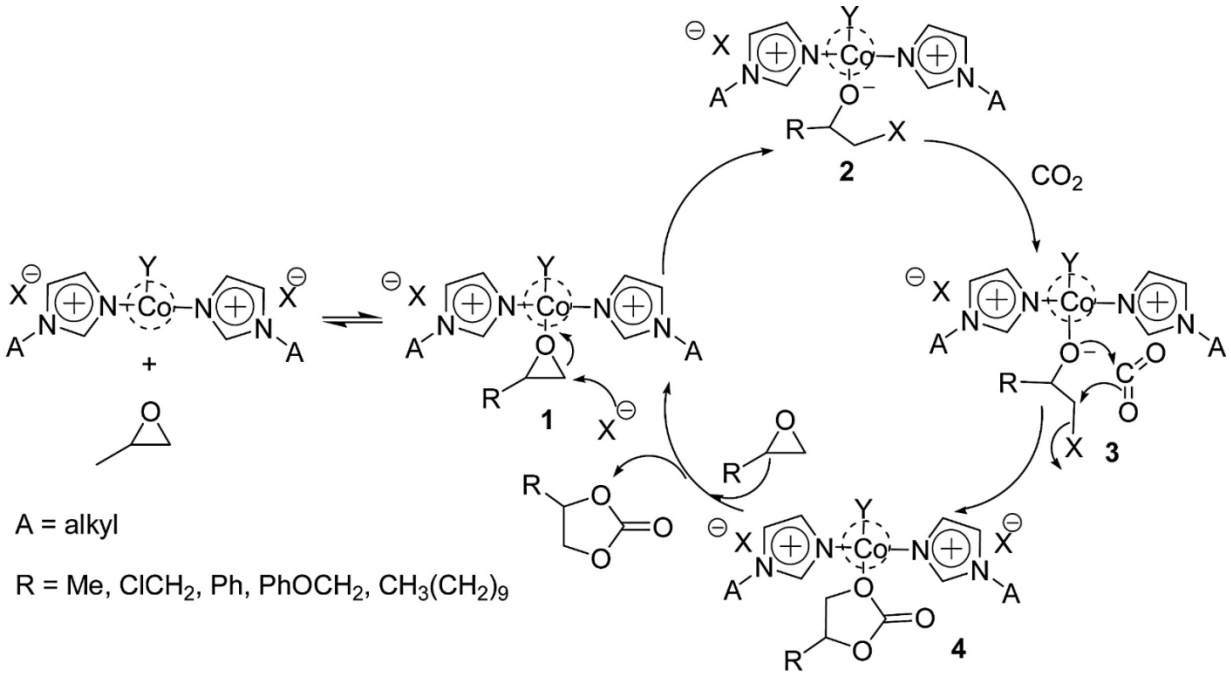

Figure 5.0.1 Proposed mechanism for the cycloaddition of CO_2 into epoxides catalyzed by Co(III) salen complexes in imidazolium-based ILs. Reprinted with permission from reference (18). Copyright © 2016 Elsevier.

5.3 References

(1) Banerjee, A.; Theron, R.; Scott, R. W. J. *ChemSusChem* **2012**, *5*, 109–116.

(2) Lang, X.-D.; He, L.-N. *Chem. Rec.* **2016**, *16*, 1337–1352.

(3) Wasserscheid, P.; Haumann, M. Catalyst Recycling Using Ionic Liquids. In *Catalyst Separation, Recovery and Recycling*, Cole-Hamilton, D. J.; Tooze, R. P; Springer: Dordrecht, The Netherlands, 2006; 183–184.

(4) Ono, F.; Qiao, K.; Tomida, D.; Yokoyama, C. *Appl. Catal. Gen.* **2007**, *333*, 107–113.

(5) Sun, J.; Fujita, S.; Zhao, F.; Hasegawa, M.; Arai, M. *J. Catal.* **2005**, *230*, 398–405.

(6) Wang, Y.; Sun, J.; Xiang, D.; Wang, L.; Sun, J.; Xiao, F.-S. *Catal. Lett.* **2009**, *129*, 437–443.

(7) Jasiak, K.; Krawczyk, T.; Pawlyta, M.; Jakóbik-Kolon, A.; Baj, S. *Catal. Lett.* **2016**, *146*, 893–901.

(8) Alvaro, M.; Baleizao, C.; Das, D.; Carbonell, E.; García, H. *J. Catal.* **2004**, *228*, 254–258.

(9) Paninho, A. B.; Ventura, A. L. R.; Branco, L. C.; Pombeiro, A. J. L.; da Silva, M. F. C. G.; da Ponte, M. N.; Mahmudov, K. T.; Nunes, A. V. M. J. *Supercrit. Fluids* **2017**, *132*, 71–75.

(10) Yu, Y.; Hu, T.; Chen, X.; Xu, K.; Zhang, J.; Huang, J. *Chem. Commun.* **2011**, *47*, 3592–3594.

(11) Chaugule, A. A.; Tamboli, A. H.; Kim, H. *Fuel* **2017**, *200*, 316–332.

(12) He, Q.; O'Brien, J. W.; Kitselman, K. A.; Tompkins, L. E.; Curtis, G. C. T.; Kerton, F. M. *Catal. Sci. Technol.* **2014**, *4*, 1513.

(13) Bernardi, F.; Scholten, J. D.; Fecher, G. H.; Dupont, J.; Morais, J. *Chem. Phys. Lett.* **2009**, *479*, 113–116.

(14) Banerjee, A.; Theron, R.; Scott, R. W. J. *Chem. Commun.* **2013**, *49*, 3227–3229.

(15) Sá, J.; Taylor, S. F. R.; Daly, H.; Goguet, A.; Tiruvalam, R.; He, Q.; Kiely, C. J.; Hutchings, G. J.; Hardacre, C. *ACS Catal.* **2012**, *2*, 552–560.

(16) Gelesky, M. A.; Umpierre, A. P.; Machado, G.; Correia, R. R. B.; Magno, W. C.; Morais, J.; Ebeling, G.; Dupont, J. *J. Am. Chem. Soc.* **2005**, *127*, 4588–4589.

(17) Buonerba, A.; De Nisi, A.; Grassi, A.; Milione, S.; Capacchione, C.; Vagin, S.; Rieger, B. *Catal. Sci. Technol.* **2015**, *5*, 118–123.

(18) Duan, S.; Jing, X.; Li, D.; Jing, H. J. *Mol. Catal. Chem.* **2016**, *411*, 34–39.

(19) Zhang, S.; Huang, Y.; Jing, H.; Yao, W.; Yan, P. *Green Chem***. 2009**, *11*, 935–938.

(20) Payagala, T.; Armstrong, D. W. *Chirality* **2012**, *24*, 17–53.

(21) Ding, J.; Armstrong, D. W. *Chirality* **2005**, *17*, 281–292.

(22) Fukumoto, K.; Kohno, Y.; Ohno, H. *Chem. Lett.* **2006**, *35*, 1252–1253.

APPENDIX A

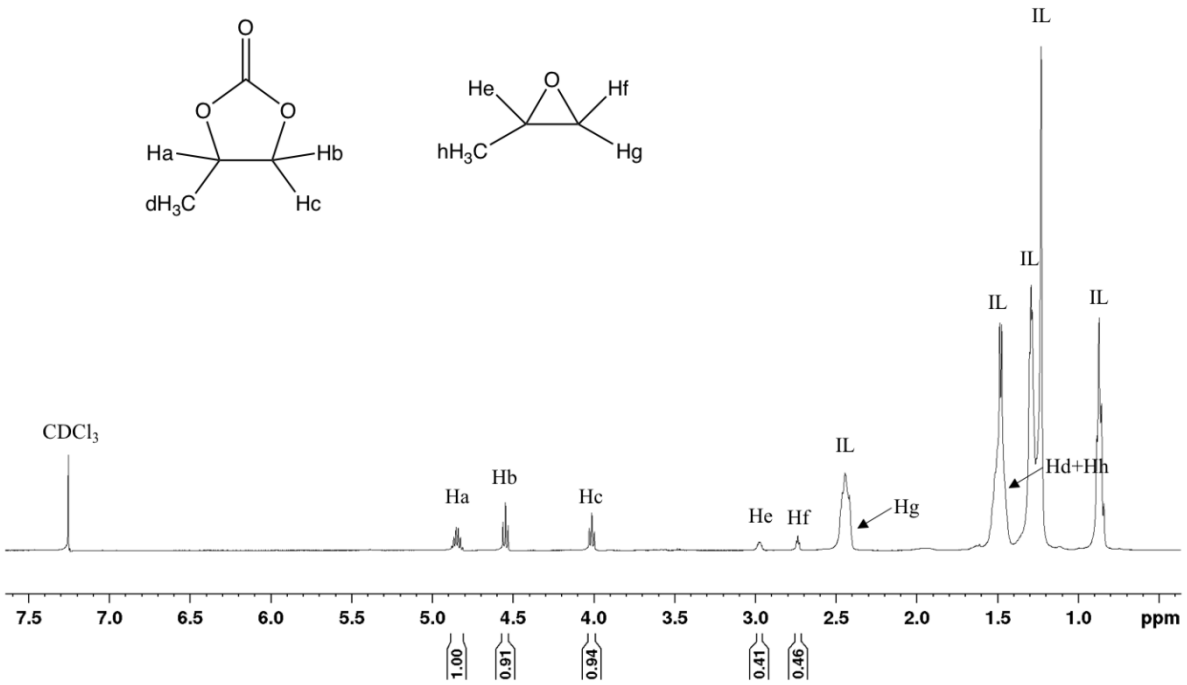

Figure A.1 Propylene carbonate reaction catalyzed by [P66614][Cl] without the use of the internal standard acetic acid. Reaction conditions used: substrate:catalyst mmol ratio of 8.49:28.6, 2.4 MPa, 3 h, 33 ºC, and stirring rate of 600 rpm.

A

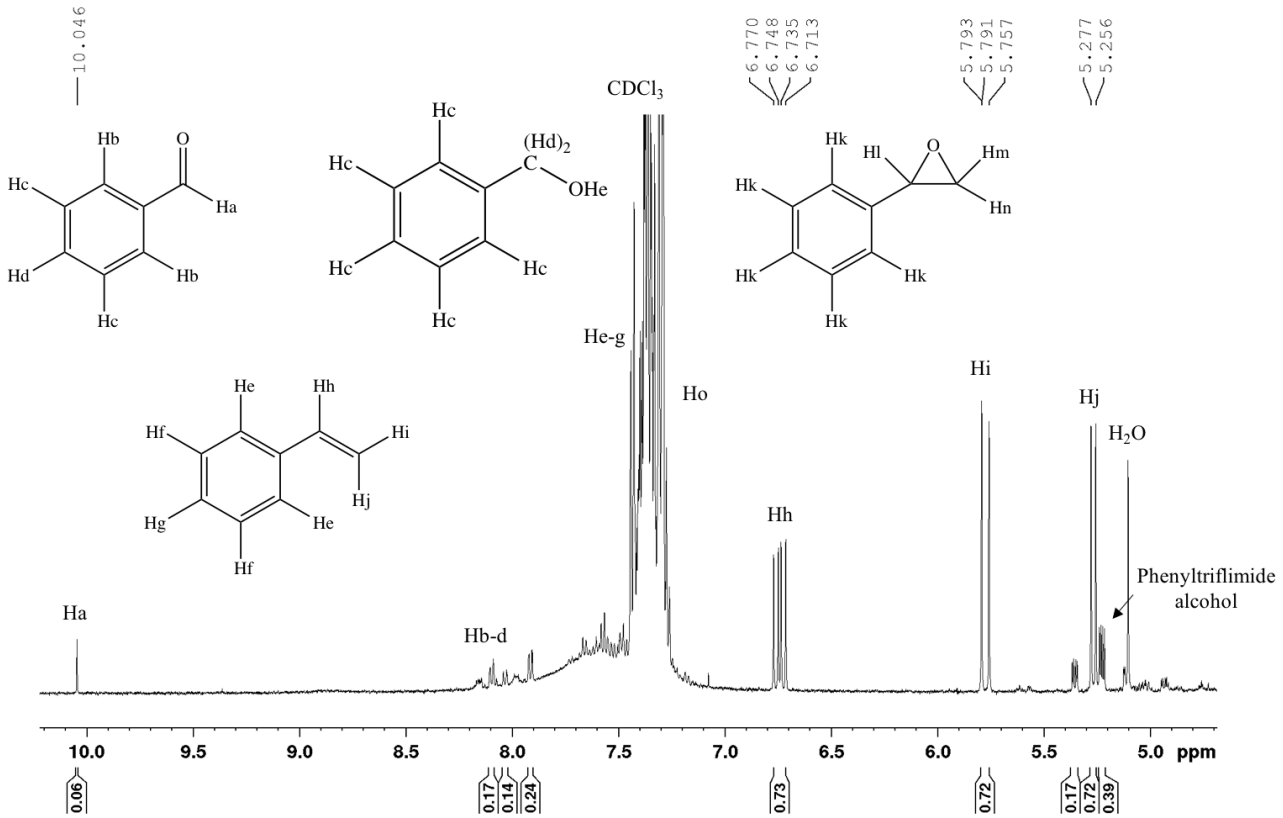
10.046
6.770
6.748
6.735
6.713
5.793
5.791
5.757
5.277
5.256
CDCl3
Hb
O
Hc
Ha
Hd
Hb
Hc
Hc
(Hd)2
C
OHe
Hc
Hc
Hc
Hc
Hk
Hl
O
Hm
Hk
Hn
Hk
Hk
Hk
He
Hh
Hf
Hi
Hj
Hg
He
Hf
He-g
Ho
Hi
Hj
H2O
Hh
Phenyltriflimide
alcohol
Ha
Hb-d
10.0
9.5
9.0
8.5
8.0
7.5
7.0
6.5
6.0
5.5
5.0
ppm
0.06
0.17
0.14
0.24
0.73
0.72
0.17
0.72
0.39

B

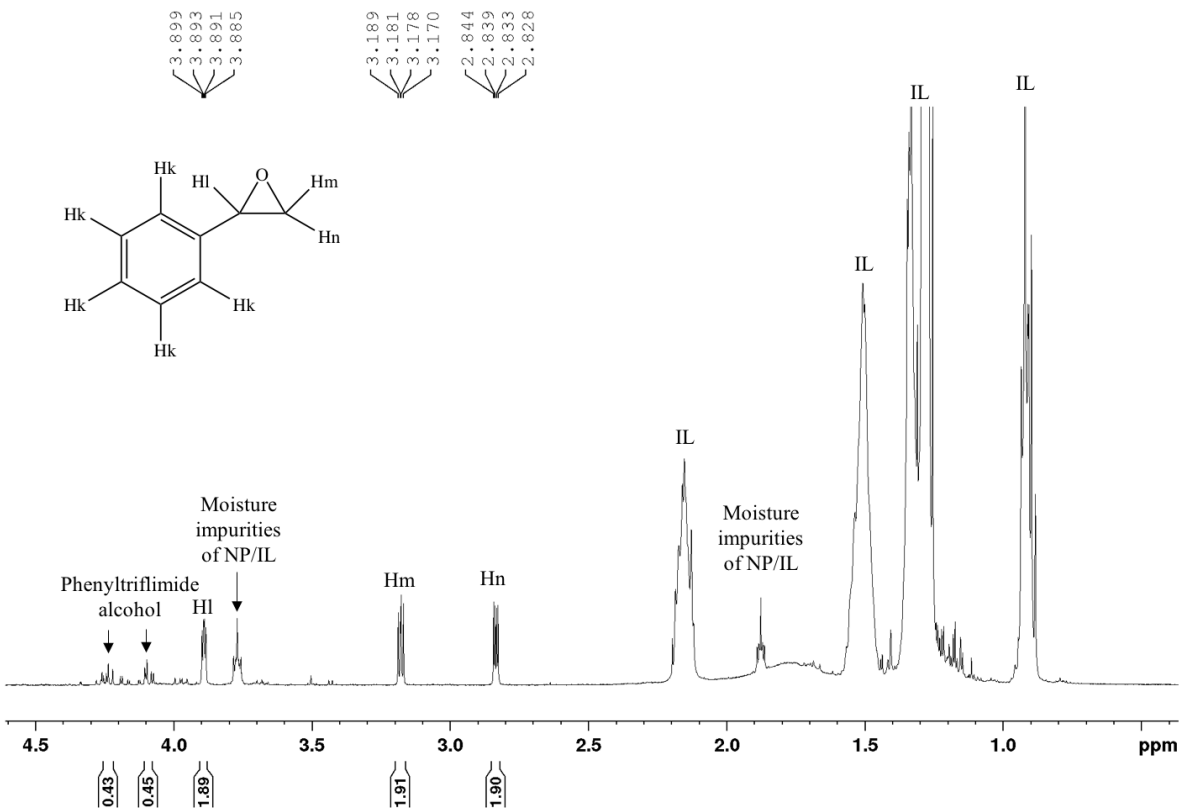

Figure A.2 Styrene epoxidation catalyzed by Au/[P66614][NTf_2]. Reaction conditions used: 5.24 mmol styrene:0.0102 mmol Au:19.7mmol TBHP, 0.1 MPa, 80 °C for 4 h. A drop of $LiBH_4$ followed by 2 drops of TBHP were added into the reaction solution after 3 h during the 4 h reaction.

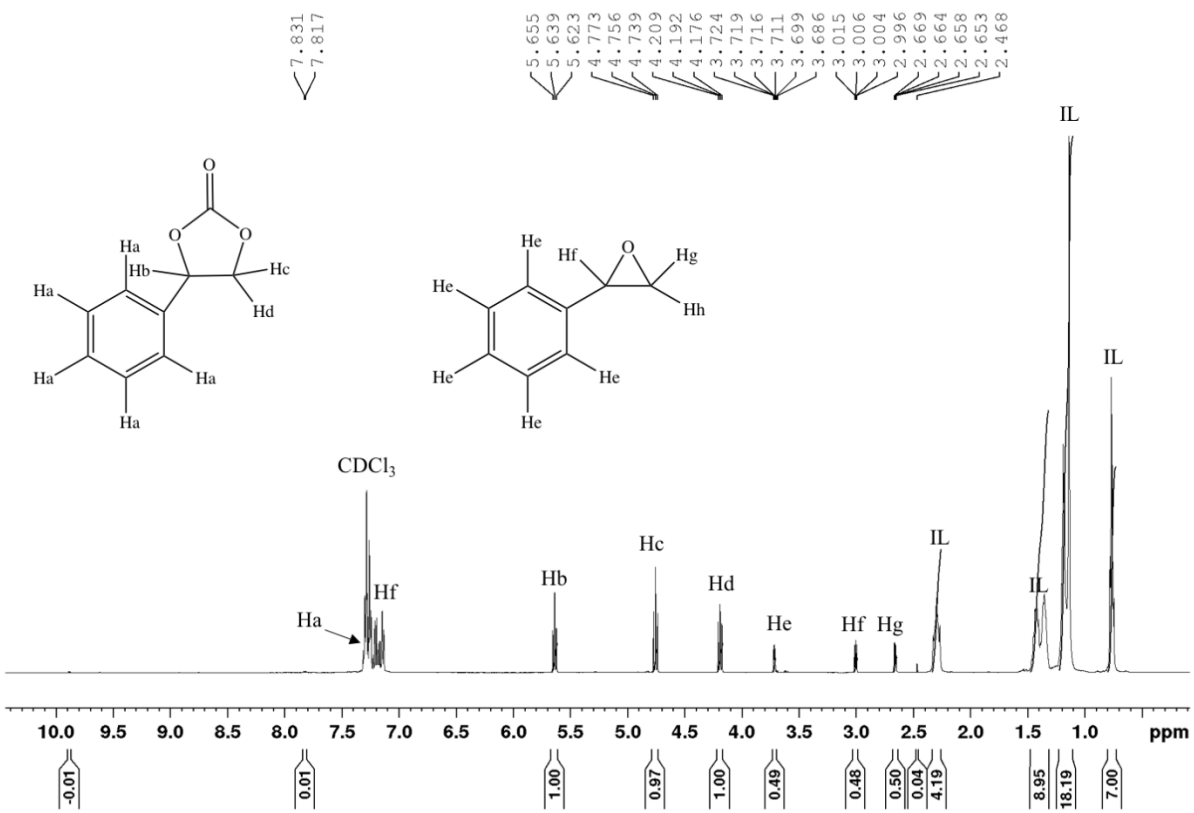

Figure A.3 Cycloaddition of CO_2 to SO catalyzed by [P66614][NTf_2]. Reaction condition used: 8.49 mmol SO:28.6 mmol IL, 55ºC, 2.4 MPa, 7 h, and 600 rpm.